PULSATING STARS AND BINARY SYSTEMS

by

Aliz Derekas

A thesis
submitted for the degree of
Doctor of Philosophy
at the
University of Sydney

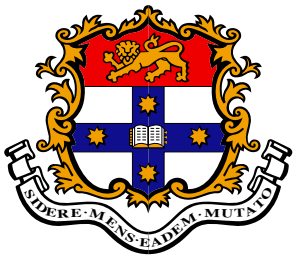

SYDNEY·AUSTRALIA
March 2009

Statement of Originality

This thesis describes work carried out at the Department of Astrophysics, University of New South Wales between February 2003 and August 2004 and at the Sydney Institute for Astrophysics within the School of Physics, University of Sydney, between February 2005 and March 2009 (with 1.5 years' suspension for maternity leave). This thesis contains no material that has been presented for a degree at this or any other university, and, to the best of my knowledge, contains no copy or paraphrase of work published by another person, except where duly acknowledged in the text.

Note that Chapters 3-9 are reproductions of papers produced in collaboration with other researchers or are in preparation. The majority of the work can be credited as my own and the division of the work between the authors is explained at the beginning of each of these chapters.

Aliz Derekas Date

Abstract

This thesis presents research on different types of variable stars, using publicly available data obtained by the MACHO Project in the Large Magellanic Cloud to find eclipsing binaries with pulsating component and my own photometric and spectroscopic observations to detect spectroscopic binary pulsators and multiperiodicity in high- amplitude δ Scuti stars. The thesis contains two major sets of work: Chapters 3, 4 and 5 summarise the results of the MACHO analysis, while Chapters 7, 8 and 9 show the results using my observations. The results were published in four refereed journal papers.

I reanalysed publicly available two-colour observations of about 6800 stars in the Large Magellanic Cloud obtained by the MACHO Project and classified as eclipsing variables. Of these only 3031 in total turned out to be genuine eclipsing binaries. I determined new periods and classified all the stars and analysed the sample.

During the process my attention was drawn to an RR Lyrae star with an enormous rate of period modulation with cycle length of about 8 years that indicated a possible binary nature for this star. I could exclude both multiple periodicity and amplitude modulation unambiguously as a cause of the period modulation. Spectroscopic follow-up observations ultimately rejected the binary hypothesis. The observed behaviour is consistent with that of the RR Lyrae stars with Blazhko effect in form of pure phase modulations, presumably due to tiny changes in the pulsation period.

Another step in the analysis of the MACHO data was a period-luminosity-amplitude study of 5899 red giant and binary stars. The period-luminosity (P–L) relations confirm the existence of a short-period, small-amplitude P–L sequence at periods shortward of sequence A. My investigation revealed that the correct position for sequence E is at the doubled periods, thus overlapping with the sequence of long secondary periods (LSPs; sequence D). The amplitudes of LSPs have properties more similar to pulsations arguing for pulsational origin of the LSP phenomenon.

I carried out a spectroscopic monitoring of high-amplitude δ Scuti stars (HADS) and Cepheid variables in order to detect binarity and collected photometry to study multiperiodicity in high-amplitude δ Scuti stars. Orbital motion was detected in two HADS, while multiperiodicity was confirmed in three cases. The first radial velocity curves in the literature were obtained for two stars. In the radial velocity survey of 40 classical Cepheids, I discovered 6 new spectroscopic binary systems. The analysis of the Hα and

photospheric metallic lines revealed that the latter are more suitable for extracting radial velocity curves, as Hα is strongly effected by the atmospheric shocks. Interestingly, the Hα minus metallic velocity difference shows a very characteristic period dependence, which strongly resembles that of the Fourier parameter R_{21} of the radial velocity curves. This suggests that the velocity difference is a sensitive kinematic proxy of the mode resonance in Cepheids and its atmospheric effects.

Finally, HH Nor is an optical double system that carried the potential of being the first RR Lyrae star in an eclipsing binary system. Spectroscopic observations of the system revealed no physical connection between the components. Further analysis of the data is still in progress.

Acknowledgments

First, I warmly thank my supervisors, Tim Bedding and László Kiss, for their advice, support and encouragement throughout my years in Sydney. I would also like to thank my parents for accepting the fact that I moved to Sydney and supporting me and my decisions all of my life. Very special thank to my mum, facing your fear of flight and traveling here to help us selflessly and giving so much love to Ben and teaching him so many things. Many thanks to my husband, László for your help and encouragement in many things which, had they been fully listed, would have filled another thesis. Thank you Nyuszi for your existence, your smile and gaze and everything I received through you. You opened a new chapter in my life and taught me things which I have never known before. I really appreciate letting me sleep many times. I am really really grateful to Ange, Stew, Harmony and your family for looking after Ben and being so good to him. Without your help, I would not have been able to finish my thesis in time.

I would like to thank Michael Ashley, my former supervisor at the UNSW for using the APT and inviting me to participate in the exoplanet search project. On a more formal note, my acknowledgments go to the followings. My studies were first supported by the International Postgraduate Research Scholarship (IPRS) programme of the Australian Department of Education, Science and Training and then by a University of Sydney Postgraduate Award. I am very thankful to the ANU RSAA, the Anglo-Australian Observatory and the CfA Time Allocating Committees for their support by providing telescope time for this project and for Prof. Chris Tinney for taking the high-quality service observations with the AAT. I am very grateful to the Postgraduate Research Support Scheme for supporting me in conference travels and providing a laptop computer to help my research. I am also very thankful to the International Astronomical Union for providing a travel grant for the IAU Symposium No. 240, Binary Stars as Critical Tools & Tests in Contemporary Astrophysics, 2006, Prague, Czech Republic. I would like to thank the School of Physics for providing productive environment for the research.

The research for this thesis has been supported by the Hungarian research grants OM FKFP 0010/2001, OTKA Grants #T042509 and #K76816, the Polish KBN grant 2P03D02124, NSF grant AST-0204908 and NASA grant NAG5-12212 and the Australian Research Council. The papers analysing MACHO data utilise public domain data obtained by the MACHO Project, jointly funded by the US Department of Energy

through the University of California, Lawrence Livermore National Laboratory under contract No. W-7405-Eng-48, by the National Science Foundation through the Center for Particle Astrophysics of the University of California under cooperative agreement AST-8809616, and by the Mount Stromlo and Siding Spring Observatory, part of the Australian National University. The NASA ADS Abstract Service was used to access data and references. This research has made use of the SIMBAD database, operated at CDS-Strasbourg, France.

Publications

The following papers published in refereed journals have been included in this thesis. For each paper, I outline my contributions at the beginning of each chapter.

Chapter 3: **A. Derekas**, L. L. Kiss, A. Udalski, T. R. Bedding and K. Szatmáry, 2004, A first-overtone RR Lyrae star with cyclic period changes, MNRAS, 354, 821-826

Chapter 4: **A. Derekas**, L. L. Kiss, T. R. Bedding, H. Kjeldsen, P. Lah and Gy. M. Szabó, 2006, Ellipsoidal Variability and Long Secondary Periods in MACHO Red Giant Stars, ApJ, 650, L55-L58

Chapter 5: **A. Derekas**, L. L. Kiss and T. R. Bedding, 2007, Eclipsing Binaries in the MACHO Database: New Periods and Classifications for 3031 Systems in the Large Magellanic Cloud, ApJ, 663, 249-257

Chapter 7: **A. Derekas**, L. L. Kiss, T. R. Bedding, M. C. B. Ashley, B. Csák, A. Danos, J. M. Fernandez, G. Fűrész, Sz. Mészáros, Gy. M. Szabó, R. Szakáts, P. Székely and K. Szatmáry, 2009, Binarity and multiperiodicity in high-amplitude δ Scuti stars by , Monthly Notices of the Royal Astronomical Society, 394, 995-1008

Chapter 8: L. L. Kiss and **A. Derekas**, 2004, "HH Nor": a double star with two variable components, Information Bulletin on Variable Stars, No. 5555

Contents

Chapter 1

Introduction

A star is a gaseous sphere that can pulsate in many different modes if sufficient excitation is provided. Pulsating stars offer a unique opportunity to study stellar interiors. Important aspects of microphysics, such as the physics of energy propagation in dense plasmas, can be understood in a way that is not possible otherwise. *Asteroseismology* has become a major discipline within stellar astrophysics, one that has generated huge investments in theory and observational works (Gautschy & Saio, 1995, 1996; Christensen-Dalsgaard, 2004; Cunha et al., 2007). The principal way of understanding pulsating stars is detailed comparison of the observed pulsational properties (most importantly, the frequencies, but also amplitudes and mode lifetimes) with theoretical models that include realistic input physics. The latter requires the knowledge of the fundamental stellar parameters as accurately as possible: mass, effective temperature and radius (hence luminosity), metallicity, evolutionary stage. Fulfilling this requirement, however, is never an easy task.

Binary stars have long been recognized as key objects for calibrating astronomical observations in terms of these fundamental stellar parameters. As a matter of fact, binarity has been up until very recently the only route to stellar masses. Even now, the alternative ways such as combining interferometry with asteroseismology (North et al., 2007) are restricted to the very nearest stars. Existing and planned sky surveys, such as Skymapper, LSST, Pan Stars, Gaia, Kepler etc. will deliver high-quality photometric observations of millions of binary stars, which are expected to reveal new insights into the structure and evolution of the whole Milky Way.

The main focus of my research has been the combination of the two classes of objects, namely pulsating stars and binary systems, in order to test theories of stellar

structure and evolution through utilising binary star astrophysics. We are still at the beginning of a long road, however, the future is bright in the light of the coming high-profile survey projects.

1.1 Close binary stars

It is commonly accepted that at least 50% of all stars reside in double or multiple systems (Abt, 1983). Components of close binary stars are so close together that we cannot resolve them. They are clearly distinguishable from visual binaries, whose components can be optically resolved. Close binaries can be detected in many different ways: directly from photometry, astrometry and/or spectroscopy, or indirectly, such as from light-time effects (see Section 2.4.1). The importance of binary stars is due to several factors, including the following: (i) they provide the only direct way to determine the mass of a star; (ii) very accurate physical characteristics (radius, mass, temperature, luminosity) can be determined; (iii) stellar structure and evolution theories can be tested; (iv) physical processes can be investigated (such as mass exchange, eruptions or other unusual stellar phenomena); (v) very accurate distance measurement is possible (uncertainties of less than 1% in certain cases); and (vi) through very accurate distance measurements, galaxy evolution can also be studied (Hilditch, 2001). Of these, the first three are relevant to this thesis.

1.1.1 Eclipsing binaries

A special class of binaries are the eclipsing binaries, in which regular light variations occur due to one of the stars passing directly in front of its companion, as viewed from the Earth. They have a very important role in astrophysics: the only direct way to measure the mass of a star accurately is through eclipsing binaries. Moreover, other stellar parameters can also be determined most accurately using them (Lacy et al., 2005; Wilson, 2007; Southworth & Bruntt, 2007; Bruntt & Southworth, 2008).

Eclipsing binary light curves are very distinctive: when the eclipses occur the total luminosity observed from the system decreases. When the hotter star is eclipsed, the deeper minimum appears in the light curve, called primary minimum. The opposite case is called the secondary minimum. The larger the temperature difference between the components, the bigger the difference in depth of the two minima. Based on the

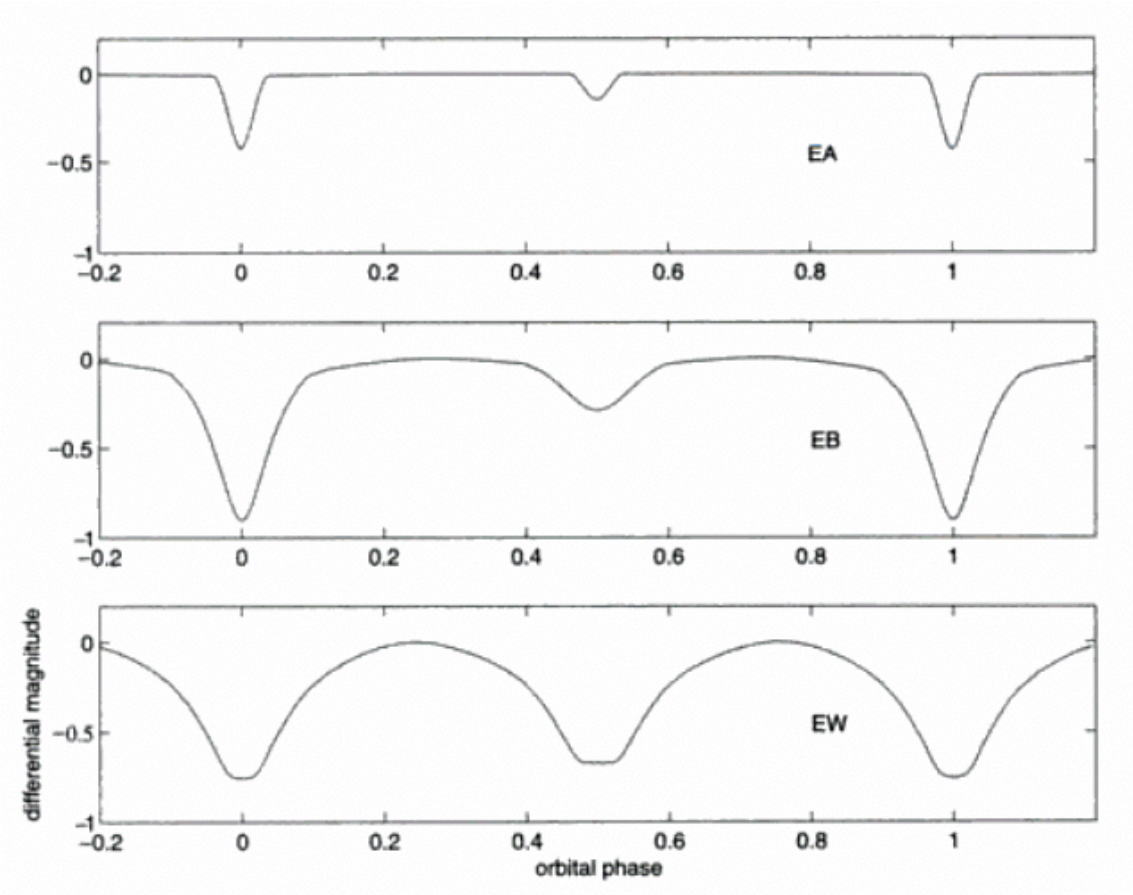

Figure 1.1 Three main classes of eclipsing binary stars based on the shape of the light curve. Figure is from Hilditch (2001).

light curve shape, eclipsing binaries are traditionally classified into three types:

1. **Algol-type binaries (EA):** The light curve contains clearly defined, sharp eclipses with an obvious beginning and end. Outside the eclipses there is very little or no variation. An example is shown in the top panel of Fig. 1.1.
2. β **Lyrae type (EB):** The light curve is quite smooth, and it is hard to distinguish the exact place when the eclipse starts or ends. Outside the eclipses the light curve varies considerably due to the non-spherical shapes of the components. In many cases there is mass transfer between the components that causes the orbital period to change. The middle panel in Fig. 1.1 shows an example for a β Lyrae type light curve.
3. **W UMa type (EW):** The light curve is very smooth (without a plateau), as shown in the bottom panel in Fig. 1.1. Mass transfer occurs until equilibrium and the

orbital period is usually shorter than 1 day. Interestingly, these objects are one of the most common type of stars (Shapley, 1948; Rucinski, 2002).

Another widely accepted classification is based on the Roche model for the surfaces of constant gravitational potential around two mass points. Binary stars can be classified into three groups: **detached, semidetached** and **contact** binaries, as introduced by Kopal (1955) by analyzing photometric light curves of eclipsing binaries as well as using results from spectroscopic observations to determine basic physical parameters (mass ratios, masses, separations and temperatures). This classification has had great impact on understanding binary evolution (Hilditch, 2001). The components of detached binaries are within their Roche lobes (top panel in Fig 1.2). One star fills its Roche lobe in semidetached systems (middle panel in Fig 1.2), while both components fill their Roche lobes in contact binaries (bottom panel in Fig 1.2). The traditional light curve-based and the Roche model classifications can be matched quite well: Algols are usually detached, β Lyraes are semidetached and W UMas are contact binaries.

As has been pointed out by one of the thesis assesors, it is worth noticing, that this traditional classification has been somewhat overcome by recent developments in the field. Fow example, 'over-contact' binary is a more logical name than 'contact binary' for both historical and astrophysical reasons Wilson (1971). Similary, the use of the β Lyrae type should not be continued, as it is a relic from an era when binary star evolution was not understood at the most basic levels. As a matter of fact, 'β Lyrae' is only a superficial light curve describer and has no structural-evolutionary meaning.

1.1.2 Measuring stellar parameters

As mentioned above, very accurate physical parameters can be determined with binary stars, even if the components are not resolved. Without going trough all the details, whose discussion is far beyond the scope of this thesis, I summarise the basics of how we can deduce these parameters from the observations, following the notation of Hilditch (2001).

The radial velocity curve of each component can be written as a function of the orbital parameters:

$$v_{rad} = K\left[\cos\left(\theta + \omega\right) + e\cos\omega\right] + \gamma, \tag{1.1}$$

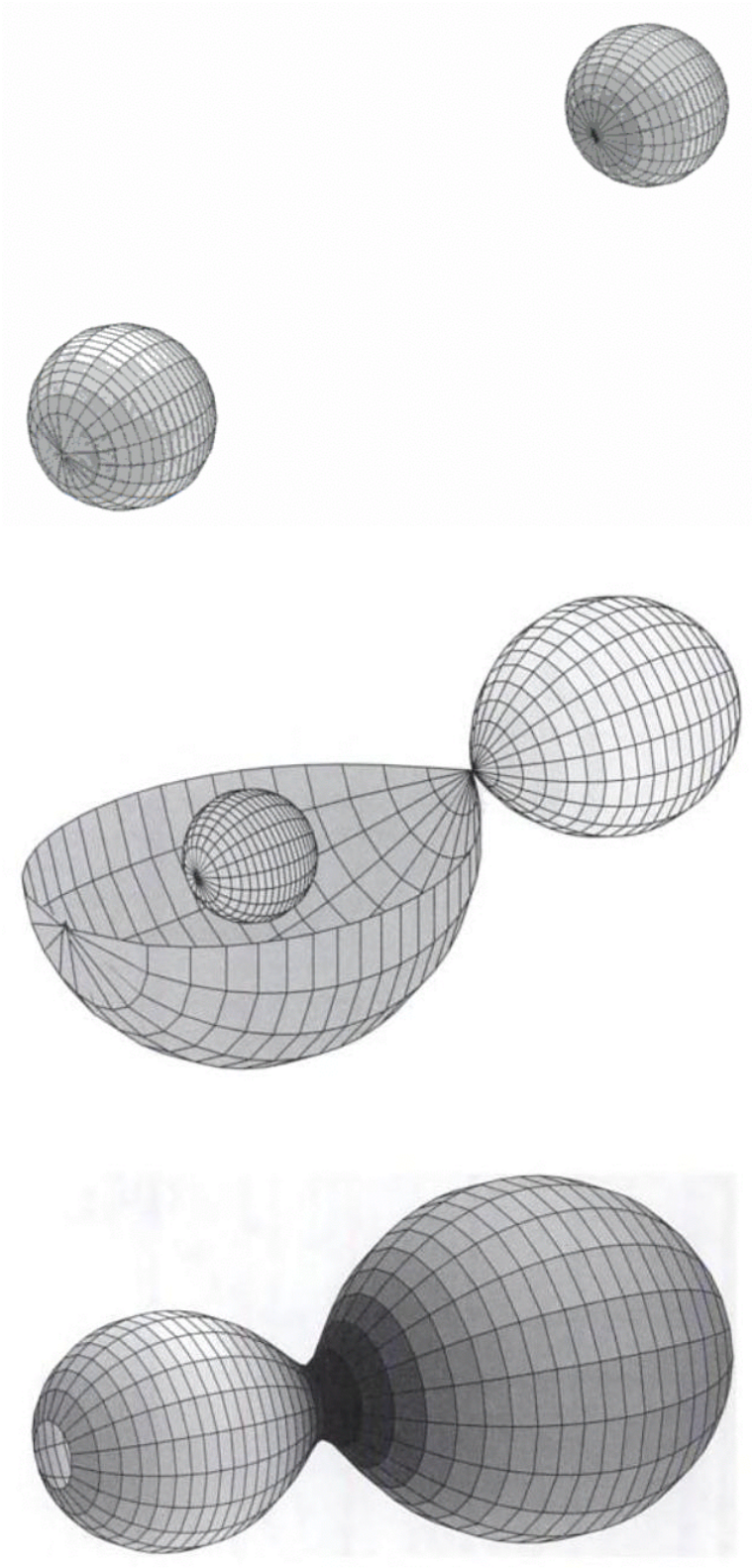

Figure 1.2 Classification of binary stars based on the Roche geometry. From top to bottom: detached, semidetached and contact binaries (Hilditch, 2001).

where $K = (2\pi a \sin i) / \left[P\left(1-e^2\right)^{1/2}\right]$ is the semi-amplitude of the velocity curve, θ is the true anomaly, ω is the argument of periastron (the orientation of the ellipse), γ is the systemic velocity (the radial velocity of the center of mass of the binary system), i is the inclination, and e is the eccentricity of the orbit.

For double-lined spectroscopic binaries, the a_1, a_2 semimajor axes can be calculated:

$$a_{1,2} \sin i = \frac{\left(1-e^2\right)^{1/2}}{2\pi} K_{1,2} P \tag{1.2}$$

and the minimum masses m_1, m_2 are given by

$$m_{1,2} \sin^3 i = \frac{1}{2\pi G} \left(1-e^2\right)^{3/2} \left(K_1+K_2\right)^2 K_{2,1} P, \tag{1.3}$$

where K_1, K_2 are the semiamplitudes of the radial velocity curves of the two components and P is the orbital period.

For single-lined binaries, we can only measure the semiamplitude of the radial velocity curve of one component and the mass function can be given with the following form:

$$f(m) = \frac{m_2^3 \sin^3 i}{\left(m_1+m_2\right)^2} = \left(1.0361 \times 10^{-7}\right) \left(1-e^2\right)^{3/2} K_1^3 P M_\odot \tag{1.4}$$

To estimate m_2 for a single-lined binary system, we need to know the orbital inclination and m_1 from other types of observations, from an empirical calibration of masses, or from theoretical models (Hilditch, 2001). For both cases, eclipsing binaries are extremely valuable because light curve models allow determining the inclination angle very accurately, so that the $\sin i$ uncertainty is removed.

In summary, close binary stars open the door to quantitative astrophysics, upon which modern stellar astrophysics, including theories of pulsating stars, has been built and calibrated.

1.2 Pulsating stars

Most pulsating stars are located in a well-defined part of the Hertzsprung-Russell diagram (HRD), in the so-called instability strip. However, some pulsating stars lie outside

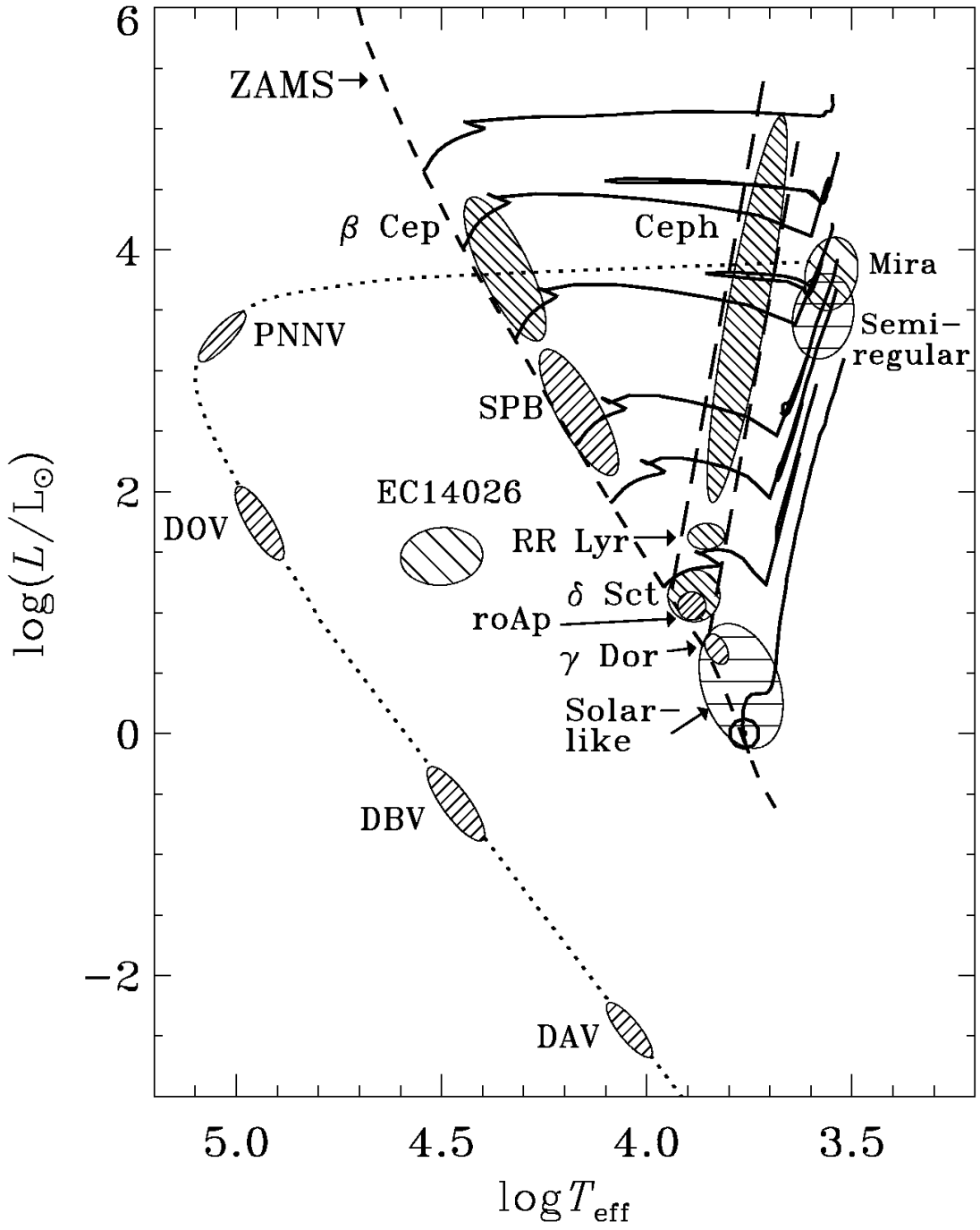

Figure 1.3 Locations of pulsating stars in the Hertzsprung-Russell diagram. The diagonal dashed line indicates the zero age main sequence (ZAMS). The nearly-vertical dashed lines show the borders of the instability strip. Stellar evolutionary tracks (black curves) are shown for 1, 2, 3, 4, 7, 12 and 20 $M_\odot$. (The figure is slightly modified from the original, which was kindly supplied by J. Christensen-Dalsgaard and Dennis Stello.)

of the instability strip, such as β Cepheids, Miras and semiregular variables. Fig. 1.3 shows the location of some of the classical pulsators in the HRD.

In this thesis δ Scuti, RR Lyrae, Cepheid and red giant variables are discussed. In the first three of these, and possibly in all four, the pulsation is driven by the κ-mechanism, which operates in the partial ionization zones (Eddington, 1941). Here, when the gas is compressed, the temperature does not rise as much as it is expected, but further ionization is produced and the opacity increases. As the layer absorbs heat during compression, it is pushed outward. During expansion, the ions recombine with electrons and release energy and the opacity decreases, as does the density. Finally, the material falls back down and a new cycle starts (Carroll & Ostlie, 2006). In red giants the pulsation may be excited stochastically by convection, as in the case in the Sun (Christensen-Dalsgaard & Frandsen, 1983) or by self-excitation (Keeley, 1970; Fox & Wood, 1982; Dziembowski et al., 2001).

Stars can pulsate in both radial and nonradial modes. In the former, the gas moves in the radial direction at every point. For the first and high overtone modes, there are nodal surfaces at which the gas is not moving. For the fundamental mode, the only node is at the centre and the whole star expands and contracts during the pulsations. The positions of the nodes within the star are determined by the variations of the internal sound speed.

Nonradial pulsation is more complicated: some regions of the surface expand while others contract. In general, stellar pulsations are characterized by their frequency and three quantum numbers: radial order n gives the number of nodes between the center and surface of the star, the angular degree ℓ and the azimuthal order m. Here $2|m|$ specifies the number of nodes in longitude and $\ell - |m|$ specifies the number of nodal lines in planes parallel to the equator. In practical applications, asteroseismology is about mode identification, that is defining the quantum numbers for each frequency measured from observations.

The simplest pulsators are radial, in which the gas moves only in radial direction. In this case, $\ell = m = 0$ and the various modes differ only in the number of radial nodes (n). Finally, there are two kinds of pulsation: in p-modes the pressure provides the restoring force for the waves, while in g-modes the gravity does. The next sections introduce the basic characteristics of the different types of pulsating variables I studied in this thesis.

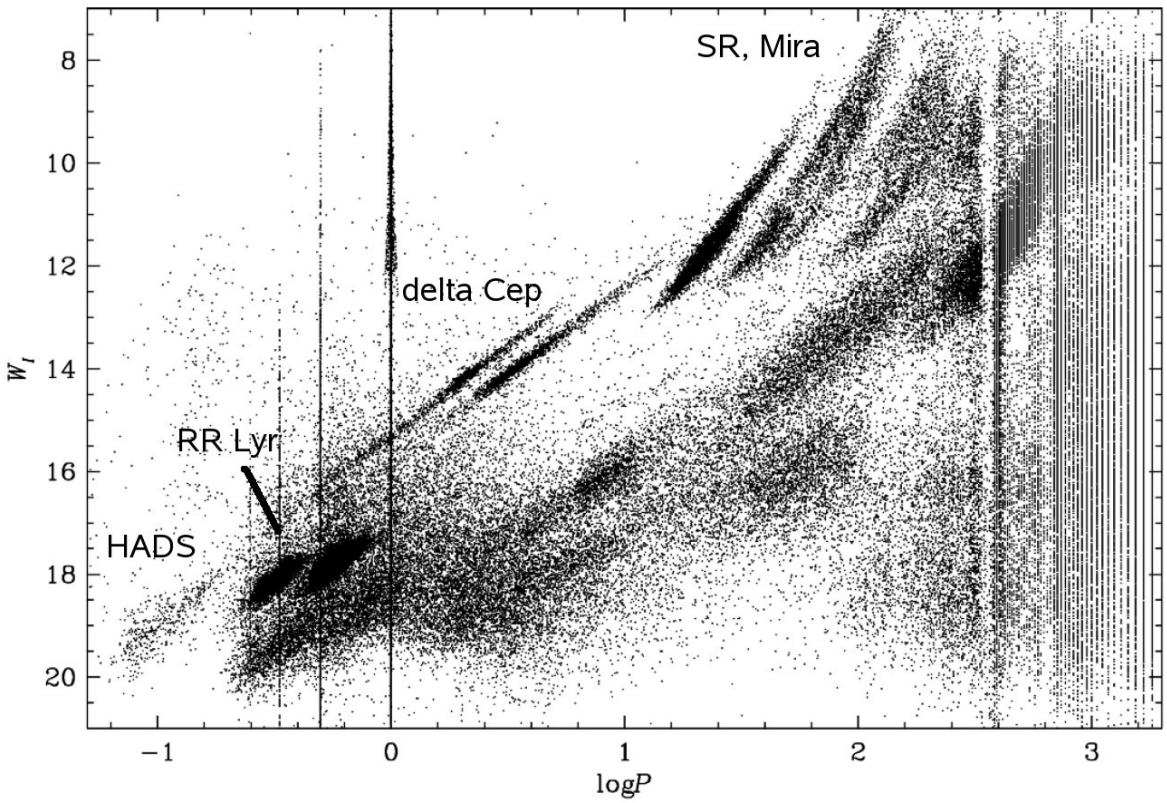

Figure 1.4 The period-luminosity relation of high-amplitude δ Scuti stars (HADS), RR Lyraes (RR Lyr), Cepheids (delta Cep) and red giants (SR, Mira), based on OGLE observations of the Large Magellanic Cloud (Soszyński, 2008a).

1.2.1 Cepheid variables

Cepheids are radially pulsating supergiants in the helium-burning stage and have spectral types of F5–G5. They are located in the upper part of the instability strip, with luminosities of $10^3 - 10^4$ times greater than the Sun (see Fig. 1.3). Population I Cepheids are called Type I Cepheids, while their Population II relatives are known as Type II Cepheids or W Virginis variables. Their pulsation is driven by the κ-mechanism, with periods ranging from a few days to more than hundred days.

A characteristic feature of Cepheids is their period-luminosity relation (see in Fig. 1.4), which was discovered by Henrietta Swan Leavitt in 1912 (Leavitt & Pickering, 1912). Since Cepheids have high luminosity, extragalactic Cepheids can easily be observed and their P–L relationship (see an example in Fig. 1.4) makes them a powerful tool for distance measurements out to about 10 Mpc (di Benedetto, 2008; Gieren et al.,

2008).

Quite a large number of Cepheids are suspected to be in binary systems. More than 60% of galactic Cepheids brighter than 8th mag have a physical companion and the same rate is expected for the fainter Cepheids (Szabados, 2003). The companion is usually a less massive main-sequence (or near-to-main-sequence) blue or yellow star (Szabados, 2006), which is very hard to detect spectroscopically. Until recently, only one galactic Cepheid was known to be in an eclipsing binary system (Antipin, Sokolovsky & Ignatieva, 2007), only a few others in the Large Magellanic Cloud (Alcock et al., 2002; Soszyński et al., 2008b). These systems are very important because they carry the potential to measure Cepheids masses directly (for more details see Section 1.1.2). This is important because Cepheid masses still need refinement, and there is a discrepancy of their masses derived by different methods: masses from stellar pulsations are 10–20% smaller than from evolutionary models (Szabados, 2006).

We have performed a spectroscopic survey of southern Cepheid variables in order to detect spectroscopic binary Cepheids. We have so far discovered 6 new spectroscopic binary Cepheids, for which the preliminary results are summarised in Chapter 10.

1.2.2 δ Scuti variables

δ Scuti stars are short-period pulsating variables of A-F spectral types, located at the intersection of the main sequence and the classical instability strip in the Hertzsprung-Russell diagram (HRD). They are either in core hydrogen-burning phase or are burning hydrogen in a shell. Their pulsation periods are between 0.02 d and 0.3 d. There are also a few δ Scuti stars among pre-main sequence stars, e.g. two pulsators in NGC 2264 (Breger, 1972) and HR 5999 (Kurtz & Marang, 1995). Presently, about 30 objects are collected in the more recent literature (Zwintz & Weiss, 2006; Zwintz, 2008). Population II members of δ Scuti stars, also known as SX Phoenicis stars, are often found in globular clusters (for a review of δ Scuti stars see e.g. Rodríguez & Breger (2001)). Most of the SX Phe stars also HADS, but not all of them (Breger, 2000).

Some δ Scuti stars pulsate purely in radial modes, while the majority pulsate with a large number of nonradial p modes simultaneously (Breger et al., 1995). Usually low-degree ($\ell \leq 3$) and low-order (n=0 to 7) p modes are detected by photometric observations, while spectroscopic studies indicate the presence of high-degree nonradial modes with ℓ up to 20 (Breger, 2000). Some data show the presence of g-modes

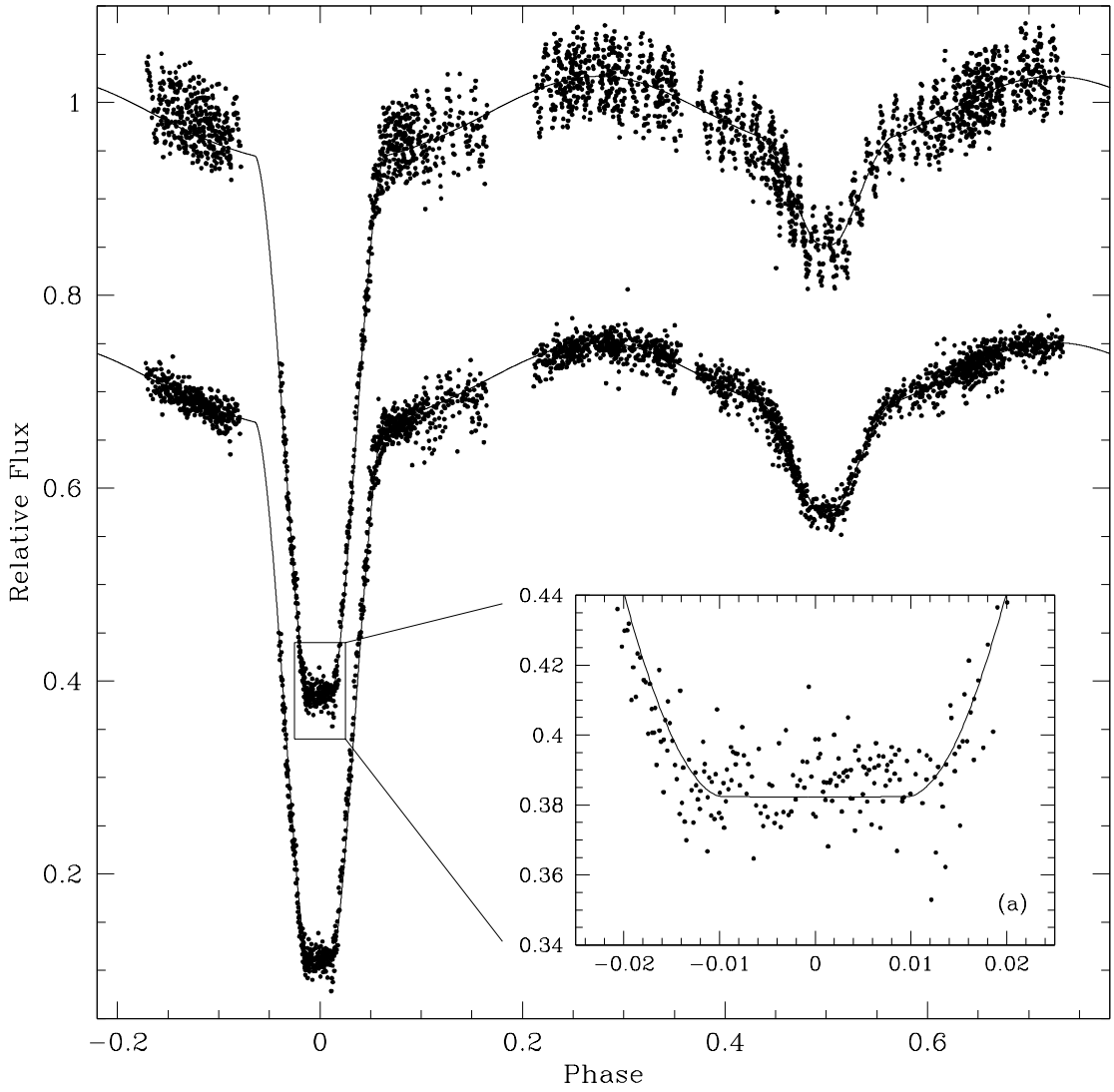

Figure 1.5 The phased light curve of the first high-amplitude δ Scuti star (HADS) discovered to be in an eclipsing binary. The upper curve is the original data, with the scatter outside the primary eclipse due to the δ Scuti pulsation. The lower curve is the same data with the δ Scuti pulsations removed. In both cases, the solid line is the fit to the original curve using the Wilson-Devinney code. Panel (a) shows the primary eclipse in more detail - there is no evidence of δ Scuti variations in this region, indicating the primary is the pulsating component. (Christiansen et al., 2007).

(Bischof & Breger, 2002; Breger et al., 1995). The photometric amplitudes range from $\sim$0.001 mag up to 1 mag. The excitation mechanism in δ Scuti stars is the κ-mechanism. The excitation zone is mainly the HeII ionization zone near 48000 K, while the H and HeI ionization zones (near 15000 K) are located near the stellar surface and may not play an important role (Breger, 2000).

The vast majority of δ Scuti stars are small-amplitude variables, pulsating with non-radial p modes. A prominent group within the family comprises the high-amplitude δ Scuti stars (HADS), which have V-band amplitudes larger than 0.3 mag. HADS are the short-period counterparts of the classical Cepheids, pulsating in one or two (sometimes more) radial modes, usually in the fundamental and first-overtone modes (McNamara, 2000). Indeed, they were once called dwarf Cepheids. The data collected by Rodríguez & Breger (2001) show, that unlike most δ Scuti stars, there are no rapidly rotating HADS ($v \sin i \leq 40$ km s^{-1}), suggesting an intimate relationship between the rotational state and the amplitude of pulsations. In recent years, the number of HADS known with multimode pulsations has grown rapidly (about 15 known), hinting a new potential for asteroseismic studies of these objects (e.g. Poretti, 2003; Poretti et al., 2005). Several investigations suggested that some of the stars may have non-radial pulsation modes present (McNamara, 2000; Poretti et al., 2005). This was confirmed for the high-amplitude SX Phe star BL Cam (Rodríguez et al., 2007) with more than 20 independent modes simultaneously excited.

The number of known binary δ Scuti stars has increased dramatically in the last few years. Some well-known examples have very detailed studies, e.g. RZ Cas (Ohshima et al., 2001; Rodríguez et al., 2004a), AS Eri (Mkrtichian et al., 2004), Y Cam (Kim et al., 2002), AB Cas (Rodríguez et al., 2004b). Soydugan et al. (2006) catalogued 25 confirmed systems and 197 candidate binaries with possible pulsating components. Pigulski & Michalska (2007) found 9 new systems in the ASAS-3 catalog data. All of these systems have low-amplitude δ Scuti companions. We discovered the first high-amplitude δ Scuti in an eclipsing binary (Christiansen et al., 2007) whose light curve is shown in Fig. 1.5. The system was found during the preparation of variable star catalog compiled from the data taken for the University of New South Wales Extrasolar Planet Search. The system is also a double-lined spectroscopic binary, which allowed us to determine the mass for the components and so the δ Scuti star. In this thesis, HADS are discussed in Chapter 7.

1.2.3 RR Lyrae variables

RR Lyrae stars are A2–F6 spectral type pulsating variables with periods between 0.2 and 2 days and amplitudes of 0.3 and 2 mag. They are Population II stars (low metallicity) and so are often found in globular clusters or in the galactic halo. Just like Cepheids, they obey a period-luminosity relation, so they are useful as distance indicators. The pulsation of RR Lyraes are driven by the κ-mechanism, similarly to δ Scuti stars and Cepheids.

According to pulsational behaviour, RR Lyrae variables are divided into three subgroups. RRab types pulsate in the fundamental radial mode and typically have asymmetric light curves. RRc types pulsate in first overtone mode and their light curves are mostly sinusoidal, with lower amplitudes and shorter periods than RRabs. Some of the RR Lyraes pulsate in more than one mode, these are usually known as RRd types. One of the most interesting pulsational features of RR Lyraes is the so-called Blazhko effect. Stars belonging to this group show amplitude and/or period change, usually over a well-defined cycle with a period in the range 5 to 100 days. Although there are a number of theories to explain this behaviour, the Blazhko effect is still poorly understood (Kolenberg, 2008). One promising theory has been proposed by Stothers (2006), whose model is based on turbulent convection inside the hydrogen and helium ionization zones which becomes cyclically weakened and strengthened, causing fluctuations of light and velocity amplitudes. Other explanations assume the presence of nonradial modes in the stars (Dziembowski & Mizerski, 2004) or involve the so-called magnetic model in which the variation is caused by the magnetic field being inclined to the rotational axis (Shibahashi, 2000). Observational campaigns to explore the phenomena have become very popular in recent years (Chadid & Chapellier, 2006; Jurcsik et al., 2006, 2008, 2009; Kolenberg et al., 2006, 2009) but the Blazhko effect is still unexplained.

Another great mystery related to RR Lyrae variables is the lack of confirmed binaries among them. There is only one unambiguous binary RR Lyrae, namely TU UMa, for which both cyclic period change and radial velocity measurements indicate a binary companion in a highly elliptical orbit (Wade et al., 1999). In Chapter 3 we present observations of an RR Lyrae star which appears to have regular period changes. This could be due to binarity, but only if the companion is a black hole. The spectroscopic follow-up of the star does not support this hypothesis, so the observed period change is caused by an unknown mechanism, perhaps phase modulation generated by the Blazhko effect.

1.2.4 Red giants

Low and intermediate mass stars (between 0.5 and 5 solar masses) become red giants when they start to run out of fuel for thermonuclear reactions in their cores. Theoretical calculations have shown that stars become red giants twice during their evolution (first on the Red Giant Branch and then on the Asymptotic Giant Branch). Each time, the star expands to several hundred solar radii with cool temperatures ($T_{\rm eff} \sim$ 3500–4500 K) and high luminosities (L $\sim 10^2$–10^4 $L_\odot$).

Most, if not all, red giants pulsate (Jorissen et al., 1997; Eyer & Mowlavi, 2008). Periods range from 10 d to 1000 d, while amplitudes varies between 1 mmag and 10 mag. Previously, pulsating red giants were classified into 5 types by the *General Catalog of Variable Stars*. The first are Mira stars, which pulsate very regularly (P=10-500 days) with very large amplitudes (order of a few magnitudes). Semi-regular (SR) variables are divided into 3 subgroups: SRa variables, which are quite regular but smaller in amplitude than Miras; SRbs, which are less regular and SRcs, which are supergiants. The fifth group contains the slow irregular (L) variables.

The last decade witnessed a new era in red giant research, mainly thanks to the large-scale microlensing programs MACHO and OGLE. Now we know that there is a more complex spectrum of behaviour among red giants. Wood et al. (1999) has found five distinct period-luminosity sequences in the LMC (Fig. 1.4): large-amplitude Mira stars pulsate in the fundamental mode, whereas smaller amplitude semiregulars are often multimode pulsators, in which various overtone modes can be excited (sequences A, B and C) and two other sequences were suggested: sequence E with red giants in eclipsing binaries and sequence D with stars that have long secondary periods (LSPs). Later, Kiss & Bedding (2003, 2004), Ita et al. (2004a,b) and others have analysed red giants in the Large and Small Magellanic Cloud observed by the OGLE-II microlensing project and found that the original five sequences have further details, including a break at the tip of the red giant branch (RGB), which is due to the existence of distinct RGB pulsators that are mixed with the more evolved asymptotic giant branch (AGB) variables.

During the process of analysing eclipsing binaries in the MACHO data, I found that the position of Sequence E in the P–L relation of red giants was not correct. It turned out that this sequence is merging into Sequence D (Soszyński et al., 2004a; Derekas et al., 2006) which perhaps suggests binary origin for the long secondary periods. We examined this possibility and found no strong evidence for it. The details are summarised in Chapter 4.

1.3 Pulsation and binarity

Pulsating stars in binaries, especially in an eclipsing system, have a very important place in astrophysics. The binarity defines the physical and geometrical parameters of the system and, as mentioned in Section 1.1, these fundamental parameters can be determined very accurately. In binaries, therefore, the physical properties of the pulsating star can be measured. Basically, this is the only way to directly measure physical parameters for pulsating stars, to compare with other determinations and models (such as evolutionary or pulsational models). Therefore, the models can be tested through these systems (Aerts, 2007).

For asteroseismology, eclipses may be very helpful in mode detection and identification, which is one of the basic problems in asteroseismic studies. In an eclipsing system the inclination is close to 90° and it is assumed, but not proved, for various classes of detached and Algol-type binaries that the components rotational axes are perpendicular to the orbital planes. Thus, pulsating stars in eclipsing binary systems are very likely to viewed nearly equator-on. This is very favorable condition to detect sectorial and $\ell = +m$ = even modes (Mkrtichian et al., 2005). During the eclipse of the pulsating component, the obscuring component acts as a geometric spatial filter with an accurately known variable shape. This produces specific pulsation amplitude and phase changes of the non-radial pulsation mode depending on the quantum number ℓ, m of the spherical harmonic and the geometry of the eclipse. The amplitudes of the odd modes are reduced and may not be visible, only the even modes may be detectable (Mkrtichian et al., 2002, 2005). As a result, using the comparison of the modeled and the observed pulsation amplitude and phase changes during eclipses, the two-dimensional (ℓ, m) spatial information about non-radial pulsations can be determined (Mkrtichian et al., 2005).

Binaries with pulsating components also give opportunity to measure the internal rotational velocity of the pulsating star through the rotational splitting of the non-radial modes. The rotation of the components can be measured with the same accuracy as the pulsation frequency. In addition, the comparison of a splitting of low-degree modes with a splitting of high-degree modes that are trapped in the sub-photospheric layers on equatorial latitudes can provide accurate information about the differential rotation (Mkrtichian et al., 2005).

Effects of binarity on pulsation is also an exciting topic. The components in many

cases are so close together that they are tidally elongated. Such distortions are expected to have an effect on the pulsation (Ulas & Demircan, 2007). Tidal forces may be able to induce pulsations which was studied by Willems & Aerts (2002) and Willems (2003), estimating theoretical stellar and orbital parameters. Another effect is the pulsation-to-orbital period synchronization, which may be detected in the resonances of the frequency of the pulsation and the orbital period. However, observations have not been able to prove this hypothesis (Mkrtichian et al., 2005). One intriguing example is an eclipsing binary with δ Scuti type component, V6 in the open cluster NGC 2126 by Gáspár et al. (2003) where the ratio is very close to 9.

These applications were all considered when my PhD project started and some of my results are directly related.

1.4 Thesis layout

This thesis presents research on different types of variable stars using publicly available data and my own observations. The main goal was to deepen our knowledge of interplay between pulsations and binarity. For this I used the data obtained by the MACHO Project in the Large Magellanic Cloud and I also took spectroscopic observations to detect spectroscopic binary pulsators. The thesis contains two major sets of work: Chapters 3, 4 and 5 summarise the results of the MACHO analysis, while Chapters 7, 8 and 9 show the results using my observations.

In my research I started to work on the eclipsing binary data taken by the MACHO Project in order to detect pulsating components by analysing the light curves. After the time consuming downloading process (every single light curve had to be downloaded individually), it quickly became obvious that the classification and the periods given in the catalog were not perfect. Therefore, I reclassified and determined periods for all 6833 stars that have been available on the MACHO website. At the end of the reclassification and period determination, 3031 stars remained as genuine eclipsing or ellipsoidal variables, which composed the sample for the later analysis. The MACHO analysis is described in *Chapter 2*.

During the visual inspection of the individual light curves, my attention was drawn to an RR Lyrae star with enormous rate of period modulation that indicated a possible binary nature for this star. This was particularly interesting because only one RR Lyrae

star is known to be in a binary system, though it is expected that at least 50% of stars have companions (Section 1.2.3). The binary hypothesis of this star could only be confirmed by spectroscopic measurements. Therefore, I monitored the star spectroscopically in two different years and was ultimately able to reject this exotic possibility. The analysis of this star resulted in an MNRAS paper that comprises *Chapter 3* of this thesis.

Having the right periods of the binary sample, I plotted them in the period-luminosity plane. Here, the pulsating red giant variables form distinct sequences. The eclipsing binaries (Seq. E, Section 1.2.4) turned out to overlap with the sequence of Long Secondary Periods (Seq. D.), when the correct periods were used in the plot. The results were published in an Astrophysical Journal Letter that can be found in *Chapter 4*. Finally, the reanalysis of the MACHO data, containing the general properties of the sample, has been published in a separate ApJ paper, described in *Chapter 5*.

During my PhD, studies I have initiated a spectroscopic monitoring of high-amplitude δ Scuti and Cepheid variables in order to detect binarity. With this I gained extensive experience in spectroscopy. A short introduction of the observations and the reduction process is given in *Chapter 6*. In addition, I obtained photometric observation of δ Scuti stars. The results on δ Scuti stars, dealing with binarity and multiperiodicity, have been published in MNRAS (*Chapter 7*), while the analysis of Cepheid data are still in progress and the preliminary results are shown in *Chapter 9*.

Chapter 8 is a short sidetrack inspired by a paper on HH Nor written by Dvorak (2004). The star was originally classified as eclipsing binary but Dvorak (2004) revised it as an RR Lyrae variable based on ASAS observations. The published light curve drew my attention because it contained both eclipsing binary and RR Lyrae features, which suggested the possibility of finding the first RR Lyrae star in an eclipsing binary system. The close examination of other sources revealed a system containing an RR Lyrae and an eclipsing binary with similar brightness. This led to the publication that is summarised in *Chapter 8*. Later on, I obtained spectroscopic observations of the two stars to show if there is a possible physical connection between them. The analysis is still in progress, with preliminary results included in the chapter.

I summarise the results and give the future prospects of the further analysis of the data in *Chapter 10*.

During my years of PhD I have been involved in other projects, closely related to the main aim of my research. I spent almost the first half of my PhD at the University of New South Wales, Sydney, Australia. There I was involved in the observations of the

UNSW exoplanet search team led by Prof. Michael Ashley. I made remote observations from Sydney with the Automated Patrol Telescope (APT) at Siding Spring Observatory. I was involved in the classification of variable stars discovered by the project, which was published in a refereed paper, on which I am the second author (Christiansen et al., 2008). The catalog contains a particularly interesting object, the first high-amplitude δ Scuti star in an eclipsing binary system (Fig 1.5). The analysis of the system was published in a separate paper on which I am the second author (Christiansen et al., 2007). These results comprised part of the PhD thesis of Jessie Christiansen (accepted in 2008).

Chapter 2

MACHO database

2.1 The MACHO data

In three papers (Chapters 3, 4 and 5) I used publicly available data taken by the MACHO project of stars in the Large Magellanic Cloud (MACHO stands for MAssive Compact Halo Objects). The observations were obtained between June 1992 and January 2000, with the 50 inch telescope at Mt. Stromlo Observatory using a two-channel system (Hart et al., 1996). The imaging system incorporated a total of eight 2048x2048 pixel CCDs into two focal planes, allowing simultaneous imaging in two colours. Two-colour data in the specifically designed MACHO blue ($B_{\rm M}$) and MACHO red ($R_{\rm M}$) bands are publicly available at the MACHO website[1].

The website contains a Variable Star Catalog, for which a classification was made with using automatic software. One can download any specific class of stars (for example, a total of 6835 stars were classified as eclipsing binaries). The search returns a table of the basic parameters of the stars (such as coordinates, period, brightness, amplitude) and a link to view the light curve or to download it (see Fig. 2.1). Unfortunately, the data for all stars cannot be downloaded in a simple way: one has to click every single star that is wanted for download and then ftp Bundle, so the whole process was very time-consuming.

The downloaded file for each star contains 36 columns with different information, including Modified Julian Date of each observations, the MACHO blue and red magnitudes, their uncertainties and other data on the position of the given star in the focal

[1] `http://wwwmacho.mcmaster.ca/`

MACHO Variable Star Search Result

Your query was: ((Classification=10)).

6835 hits

Help | New Search | Previous | Next | ftp Bundle

Light Curve	Field. Tile.Seqn	Location (J2000)		Variability Index	Classification	# Obs	Obs w/2 Pts	Focal Plane	# Pts	Period (Days)	Magnitude Ave (K-C)	Amplitude Ave	Sup RSA	Sig	Chi2r
View	82.8404.38	RA	5:32:12.4080	17.22	EB	846	815	r	835	534.6041	15.806 R	0.268	2.15	0.108	16.14
Bundle		Dec	-69:15:58.3200					b	823	536.5728	15.464 V	0.222	1.49	0.071	7.7
View	82.8404.48	RA	5:32:3.2400	15.97	EB	846	364	r	400	1.0321	15.826 R	0.636	2.41	0.143	28.29
Bundle		Dec	-69:14:36.2400					b	599	1.032	15.502 V	0.611	3.23	0.141	36.5
View	82.8404.211	RA	5:32:24.1680	2.97	EB	846	708	r	733	0.4988	17.344 R	0.089	1.69	0.052	3.54
Bundle		Dec	-69:14:6.7200					b	811	0.4998	17.071 V	0.123	2.59	0.062	7.42
View	82.8404.851	RA	5:32:7.3200	1.02	EB	846	813	r	835	3.8282	18.79 R	0.746	1.13	0.125	1.51
Bundle		Dec	-69:15:42.4800					b	821	3.8285	18.796 V	0.55	1.16	0.126	1.59
View	82.8405.15	RA	5:31:50.8800	69.8	EB	844	795	r	833	93.1887	14.175 R	0.572	1.87	0.133	47.06
Bundle		Dec	-69:11:47.0400					b	805	93.1887	14.479 V	0.711	2.12	0.172	100.4
View	82.8405.172	RA	5:31:47.4480	7.1	EB	844	795	r	832	0.422	17.719 R	0.468	0.85	0.121	20.37
Bundle		Dec	-69:10:59.8800					b	805	0.422	17.431 V	0.483	0.85	0.118	26.24
View	82.8407.1086	RA	5:31:51.3120	1.28	EB	847	769	r	782	28.0586	17.482 R	0.107	0.89	0.047	1.9

Figure 2.1 A sample page from the MACHO Project Variable Star Catalog Retrieval Form.

plane, which were used for the standard photometric calibrations to Johnson's V and R magnitudes.

For the reasons mentioned in Sect. 1.4, I have reclassified all 'eclipsing binary' stars and re-determined their periods.

2.2 Techniques for period searches

Period determination for the downloaded sample consisted of using several different techniques, each with certain advantages and disadvantages. The MACHO observations were made nightly over 8 years. That is a sparse sampling, especially for periods of a few days, so the period determination is not simple. After extensive tests of various methods, I ended up with a two-step process. For the first step, I used the Phase Dispersion Minimization (PDM) method, which gave a reasonably good approximate period. During this process, I visually inspected all the phase diagrams to re-classify the sample, as well as to filter out whether the actual period was an alias or just slightly inaccurate.

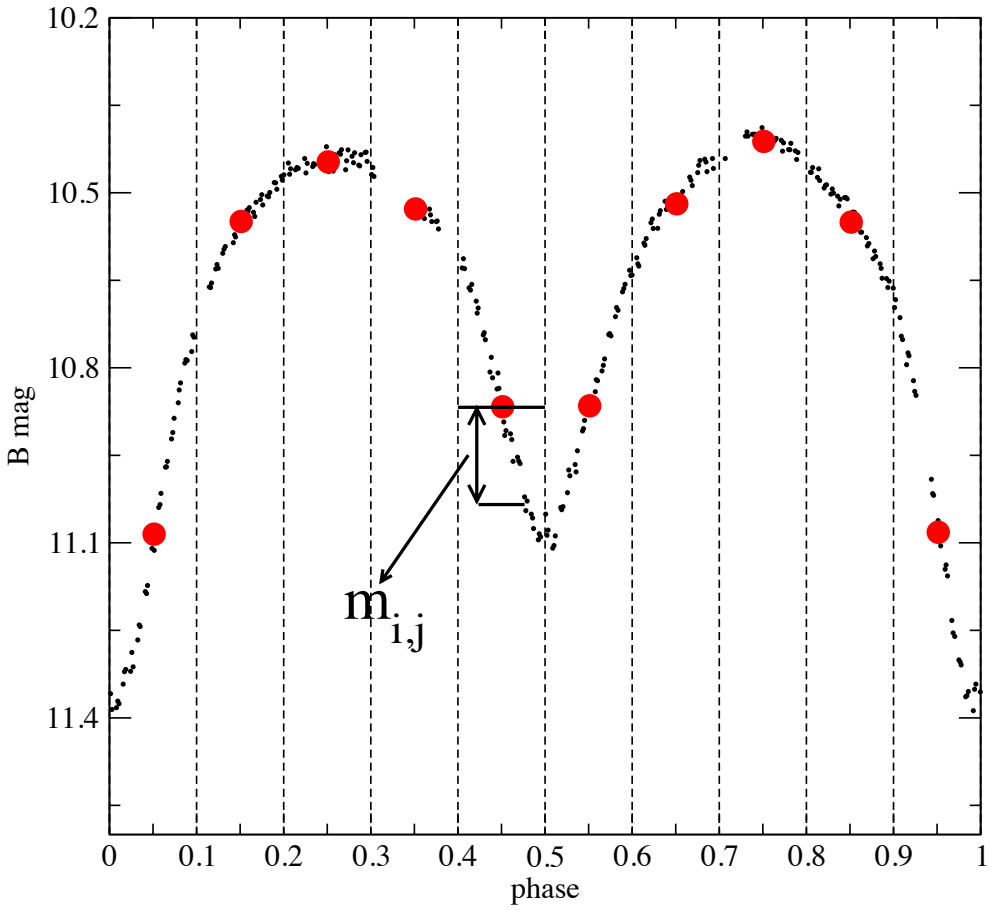

Figure 2.2 A simple illustration of the Phase Dispersion Mimimization method. The dashed lines indicate the boundaries of the bins.

In the case of an alias, I multiplied the PDM period by different constants (in most cases by 2) until the shape of the curve was consistent with that of an eclipsing binary. In the second step, I used the String-Length method to improve period determination. In the following sections, I describe these two methods in detail.

2.2.1 Phase Dispersion Minimization

Phase Dispersion Minimization is a well suited period determination technique in the case of a non-sinusoidal time variation covered by irregularly spaced observations (Stellingwerf, 1978), such as the MACHO observations. The method is based on searching for the period that produces the least possible scatter about the phased light curve. It involves summing the squares of the differences in the ordinate from one data point to

the next (Wolk, 1996). Fig. 2.2 shows a simple sketch to illustrate how PDM works. The dispersion is calculated with the following form:

$$s_j^2 = \sum_{i=1}^{n_j} \left(m_i - \overline{m}_j\right)^2 / \left(n_j - 1\right), \tag{2.1}$$

where m_i is the observed magnitude, $\overline{m}_j = \sum_{i=1}^{n_j} m_i/n_j$ is the mean magnitude. The period resulting in the smallest sum gives the true period:

$$s^2 = \sum_{j=1}^{m} s_j^2 \tag{2.2}$$

An important part of this method is to find the optimal bin size of the phase diagram. If there are too few bins, the method will be insensitive to the steep features of the light curve, such as a very deep minimum of an eclipsing binary. For too many bins, there could be too few points per bin, hence the estimate of s could be less certain. After performing some test calculations, we found that ten bins provided the optimal results.

We calculated 600 000 trial phase diagrams for each star, covering a wide range of periods between 0.085 days and 1000 days (from 0.001 cycles/day to 12 cycles/day, with equidistant steps in frequency). The one producing the least scatter in the phase diagram was accepted as the PDM period.

However, PDM did not always give the true period. In many cases, it gave a harmonic or subharmonic of the true period, which was due to the fact that eclipsing binary light curves quite often contain two very similar but not identical half-cycles. This was corrected by visual inspection of the individual phase diagrams, multiplying the PDM period with a constant. In other cases, PDM was not sensitive enough to sharp variations of the light curve (such as a steep minimum), so the periods needed to be refined slightly. For this I used the String-Length Minimization method, described below.

2.2.2 String-Length Minimization

The String-Length Minimization method or Lafler-Kinman statistic (hereafter L-K statistic) was originally developed to determine periods of RR Lyrae stars from small samples of single-passband observations made by Lafler & Kinman (1965) but the statistic has quite general applications beyond using simple photometry (Clarke, 2002). The L-K

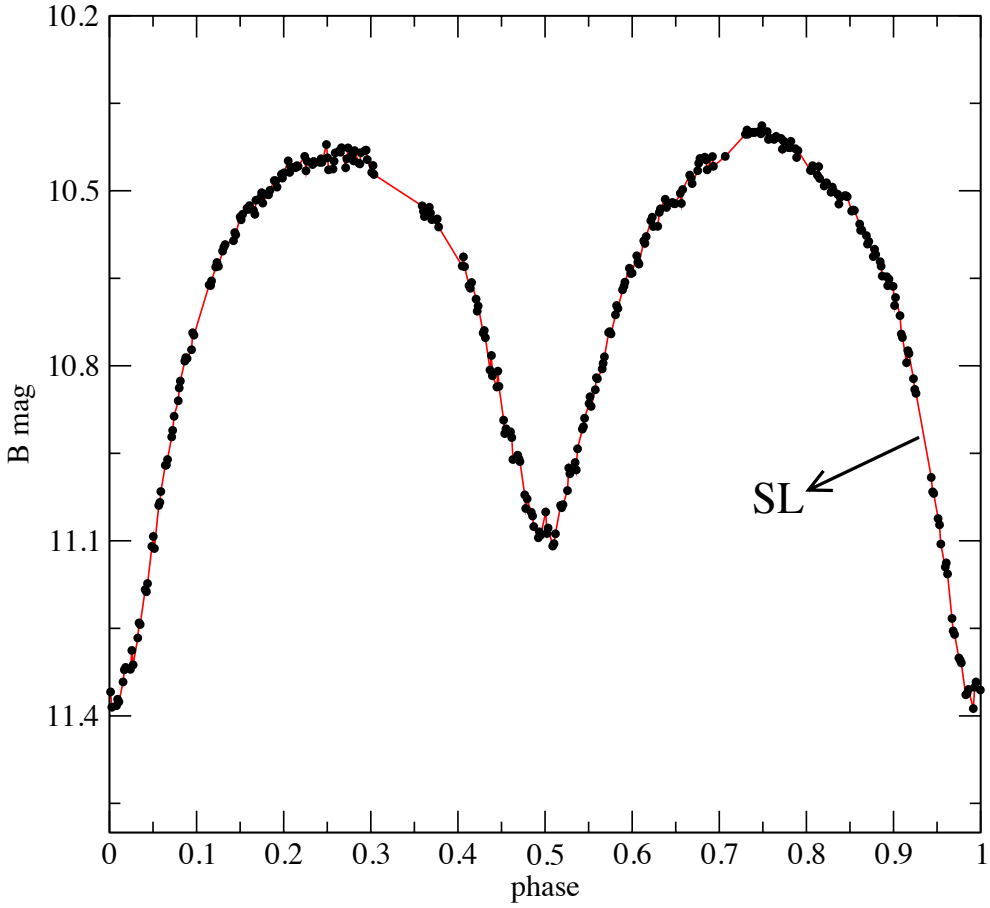

Figure 2.3 A schematic illustration of the String-Length Minimization method.

statistic measures the quality of a light curve for a given trial period by using the sum of the squared differences in magnitude between observations made at adjacent phases (Sandquist & Shetrone, 2003):

$$SL^2 = \sum_{i=1}^{n-1} \left((m_{i+1} - m_i)^2 + (\varphi_{i+1} - \varphi_i)^2 \right), \tag{2.3}$$

where $\{\varphi_i, m_i\}_{i=1}^{n}$ is a folded dataset sorted in phase; φ_i and m_i are the phase and the magnitude of the observations taken at time t_i (so that $\varphi_i = [(t_i - t_0)/P]$, where t_0 was chosen as an epoch of the deeper minimum, P is the period, [ ] is the fractional part). The best period here was the one that minimized SL^2. In our case, we applied the SL method for 1000 periods within $\pm 1\%$ of the best PDM period. The typical period improvements resulted in a change in the 5-6th decimal place, an example is shown in

Fig. 5.1 in Section 5.

For longer datasets (containing at least a few years of observations) the period can be further improved with the classical O–C method. Furthermore, period change may also occur in a number of stars (coming from different reasons, such as evolutionary, instability in the star, or multiplicity) which can also be detected with the O–C method. The next section gives a basic summary of this simple method I have used both for the MACHO stars (Chapters 3 and 10) and ones I observed spectroscopically (Chapter 7).

2.3 The O–C method

For period variations of single-periodic stars, I used the classical O–C method (observed *minus* calculated), which is very effective for detecting tiny period changes. However, the shape of the diagram strongly depends on the period used in the calculation, which may cause problems in the interpretation of the real nature of variation. Therefore, the blind use of the O–C technique has been strongly criticised by Lombard and Koen in their series of papers (e.g. Lombard & Koen (1993); Koen & Lombard (1995); Koen (1995); Lombard (1998)), which underline the importance of the evaluation of the model residuals. For this, they developed various statistical methods by analysing the autocorrelation of the residuals. This is crucial when studying long-period stars (e.g. Mira variables) with relatively large stochastic scatter of the period but in the case of stars presented in this thesis, one does not expect such intrinsic period scatter. For these, gradual evolutionary period changes might be constrained with the O–C technique.

The O–C method can be used in studying monoperiodic stars to achieve very accurate (order of $10^{-6} - 10^{-7}$) period determination/refinement.

Let us assume that we know the following parameters of an observed star:

t_0: the accurate time of a well defined, observed event (such as the maximum or the minimum of a light curve), called *epoch*.

P_0: the known period when the event occurred ($P_0 = t_1 - t_0$: the time between two maxima or minima).

From the observations, one can determine the occurrence of the maximum or minimum brightness, so an observed time (O=observed) is available for us. One can also calculate the occurrence of the maximum or minimum using the epoch and the period by adding the elapsed time (the period (P_0) multiplied with the number of cycles since the known

epoch occurred) to the epoch (C=calculated). We can determine the O–C value of a given time (t_n) of a maximum or minimum brightness with the following equation:

$$O - C = t_n - (t_0 + n\ P_0,) \tag{2.4}$$

where n is the number of cycles. Plotting the O–C difference as a function of time (or cycle number) gives the O–C diagram. The pattern of the diagram can tell whether the assumed parameters were correct. As an example, assume that the period is continuously increasing. Let the period change in every $(t_{i+1} - t_i)$ cycle be $\delta P = P_{i+1} - P_i$. The observed time (t_n) of the maximum or minimum in cycle is:

$$t_n = t_0 + n\ P_0 + \sum_{i=1}^{n} i\ \delta P = t_0 + n\ P_0 + \frac{n\,(n-1)}{2}\delta P \tag{2.5}$$

Let us now calculate the O–C diagram using a T' and P' ephemeris: $t_c = T' + E \cdot P'$, where E is the estimated value of n (cycle number). This is a very important parameter in the calculation of the O–C diagram and can be only given accurately if the period does not change significantly during the gaps of the observations.

Let us assume that $E = n$, $T' \approx T_0$ and $P' \approx P_0$, so the O–C can be calculated as follows:

$$\begin{aligned} O - C = t_n - t_c = t_0 + n\ P_0 + \frac{n\,(n-1)}{2}\delta P - (T' + n\ P') = \\ = t_0 - T' + n\,(P_0 - P') + \frac{n\,(n-1)}{2}\delta P = \\ = \Delta t + n\ \Delta P + \frac{n^2}{2}\delta P - \frac{n}{2}\delta P = \end{aligned}$$

$$= \Delta t + n\left(\Delta P + \frac{\delta P}{2}\right) + n^2\ \frac{\delta P}{2} \tag{2.6}$$

Therefore, if the period is increasing continuously, the O–C diagram turns out to be a parabolic function. Similarly, it can be shown that if the period is continuously decreasing, the second order coefficient of the parabolic function will be negative. Fitting the O–C diagram with a parabolic function, one can give the parameters of the correction: Δt: epoch correction, ΔP: period correction and δP: rate of period change, which is

also designated as β. (Note that δP is also in the first order coefficient but it is negligible compared to ΔP).

If the period is not changing, the O–C is reduced to a straight line. Depending of the correctness of the period used in the calculation, the O–C diagram has different slope. The value of the slope gives the period correction.

The resulting formula of the O–C shows that it is only defined at discrete times. However, the O–C diagram is usually taken as a quasi-continuous function if based on a long time interval. An interesting application of the O–C method is given in the next section.

2.4 Binarity search techniques in pulsating stars

There are various methods to detect binarity of pulsating stars. Both photometry and spectroscopy can be used.

2.4.1 The light-time effect

The O–C diagram can be used to detect binarity or multiplicity through the well-known light travel time effect. If a star is in a binary (or multiple) system, the pulsation period may show cyclic changes which can be detected in the O–C diagram. During one orbit the distance between the star and the observer changes, hence the light coming from the star has to travel different distances at different points in the orbit, so the frequency of the pulsation suffers modulation. This is called the light-time effect (LITE). An example is shown in Fig. 2.4, for a star that I studied in my M.Sc. thesis (Derekas et al., 2003).

Suppose that we have a pulsating star in a binary system. At time t_n, O–C of the pulsations is given by:

$$O - C = \frac{1}{c} \int_{t_0}^{t_n} (v_r - v_0)\, dt, \tag{2.7}$$

where t_0 is a fixed epoch, c is the speed of light, v_r is the radial velocity of the pulsating star and v_0 is the radial velocity of the center of mass. Therefore, the O–C diagram is the integral of the radial velocity curve. From these, the O–C can be expressed as a function of the orbital parameters (Vinkó, 1993):

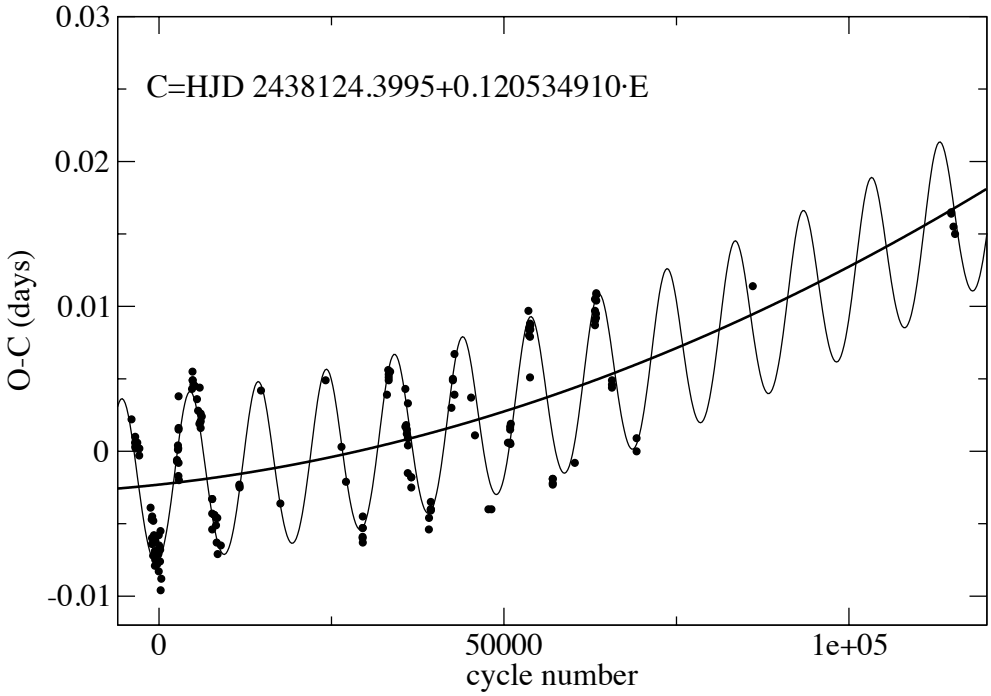

Figure 2.4 An example for the light-time effect: the O–C diagram of SZ Lyn, a high-amplitude δ Scuti star that is in a binary system with orbital period of $\sim$1190 d. The solid line shows a parabolic fit that implies a continuous period increase that may be due to stellar evolution. Figure taken from Derekas et al. (2003).

$$O - C = \frac{a \cdot \sin i}{c} \left(1 - e^2\right) \left[\frac{\sin\left(v_n + \omega\right)}{1 + e \cdot \cos v_n} - \frac{\sin\left(v_0 + \omega\right)}{1 + e \cdot \cos v_0}\right], \tag{2.8}$$

where a is the semi-major axis, i is the inclination, e is the numeric eccentricity, v_i is the mean anomaly and ω is the argument of the periastron.

Considering that the time dependency of the mean anomaly is calculated from the eccentric anomaly and numerical solution of the Kepler equations, we can conclude that there is no analytic formula for the time dependency of the O–C diagram. In practice, O–C diagrams are fitted with Eq. 2.8, from which one can calculate three orbital parameters. As a simple approximation, the amplitude of the O–C variations gives the projected semi-major axis, hence indicating the mass of the invisible companion.

This method is used in Chapter 3 for an RR Lyrae star to analyse cyclic period modulation that might be due to binarity.

2.4.2 Eclipsing binaries with pulsating components

When one or both components of an eclipsing binary system are pulsating star, it is clearly detectable in the light curve: outside the eclipses there are regular brightness changes (with the pulsation period) and/or during the eclipse(s) (depending on the parameters of the system).

In order to analyse the pulsation, one way to proceed is to subtract the eclipsing variation from the light curve. This can be done by applying light curve fit, such as Wilson-Devinney code (Wilson & Devinney, 1971). After this, the classical way of period analysis can be performed. This approach, however, suffers from several drawbacks (e.g. it makes no attempt to deal with changes in eclipse geometry that are caused by the pulsations; the residual observed pulsation wave will have variable amplitude because the pulsational variation is reduced by eclipses) and hence, a coherent analysis of eclipsing variations and pulsation phenomena is highly desirable.

For longer datasets, such as the MACHO data, one has to take into account possible binary period change in the subtraction of the binary solution. This can be determined with the classical O–C method (Section 2.3). In Chapter 10, I show preliminary results of O–C diagrams from the MACHO eclipsing binary database.

2.4.3 Spectroscopic methods for detecting binarity

While photometric methods are not always conclusive about the physical relationship of the companion and the pulsating star, spectroscopic radial velocity data can give the definite proof.

If the spectrum is double-lined, it is a clear indication for the presence of a companion. The radial velocity curves of both components can be measured and the physical parameters of the system can be calculated.

On the other hand, in many cases only the pulsating star can be detected in the spectrum (single-lined spectroscopic binaries), because the companion is much fainter. As the two components are orbiting around the barycentre, the orbital motion can be revealed in the radial velocity shift of the atmospheric pulsation. The size of this velocity shift depends on the physical and orbital parameters of the system (masses, semimajor axis, inclination, etc.). A very nice example for the continuously changing shift in the systemic velocity is shown in Fig. 7.2 and the phased γ-velocities are shown in Fig. 7.4.

Chapter 3

A first-overtone RR Lyrae star with cyclic period changes

This chapter is reproduced from the paper *A first-overtone RR Lyrae star with cyclic period changes* by **A. Derekas**, L. L. Kiss, A. Udalski, T. R. Bedding, K. Szatmáry, 2004, Monthly Notices of the Royal Astronomical Society, 354, 821. Section 3.5 was added later and does not appear in the published paper.

I downloaded and conducted the full analysis of the data. The code I needed for period determination (PDM and string-length) was developed by László Kiss. I took spectroscopic observations, and reduced and analysed them.

Abstract

A detailed light curve analysis is presented for a first-overtone RR Lyrae star, MACHO* J050918.712−695015.31, based on MACHO and OGLE-III observations. As a foreground object of the Large Magellanic Cloud, it gives an extraordinary opportunity to study an almost continuous, 12-year long dataset of a relatively bright ($V \approx 15\overset{\mathrm{m}}{.}0$) RRc star with rapid period change. Cyclic period modulation is suggested by the O–C method, where the cycle length is about 8 years. With the available unique dataset, we could draw strong limits on other light curve changes that may be associated to the period modulation. We could exclude both multiple periodicity and amplitude modulation unambiguously. Any theoretical model should reproduce the observed lack of photometric modulations. Simple arguments are also given for possible

hydromagnetic effects. Spectroscopic follow-up excluded the possibility of the presence of a companion.

3.1 Introduction

Period changes in RR Lyrae stars have been an intriguing issue since the discovery of this phenomenon (Bailey, 1913; Prager, 1939). Numerous studies have been carried out for RR Lyrae stars in globular clusters (e.g. Szeidl, 1975; Wehlau et al., 1992; Rathbun & Smith, 1997; Jurcsik et al., 2001) and in the galactic field (see a collection of field stars in Firmanyuk (1976, 1982) and a recent re-analysis of a particular object by Jurcsik et al. (2002). Stellar evolution is expected to cause very slow continuous changes in period (Lee, 1991; Cox, 1998), but the observations tend to reveal abrupt and/or cyclic changes that are too fast to be explained in this way. The Blazhko effect (Blazhko, 1907), which refers to amplitude modulation in RR Lyrae stars, does not yet have a generally accepted explanation (Chadid et al., 2004) and is also known to be associated with period modulations. To make the overall picture even more complicated, Paparó et al. (1998) found opposite period changes in the modes of two double-mode RR Lyrae stars in M15. A number of theoretical studies have attempted to explain period changes in RR Lyrae stars with various mechanisms, such as mixing events in the semiconvective zone (Sweigart & Renzini, 1979). Good reviews can be found in Rathbun & Smith (1997) and Smith (1995, 1997). Understanding these period variations remain an important unsolved problem in the stellar pulsation theory (Alcock et al., 2000c).

Globular clusters that are rich in RR Lyrae variables offer a good opportunity to study period changes. For example, Rathbun & Smith (1997) studied the period changes of RR Lyrae variables in seven globular clusters by collecting all data in the literature over 50 years. They found that the rates of period changes of fundamental-mode RR Lyrae (RRab) stars are usually larger than those of first-overtone (RRc) and double-mode (RRd) variables. However, they concluded that current theories did not explain the irregular period changes. More recently, Jurcsik et al. (2001) presented an analysis of the RR Lyrae variables of ω Centauri. They studied O–C diagrams of altogether 126 RRab, RRc and RR Lyrae-like stars and found that the period changes of most RRab were in good agreement with the evolutionary model predictions, but those of the first-overtone RRc-type stars showed a much more complex, irregular behaviour (Jurcsik et al., 2001).

Despite the great value of cluster RR Lyrae stars, no one has ever followed a cluster continuously with the same instrument for many years or decades. The essentially random samples over many decades with various instruments do not provide a homogeneous view of the period changes of RR Lyrae variables. The situation changed in the early 1990s, when microlensing projects started monitoring the sky towards the Large and Small Magellanic Cloud and the Galactic Bulge, providing continuous photometric observations of millions of stars during several years. Of these, MACHO and OGLE projects had the best coverage. These data present a great opportunity for investigating period changes of RR Lyrae stars. Alcock et al. (2000c, 2004) analysed MACHO light curves for more than 1000 RRc stars and found that 10% showed strong period changes, whose strength and patterns excluded simple evolutionary explanations. Meanwhile, Soszyński et al. (2003) compiled a more complete catalog of $\sim$ 7600 RR Lyrae stars in the LMC based on the OGLE-II observations. It remains for a future study to combine these two sources of data for examining period changes over a longer time base.

Although a large amount of data is available for the RR Lyrae stars in the Large Magellanic Cloud, there is a major drawback with these stars: they are very faint at the distance of the LMC ($\mathrm{V} \approx 19.0\mathrm{mag}$). Hence, the signal-to-noise ratio (S/N) of the MACHO observations for the LMC RR Lyrae stars is very low (Alcock et al., 2000c) and neither light curve parameters nor their changes can be determined accurately. Although OGLE-II RR Lyrae observations have higher S/N ratio due to better seeing and more advanced photometric reductions technique, they were carried out over a shorter time span and with only a single filter. These problems could be circumvented if we found suitably bright foreground stars in the MACHO and OGLE databases. During an analysis of more than 6000 MACHO variable stars (Derekas et al. in prep.), we noticed MACHO* J050918.712$-$695015.31 (hereafter M0509$-$69), an RR Lyrae star with intriguing period changes. At magnitude $\mathrm{V} \approx 15.0\mathrm{mag}$, period $\mathrm{P} = 0.328\mathrm{d}$ and amplitude $\mathrm{A_{blue}} \approx 0.5\mathrm{mag}$, this star offers a unique opportunity, because of its high S/N ($\sim 80 - 120$ in the MACHO data and $\sim 120 - 130$ in the OGLE-III data) light curve, for analysing the correlation between period changes and light curve shape variations. This is expected to tell us something about the physical mechanism causing the modulations. We note that M0509$-$69 was also included in the study of Alcock et al. (1997b), who discussed 20 foreground RR Lyrae stars towards the LMC and noticed the changing period of this star.

The main aim of this work is to demonstrate the period modulation of M0509$-$69, and show that it is not accompanied by any variations in amplitude or light curve shape.

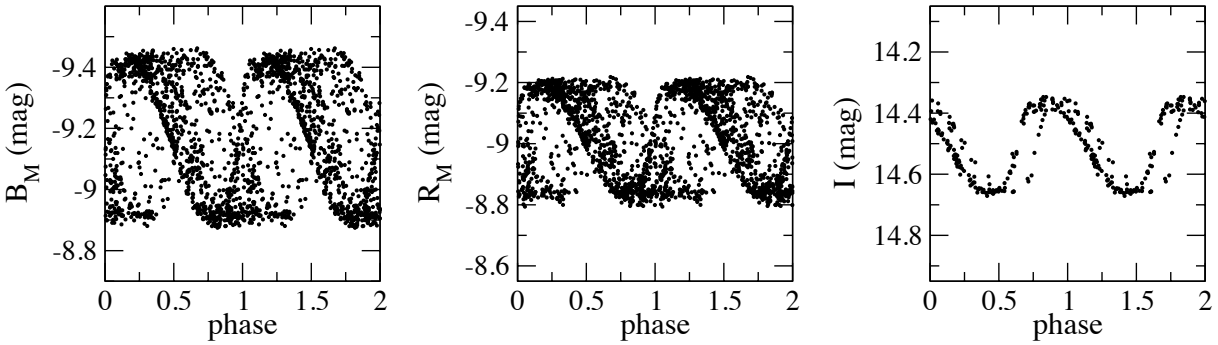

Figure 3.1 The phase diagram for M0509−69 in three colours: MACHO blue, MACHO red and OGLE.

Our study exploits the homogeneity, the continuity and the 12-year long time span of the combined MACHO and OGLE-III CCD observations. In Sect. 3.2 we describe the data and their basic analysis. We show several pieces of evidence for pure period modulation of M0509−69 in Sect. 3.3. Finally, we briefly discuss possible mechanisms in Sect. 3.4.

3.2 Initial data analysis

Our attention was drawn to this star during an on-going study of MACHO variable stars, that are classified as eclipsing binaries in the on-line MACHO Variable Star Catalog. The MACHO observations were obtained between June 1992 and January 2000, with the 50 inch telescope at Mt. Stromlo Observatory using a two-channel system (Hart et al., 1996). Two-colour data in the specifically designed MACHO blue ($B_{\rm M}$) and MACHO red ($R_{\rm M}$) bands are publicly available at the MACHO website[1]. Stars have been classified by an automatic software and we downloaded individually every target, 6835 in total. However, it became obvious very quickly that the classification was not perfect, as large fraction of "eclipsing binaries" was found to be Cepheids, RR Lyrae stars or long-period variables. We therefore decided to re-classify all stars and during this procedure we noted the peculiar light curve of M0509−69. Whereas the period and amplitude unambiguously place this star among the first-overtone RR Lyraes (Poretti, 2001), the light curve showed enormous phase modulations.

In light of the strange behaviour of M0509−69 in the MACHO data, we decided to supplement them with OGLE observations. Unfortunately, this object is located outside

[1] `http://wwwmacho.mcmaster.ca/`

the fields covered during the second phase of the OGLE project (Udalski et al., 1997) so that OGLE-II photometry from 1997–2000 is not available. However, this field was covered in the OGLE-III phase, which started in June 2001, and the star is continuously monitored up to now. Thus the gap between the MACHO and OGLE-III observations is only 621 days. The OGLE observations were obtained with the 1.3 m Warsaw telescope located at Las Campanas Observatory, Chile, which is operated by the Carnegie Institution of Washington, equipped with 8192×8192 pixel mosaic camera. Photometry was derived with the standard OGLE data pipeline based on DIA image subtraction technique (Udalski, 2003). Observations were done through I-band filter.

As the first step of the analysis of M0509−69, we searched for the period using the Phase Dispersion Minimization method (Stellingwerf, 1978), then we refined that period using the String Length method (Lafler & Kinman, 1965; Clarke, 2002). The phase diagram with the finally adopted period (Sect. 3.2) is plotted in Fig. 3.1. Both the phase diagram and random checks of short subsets suggested a strong period modulation, so we therefore determined epochs of maximum light to construct the classical O–C diagram. To this, we divided the whole dataset into 50-day long subsets, which did not show any noticeable phase shift. Then we phased each subset with the period given by the String Length method (0.32806 days). When there were too few points within 50 days, then we used 100-day long subsets. The best of these phase diagrams was fitted with a fourth-order Fourier-polynomial. This polynomial was used as a master curve – allowing both vertical and horizontal shifts to fit every other phase diagram. The same procedure was applied for the OGLE-III data. From the resulting phase shifts, the period and the epochs of each phase diagram, we calculated the times of maximum light, listed in Table 3.1. Typical uncertainties are about 0.001–0.0015 days.

Finally, we note that downloadable MACHO data are in Modified Julian Date, so that we had to add 0.5 days to all epochs of maximum.

3.3 Results

3.3.1 Multiple periodicity

We examined the possibility of multiple periodicity in the MACHO blue-band light curve of M0509−69. We chose this set because of the higher amplitude, thus better S/N. The frequency analysis was carried out by standard Fourier-analysis using Period98 of

Table 3.1 Times of maximum for M0509−69.

$HJD_{\max}$	filter	$HJD_{\max}$	filter
2448885.1603	R_M	2449937.4734	B_M
48885.1712	B_M	50037.2174	B_M
48948.1480	B_M	50039.1748	R_M
48950.1030	R_M	50139.2403	R_M
48997.0187	B_M	50139.2513	B_M
49001.2712	R_M	50241.9485	B_M
49045.2343	B_M	50243.9034	R_M
49050.1431	R_M	50342.3490	B_M
49095.0899	B_M	50349.2265	R_M
49099.9961	R_M	50436.1742	R_M
49146.9115	B_M	50446.3549	B_M
49152.4765	R_M	50543.1468	B_M
49197.4241	B_M	50547.0712	R_M
49200.3659	R_M	50649.4351	R_M
49253.1684	R_M	50653.3818	B_M
49253.1796	B_M	50749.4961	R_M
49292.5371	R_M	50749.5064	B_M
49303.3733	B_M	50850.2163	R_M
49397.1685	R_M	50850.2268	B_M
49397.1801	B_M	50955.2051	B_M
49447.0279	R_M	51034.5776	R_M
49452.2878	B_M	51074.6031	B_M
49497.2208	B_M	51120.1905	R_M
49497.5391	R_M	51181.5408	B_M
49547.4005	R_M	51290.1142	B_M
49551.3507	B_M	51317.9810	R_M
49597.2600	R_M	51394.4042	B_M
49599.2387	B_M	51432.4460	R_M
49648.4325	R_M	51502.3273	B_M
49652.3801	B_M	51516.0922	R_M
49697.3256	B_M	52227.1610	I
49699.2805	R_M	52333.7701	I
49749.1449	R_M	52578.8074	I
49752.1087	B_M	52667.7100	I
49834.1273	B_M	52895.0690	I
49836.0847	R_M	52995.7926	I
49936.4784	R_M		

Sperl (1998). The calculated amplitude spectrum is shown in the top panel of Fig. 3.2. The main peak at $f_0 = 3.048222d^{-1}$ is in very good agreement with the result by the String Length method ($3.048223d^{-1}$). Usual prewhitening steps resulted in the same behaviour as the one found for RR1-PC-type stars by Alcock et al. (2000): the prewhitened frequency spectrum contained significant remnant power very close to the main component. As was shown in Alcock et al. (2000c), this can be attributed to long-term period and/or amplitude change. Since the procedure of determining epochs of maximum proved the stability of the amplitude (i.e. every phase diagram could be fitted very well with the master curve), we checked for the presence of multiple periodicity in two different ways. Firstly, we did regular prewhitening in the best three 50-day long subsets to check the residual frequency spectra for any significant peak unrelated to the pulsational frequency. For that reason, we fitted and subtracted not only f_0, but $2f_0$, $3f_0$ and $4f_0$ from the subsets. None of the residual spectra contained a significant peak other than $5f_0$, after which we could not find anything else.

Secondly, we subtracted individually fitted Fourier-polynomials from every subset in form of

$$m = A_0 + \sum_{i=1}^{4} A_i \cdot \sin\left(2\pi i f t + \phi_i\right), \tag{3.1}$$

where the amplitudes and phases were fitted with Period 98. After subtracting each polynomial, we re-united the residual light curves and calculated the frequency spectrum of the whole set. As expected from the asymmetric shape of the mean light curve, we detected only $5f_0$ and $6f_0$ with amplitudes of $0\overset{\mathrm{m}}{.}0064$ and $0\overset{\mathrm{m}}{.}0045$. After subtracting these two frequencies, the S/N ratios (Breger et al. , 1993) of the next three peaks were about 4, close to the limit of significance. We could identify these frequencies as close remnants of the primary peak and its harmonics or daily aliases. Finally, we arrived at pure white noise (bottom panel in Fig. 3.2), confirming the monoperiodic nature of M0509−69. Similar results were given by the red data too, but their S/N is lower than that of the blue data, which we preferred in our analysis.

3.3.2 The O–C diagram

Having excluded multiple periodicity, the O–C diagram was made from the times of maxima in Table 3.1. Initially, we used the period given by the String Length method, with the following ephemeris: $HJD_{\max} = 2449197.4241 + 0.32806 \times E$. It showed very clear cyclic period changes without colour dependence (i.e. the blue and the red O–C

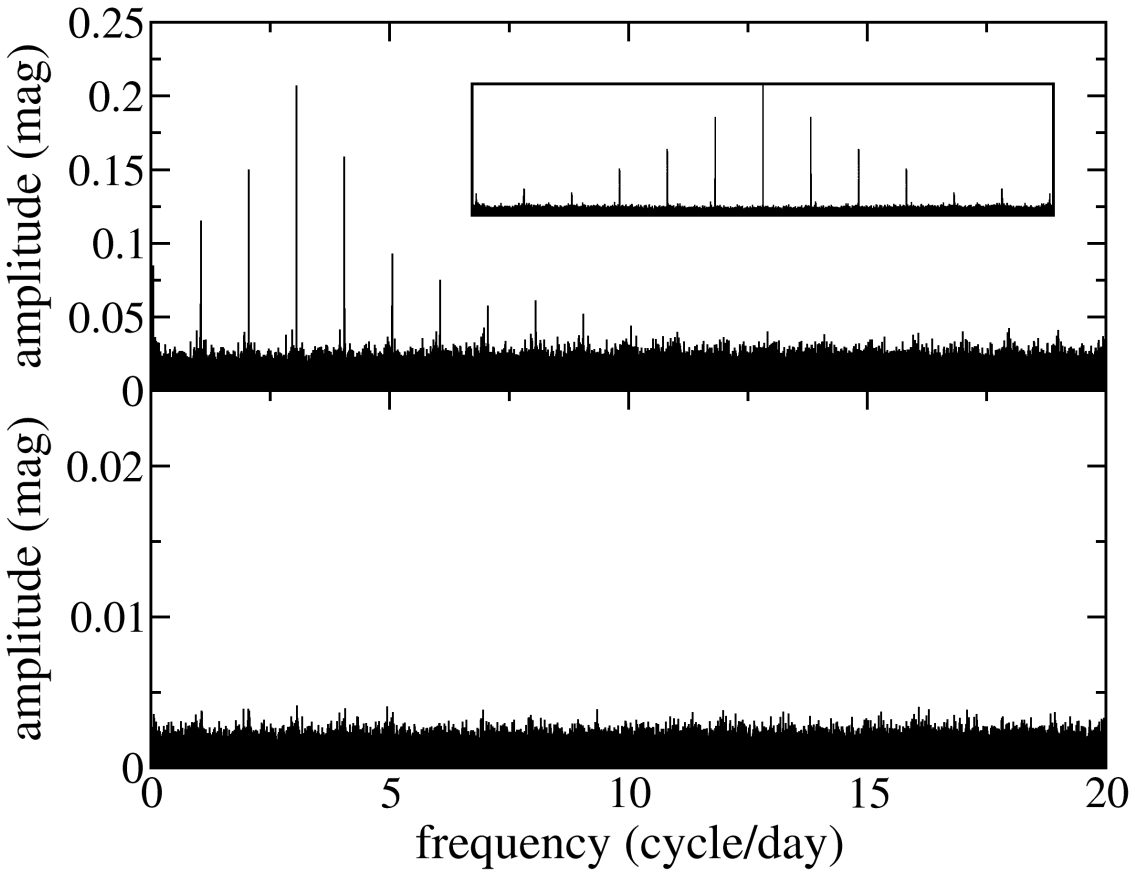

Figure 3.2 The Fourier spectra of the complete blue colour dataset (*top panel*) and the residuals, after removal of the main period, harmonics and aliases (*bottom panel*). The insert shows the window function on same frequency scale.

points drew the same curve).

There is a well-known problem with the O–C method: although it is a very effective tool to detect tiny period changes, the shape of the diagram strongly depends on the period used in the calculation. Moreover, it can be discontinuous after long periods, so that we analysed the O–C diagram using the continuous method suggested by Kalimeris et al. (1994). In this approach, both the period and its rate of change are continuous functions of time. Rather than using various assumptions on period change (e.g. assuming constant change of period and thus fitting parabola to the O–C; or fitting straight lines to selected parts of the O–C), we determined the "instantaneous" periods from every neighbouring pair of subsets, simply as the local derivative of the O–C plot plus the period used in the ephemeris (P_e). The difference between the "instantaneous" period and P_e is plotted in the bottom panel of Fig. 3.3. As can be seen here, the period change

is enormous: the difference between the longest and the shortest period is about 12 seconds; in other words, the relative period change is $\pm 2 \cdot 10^{-4}$!

The use of the "instantaneous" period has a further advantage: this way we can combine MACHO and OGLE-III data without involving systematic phase shift between the $B_{\rm M}$ and I bands. We checked several foreground RR Lyraes with simultaneous MACHO and OGLE-II observations (Zebrun et al., 2001) and found that I-band maxima are usually within $0.01-0.03$ in phase relative to $B_{\rm M}$-band maxima. With the "instantaneous" period, even this small effect is eliminated.

Finally, we corrected the period by assuming that the time-span of the combined MACHO+OGLE-III data is long enough to average out the period modulation. In other words, we searched for that period which resulted in zero mean period difference in the bottom panel of Fig. 3.3. The resulting ephemeris is the following:

$$HJD_{\rm max} = 2449196.9241 + 0.328038(2) \times E, \tag{3.2}$$

and the finally adopted O–C diagram in the top panel of Fig. 3.3 was also calculated with this ephemeris.

3.3.3 Amplitude modulation

Some RR Lyrae stars show cycle-to-cycle changes in the shape of their light curves, which can be caused either by double-mode pulsation (in RRd stars) or the still-puzzling Blazhko-effect. Since double-mode pulsation was ruled out in Sect. 3.1, what remains to be checked is the possibility of amplitude modulation.

Although the master curve fitted very well all subsets, we wanted to examine quantitatively the possibility of light curve shape change. Therefore, we fitted fourth-order Fourier-polynomials to each subset using equation (3.1) at the primary frequency and its harmonics. Then we measured the light curve shapes with the Fourier parameters (Simon & Teays, 1982), of which we show particular results for $R_{21} = A_2/A_1$ and $R_{31} = A_3/A_1$ (these are the most accurate parameters). Fig. 3.4 shows the relative variations of R_{21} and R_{31}. The error bars are quite large (because the light curve is not too asymmetric, so that higher harmonics are fairly weak), but it is evident that there were no measurable shape changes.

Since individual subsets rarely contained enough data points for determining accu-

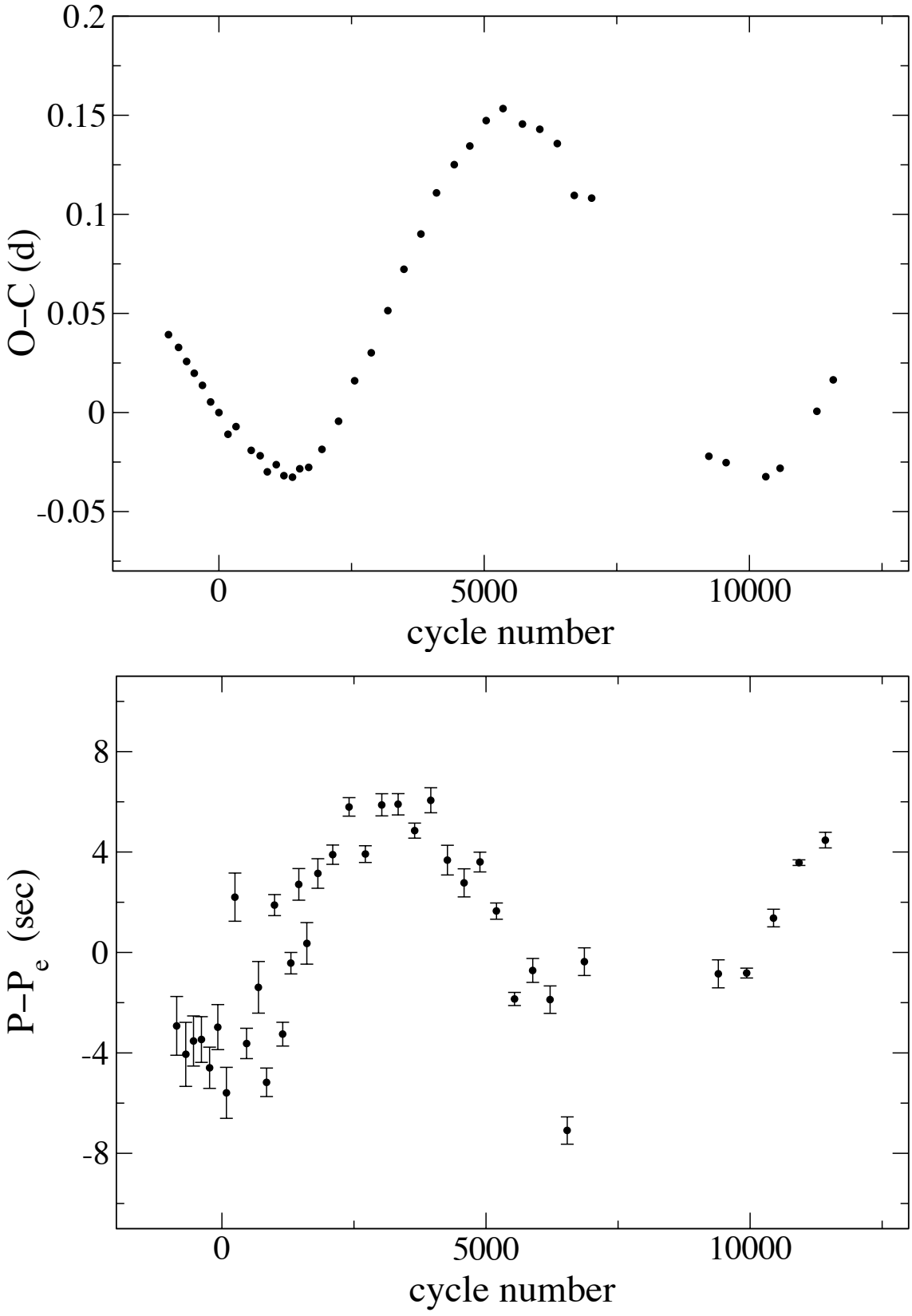

Figure 3.3 *Top panel*: the O–C diagram of M0509−69 from $B_{\rm M}$ and I data. *Bottom panel*: the "instantaneous" period. The error bars are the 3σ errors of the fits.

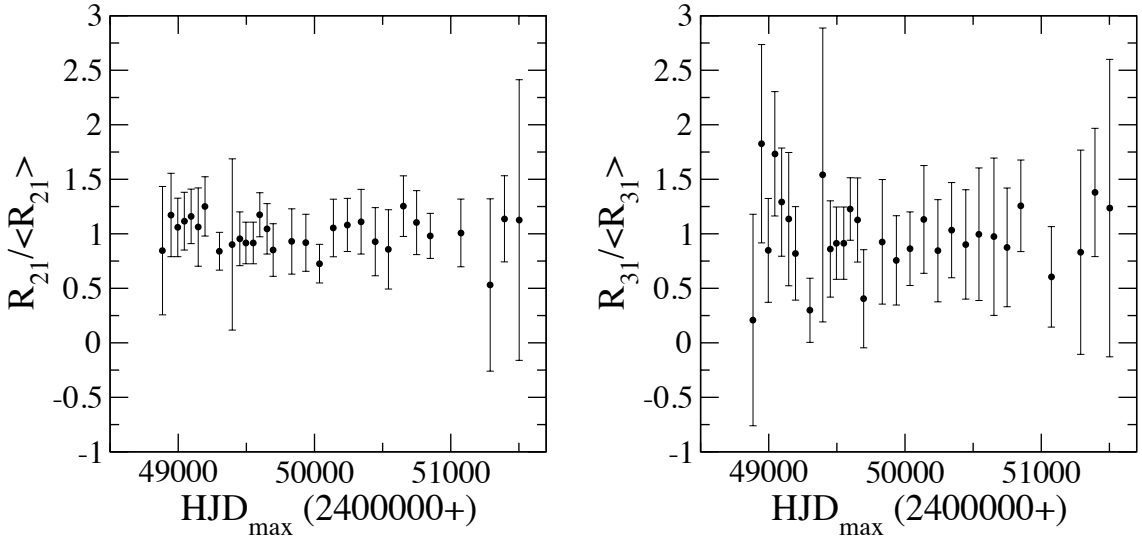

Figure 3.4 The relative variations of R_{21} and R_{31}.

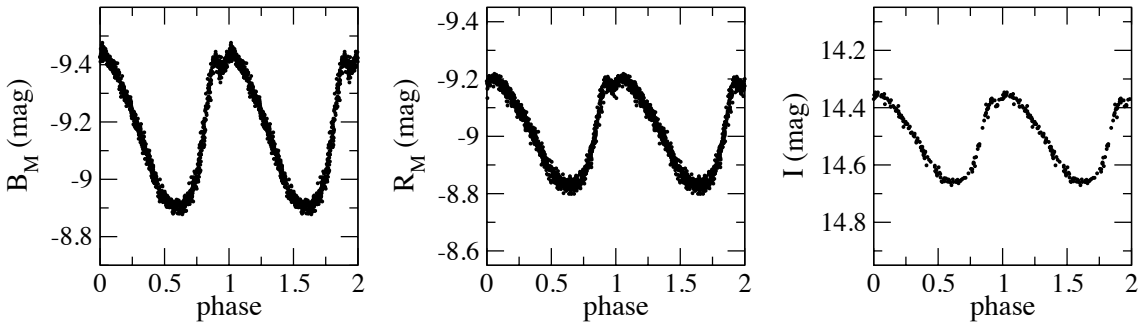

Figure 3.5 The phase diagrams after eliminating the phase shifts between all subsets.

rate Fourier-parameters, we also examined the correlation between the period change and the light curve shape using five subsets around the minimum and five around maximum of the "instantaneous" period. Then we corrected these phase diagrams for any phase shifts to form high-quality, continuous phase diagrams representing the two extrema of the period. Then we fitted sixth-order Fourier polynomials to both phase diagrams and the resulting parameters are shown in Table 3.2. As can be seen, none of the Fourier-coefficients differs significantly for the two cases. This means that we could not detect any light curve change associated with the period variation. This conclusion is also supported by the phase diagram of the whole MACHO and OGLE-III datasets (Fig. 3.5), where we shifted every subset to match the master curve in phase. The well-defined shapes show no evidence for any additional variation in light curve shape.

Table 3.2 The coefficients of the sixth-order Fourier polynomials around the minimum and the maximum of the period.

parameter	values at $P_{\min}$	values at $P_{\max}$
a_0	–9.165 ± 0.003	–9.168 ± 0.001
a_1	–0.278 ± 0.005	–0.270 ± 0.005
a_2	–0.046 ± 0.004	–0.044 ± 0.005
a_3	0.023 ± 0.005	0.022 ± 0.005
a_4	0.024 ± 0.004	0.016 ± 0.005
a_5	–0.017 ± 0.005	–0.010 ± 0.005
a_6	–0.015 ± 0.004	–0.008 ± 0.005
ϕ_1	1.249 ± 0.016	1.251 ± 0.018
ϕ_2	–3.780 ± 0.104	–3.639 ± 0.112
ϕ_3	0.602 ± 0.182	0.492 ± 0.228
ϕ_4	2.007 ± 0.199	2.303 ± 0.312
ϕ_5	–0.181 ± 0.256	–0.313 ± 0.476
ϕ_6	0.332 ± 0.324	0.155 ± 0.580

3.4 Discussion

It is obvious from Fig. 3.3 that the period change seems to be cyclic, which implies there must be some (quasi)periodic mechanism affecting the pulsation. The shape of the curve in the bottom panel of Fig. 3.3 is largely independent of the period used for the O–C diagram (provided that it is close to the real mean period), so that the observed change cannot be explained by some numerical artifact caused by a wrong period in the ephemeris.

As a first possibility, we consider light-time effect (LITE) due to orbital motion in a binary system. Although it was suggested for several RR Lyrae stars that their cyclic O–C diagrams were caused by LITE, so far this was supported by spectroscopic observations only for TU UMa (Wade et al., 1999). For M0509−69, the half-amplitude of the O–C in Fig. 3.3 is A(O−C)=0.09 d, while the time separation of the two minimum is 2900 d. Assuming that $A(O-C) = \frac{a \sin i}{c}$, the estimated semi-major axis is about $15.5/\sin i$ AU. Given $P_{\rm orb}$=2900 d ≈ 7.95 yr; the minimum mass of the system would be almost $60 M_{\odot}$.

Although there are models that predict the existence of detached black hole binaries with $M_{BH} = 10 - 20$ M$_{\odot}$ and $M_{sec} = 0.3 - 1$ M$_{\odot}$ (see, e.g., Table 1 in Podsiadlowski et al., 2003), the secondary components in these theoretical systems are not expected

to follow the evolution of "normal" stars with the same masses. This is because they are descendants of more massive progenitor stars that transferred most of their masses to the black hole primaries (but models also predict that they can evolve through the classical instability strip, even becoming "RR Lyrae-like" variables). In principle, we cannot exclude this possibility until it is checked by spectroscopy (any sign of orbital motion should be relatively easily detectable spectroscopically even at $V = 15$ mag), although $60 M_{\odot}$ seems extraordinary large. Also, the high occurrence rate of strong period changes in RR Lyrae stars argues against this exotic explanation.

Stellar evolution can be safely excluded, since both the strength and the cyclic nature of the period change exceed theoretical expectations by orders of magnitudes (Smith, 1995).

Another interesting possibility is related to hypothetic hydromagnetism. Stothers (1980) argued that RR Lyrae stars may be considered as fair analogues of the Sun. He proposed that radius changes may be driven by some sort of magnetic activity, which in turn would cause observable period changes. The correlation between the frequency changes and the magnetic variations was confirmed by Howe et al. (2002), who performed a detailed study on the solar cycle frequency shifts in global p-modes of the Sun. They found that the latitudinal distributions of the frequency shifts shows close temporal and spatial correlation with the unsigned surface magnetic flux.

In our case we can calculate the radius change of M0509−69 from the period-density relation, i.e. $P\sqrt{\rho} = \mathrm{Q}$. Substituting the values determined from the bottom panel in Fig. 3.3, it follows:

$$\frac{\Delta R}{R} = \frac{2}{3} \cdot \frac{\Delta P}{P} \approx \frac{2}{3} \cdot \frac{6}{28342} \approx 1.4 \cdot 10^{-4}. \tag{3.3}$$

Note that this equation is an approximation that omits a term that contains the magnetic energy (see Stothers, 1980).

Very recently, Noël (2004) presented an analysis of 13 years of apparent radius measurements of the Sun. Interestingly, he found a correlation between the solar radius variation and the sunspot numbers, related to the solar magnetic activity. Based on the data in his fig. 5, the relative change of the solar radius was about $\Delta R/R \approx 4 \cdot 10^{-4}$. Assuming that RR Lyrae stars can show solar-like magnetic activity cycles, these two similar relative radius changes seem to support the hypothetic hydromagnetic period change.

We know little about the presence of magnetic fields in RR Lyrae stars. Most re-

cently, Chadid et al. (2004) presented high-precision longitudinal magnetic field measurements of RR Lyrae itself taken over 4 years. Their results provided no evidence for a strong magnetic field in the photosphere of this star, which was often postulated in various explanations for the Blazhko effect (see, e.g. Jurcsik et al., 2002). If the period change in M0509–69 is indeed caused by solar-type magnetic activity, this field might be quite difficult to detect observationally. In fact, the only Blazhko-related phenomena that have been detected so far seem to be small line-profile variations (possibly related to non-linear pulsations; Chadid et al., 1999; Chadid, 2000) and even these are only detectable with high S/N high-resolution spectra.

Although the effects of hydromagnetism on pulsating stars are not well understood, we conclude that the Stothers-mechanism can perhaps explain the pure period modulation of M0509−69. However, new theoretical investigations are necessary to interpret this observed behaviour. Detailed models should also address the absence of any light curve shape change and multiple periodicity.

3.5 Spectroscopic follow-up

After publishing the analysis of the combined MACHO and OGLE data, I decided to test the presented binary hypothesis with radial velocity measurements. Here I summarise the results of the spectroscopic follow-up.

As discussed in Section 3.4, one explanation for the large period modulation can be the orbital motion in a binary system. The parameters of the O–C diagram implied a minimum mass of the system as $60\ M_{\odot}$, implying a black hole as the companion. Only spectroscopic measurements can confirm or exclude unambiguously the existence of such a companion, hence we obtained spectroscopic observations. If the RR Lyrae were orbiting a $60\ M_{\odot}$ black hole, the expected velocity change would be about 60 km s^{-1} over one orbit.

I took data with the 2.3 m telescope at Siding Spring Observatory, Australia in December 2004 and 2005, on 6 nights in total. The spectra were reduced with standard tasks of IRAF, described in Chapter 6. The radial velocities were determined with the task *fxcor*, applying cross-correlation method using a well-matched theoretical template spectrum chosen from Munari et al. (2005). The velocities were measured from the 50 Å region centered on the Hα line. The resulting radial velocity curve is shown in

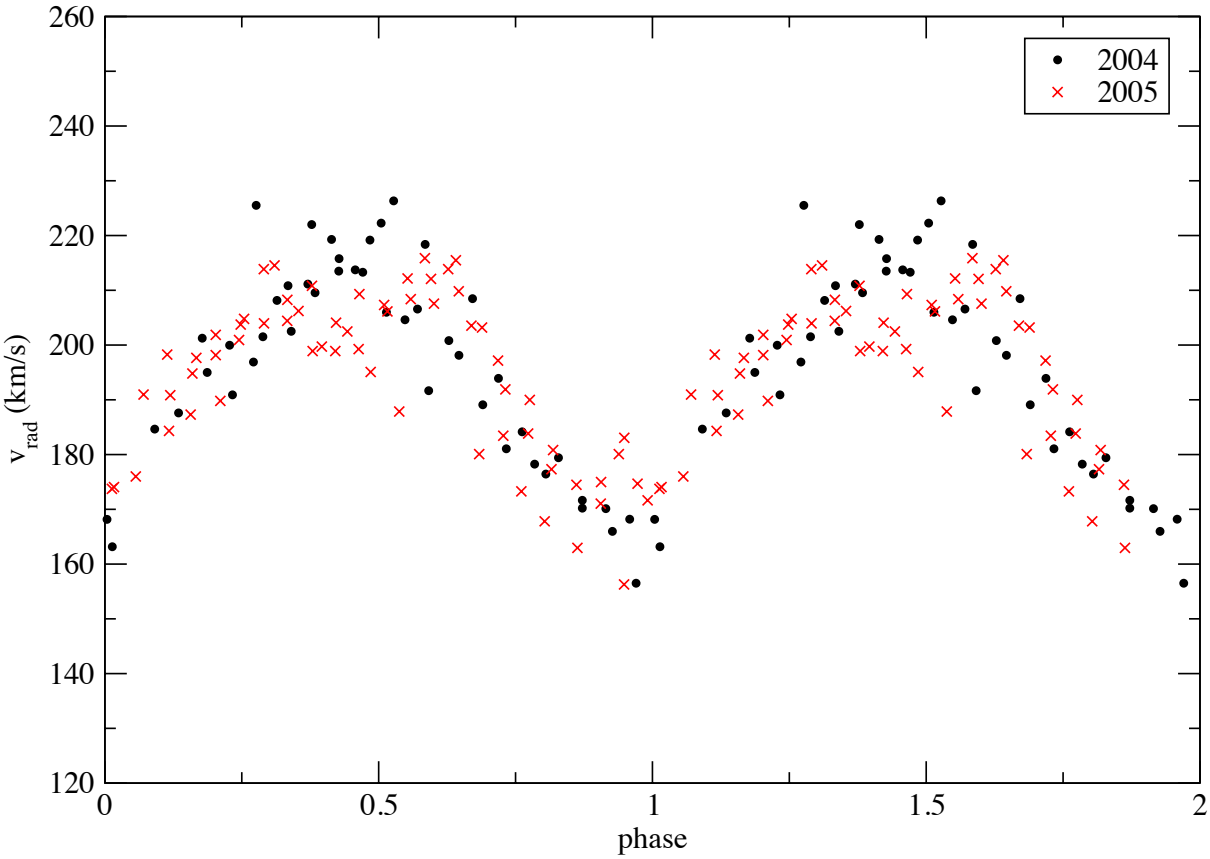

Figure 3.6 The phase diagram of the radial velocity measurements obtained in 2004 (black dots) and 2005 (red crosses). The latter data have been shifted by ∼0.1 in phase for the best match, indicating significant period change over one year.

Fig. 3.6.

The mean velocity is ∼190 km s^{-1} which is consistent with a high-velocity halo star (the LMC is at about +300km s^{-1}, so that the foreground status of the star, in addition to being ∼4 mag brighter than the LMC RR Lyraes, is confirmed kinematically).

The full amplitude of the radial velocity curve is ∼55 km s^{-1}. The data obtained in two different years (black dots in 2004, red crosses in 2005) do not show any shift in radial velocity and overlap very well, suggesting no evidence for orbital motion. Moreover, the data indicated a phase shift of about 0.1 between 2004 and 2005, showing that the period change continued at a similar rate as before. Fig 3.7 shows the O–C diagram as a function of time (HJD) adding the points where our spectra were taken (at HJD=245367 and HJD=53721, dashed lines). The O–C takes very different values at the time of the two observations, meaning that if the binary hypothesis were correct, the

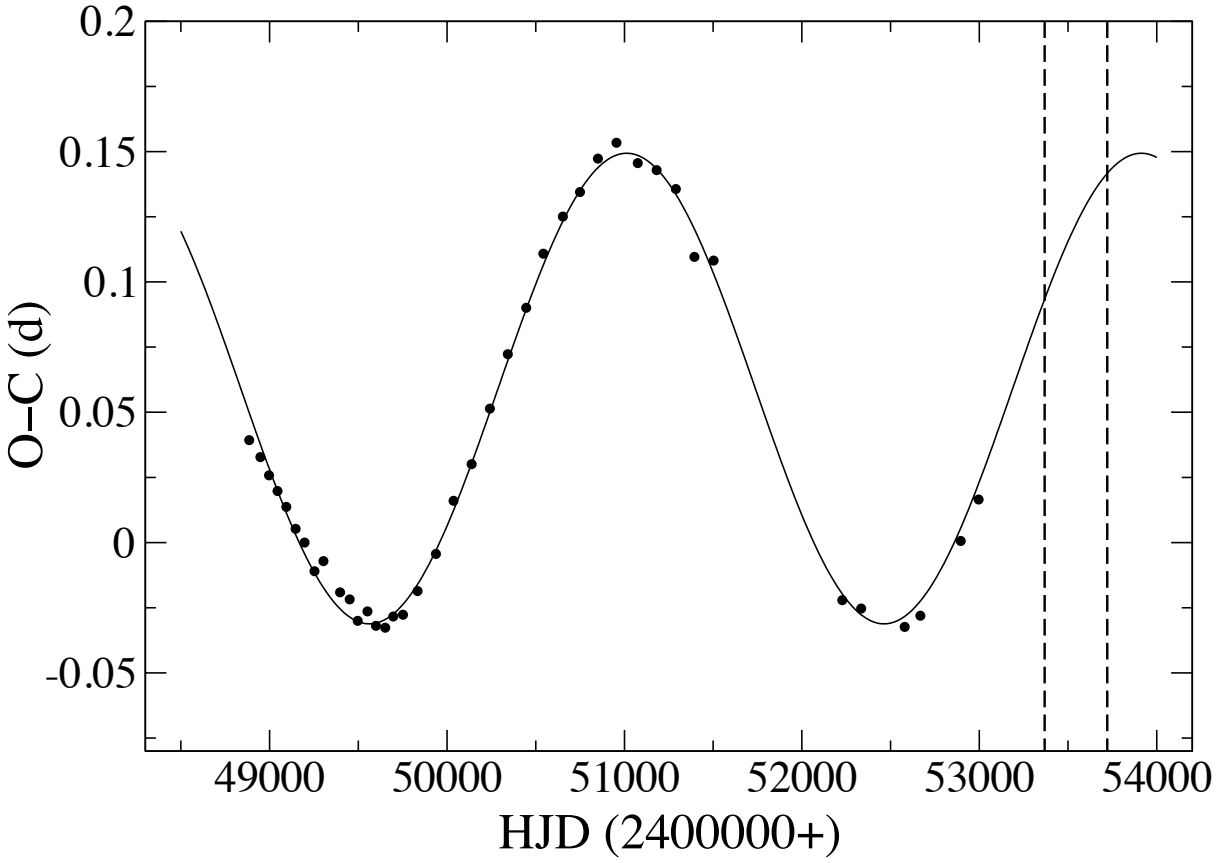

Figure 3.7 The O–C diagram as a function of time. The two vertical dashed line show the time when the spectra were taken.

components should have moved physically which should have been detected in the radial velocity data. The lack of change in γ-velocity exclude the exotic black hole binary hypothesis undoubtly. In other words, radial velocity data imply that the cyclic period change is intrinsic to the star and is not caused by external factors such as light-time effect. The Stothers (2006) theory seems to be a good explanation, a conclusion that is supported by recent results on Blazhko-type RR Lyraes (Jurcsik et al., 2008, 2009).

Chapter 4

Ellipsoidal Variability and Long Secondary Periods in MACHO Red Giant Stars

This chapter is reproduced from the paper *Ellipsoidal Variability and Long Secondary Periods in MACHO Red Giant Stars* by **A. Derekas**, L. L. Kiss, T. R. Bedding, H. Kjeldsen, P. Lah, Gy. M. Szabó, 2006, Astrophysical Journal, 650, L55

I downloaded and conducted the analysis of the data. The code I used for period determination (PDM and string-length) was developed by László Kiss. The periods and 2MASS K-magnitudes for pulsating red giants P–L relations were kindly provided by László Kiss and Phillip Lah. The multivariate ϵ-test was performed by Gyula Szabó.

Abstract

We present a period-luminosity-amplitude analysis of 5899 red giant and binary stars in the Large Magellanic Cloud, using publicly available observations of the MACHO project. For each star, we determined new periods, which were double-checked in order to exclude aliases and false periods. The period-luminosity relations confirm the existence of a short-period, small-amplitude P–L sequence at periods shortward of Seq. A. We point out that the widely accepted sequence of eclipsing binaries between Seqs. C and D, known as Seq. E, does not exist. The correct position for Seq. E is at periods a factor of two greater, and the few stars genuinely lying between Seq. C and D are under-luminous Mira variables, presumably enshrouded in dust.

The true Seq. E overlaps with the sequence of Long Secondary Periods (Seq. D) and their P–L relation is well described by a simple model assuming Roche geometry. The amplitudes of LSPs have properties that are different from both the pulsations and the ellipsoidal variations, but they are more similar to the former than the latter, arguing for pulsation rather than binarity as the origin of the LSP phenomenon.

4.1 Introduction

The multiplicity of red giant period-luminosity (P–L) relations has been a major discovery on the road to interpreting complex light variations of these stars. Following the two seminal papers by Wood et al. (1999) and Wood (2000), a picture has emerged that can be summarised as follows: large-amplitude Mira stars pulsate in the fundamental mode, whereas smaller-amplitude semiregulars are often multimode pulsators, in which various overtone modes can be excited (see also Bedding & Zijlstra, 1998). Besides the pulsating P–L sequences (Seq. A, B and C, as labeled by Wood et al. (1999)), two other sequences were suggested: Seq. E with red giants in eclipsing binaries and Seq. D with stars that have long secondary periods (LSPs). The latter pose a great mystery and the nature of their slow variations is still not understood, with several different mechanisms proposed (Olivier & Wood, 2003; Wood et al., 2004).

The basic picture of multiple P–L relations has been confirmed by many independent studies, mostly based on K-band magnitudes. It has emerged that the original five sequences have further details, including a break at the tip of the Red Giant Branch (RGB), which is due to the existence of distinct RGB pulsators that are mixed with the more evolved AGB variables (e.g. Ita et al., 2002; Kiss & Bedding, 2003, 2004; Ita et al., 2004a,b; Soszyński et al., 2004a; Fraser et al., 2005). Almost all authors have accepted the existence of the distinct sequences of red giant binaries (Seq. E) and LSP stars (Seq. D). The only exception was Soszyński et al. (2004b), who showed that Seqs. E and D seem to merge at a specific luminosity (as measured by the Wesenheit index) and suggested that this may imply the binary origin of LSPs.

Here we report on a combined analysis of MACHO observations of eclipsing binaries and red giants in the Large Magellanic Cloud, which shed new light on these stars and on the LSP phenomenon.

4.2 Data analysis and results

Our results are based on two sets of publicly available almost eight-year long MACHO light curves. A detailed description of the MACHO project can be found in Cook et al. (1995). Some of the data are offered for download through the MACHO website[1], where one can choose specific samples based on an automated classification of variability type. Using the Web interface, we individually downloaded all light curves classified as eclipsing binaries (6833 stars) and as red giant variables (classified as Wood A, B, C and D classes; 2868 stars).

Chapter 2 describes the methods of analysis in details. Periods were first estimated using the Phase Dispersion Minimization method (Stellingwerf, 1978). We then checked all the folded light curves by eye and refined the periods with the String–Length method (Lafler & Kinman, 1965; Clarke, 2002), which is more reliable than PDM when the light curve contains long flat sections and very narrow minima, as is the case for many eclipsing binaries. Also, in many cases PDM gave harmonics or subharmonics of the true period, which was only recognized through the visual inspection of every phase diagram. We also examined the colour variations to identify and exclude pulsating stars with sinusoidal light curves. After this analysis, 3031 stars remained as genuine eclipsing or ellipsoidal variables.

Next, we classified the binary sample using Fourier decomposition of their phase diagrams. Rucinski (1993) showed that light curves of W UMa systems (contact binaries) can be quantitatively described using only two coefficients, a_2 and a_4, of the cosine decomposition $\sum \mathrm{a_i} \cos(2\pi \mathrm{i}\varphi)$. Pojmański (2002) tested the behaviour of semi-detached and detached systems in the $\mathrm{a}_2 - \mathrm{a}_4$ plane by decomposing theoretical light curves into Fourier coefficients. We found that only stars with "W UMa-like" light curve shape composed the sequence (which is plotted in Fig. 4.1), while detached and semi-detached systems are spread everywhere in the P–L plane.

Our second set of light curves were those of the 2868 publicly available MACHO red giant variables. Since they often show multiply periodic light variations, we determined periods with iterative sine wave fitting. As a measure of significance, we also estimated the S/N ratio of the peaks in the Fourier spectra. Since the noise in the Fourier spectrum increased toward lower frequencies, different values of the S/N were used when determining whether a peak was real for different period-luminosity relations (S/N cutoff

[1] http://wwwmacho.mcmaster.ca

was set to 3 for Seq. A′, 4 for Seq. A, 6 for Seqs. B, C and 10 for Seq. D). We omitted periods close to 1 yr, because many light curves show variations with this period that are not real. As a result, a total of 4315 significant frequencies were identified for the 2868 stars.

We studied these two samples in the P–L plane. In order to reduce the effects of interstellar extinction and allow a direct comparison with previous results in the literature, we plotted the period–K magnitude relation. We obtained near infrared magnitudes by cross-correlation with the 2MASS All-Sky Point Source Catalog[2], with a search radius of 3″. The resulting P–L diagram is shown in the top panel of Fig. 4.1.

To our surprise, the P–L relation of the binary sample did not follow Seq. E, as we had expected. Instead, they overlapped with Seq. D, which at first sight appears to give strong evidence for the binary origin of Seq. D and prompted us to investigate the issue in more detail.

4.3 Discussion

The combined P–L plot in Fig. 4.1 shows the well-known complex structure of distinct sequences. Besides sequences A, B, C, D and E, we also detect the existence of the faintly visible new short-period P–L sequence (Seq. A′) on the left-hand side boundary of the diagram (labeled as a_4 and b_4 in Soszyński et al. (2004a) and P_4 in Kiss & Lah (2006)). The eclipsing stars (pluses) seem to merge with Seq. D rather than forming Seq. E as adopted in the literature (Wood et al., 1999; Wood, 2000; Kiss & Bedding, 2003, 2004; Ita et al., 2004a,b; Noda et al., 2004; Fraser et al., 2005).

To clarify this issue, we re-checked periods for: (i) stars on Seq. E in Fig. 1 of Wood (2000), for which the identifiers and basic data were kindly provided by Peter Wood; (ii) stars on Seq. E in our Fig. 4.1 (black dots). In both cases, it turned out that for most of the objects, the given periods were half of the true ones, as one might expect from a Fourier analysis of eclipsing binary light curves. We have carefully double-checked all individual light curves on Seq. E and D and corrected the periods (see Fig. 4.2). The final P–L plot is shown in the bottom panel of Fig. 4.1.

As a result of the period correction, the sequence between C and D, which is known as Seq. E in the literature, has completely disappeared. A few stars remain in the gap

[2]http://irsa.ipac.caltech.edu

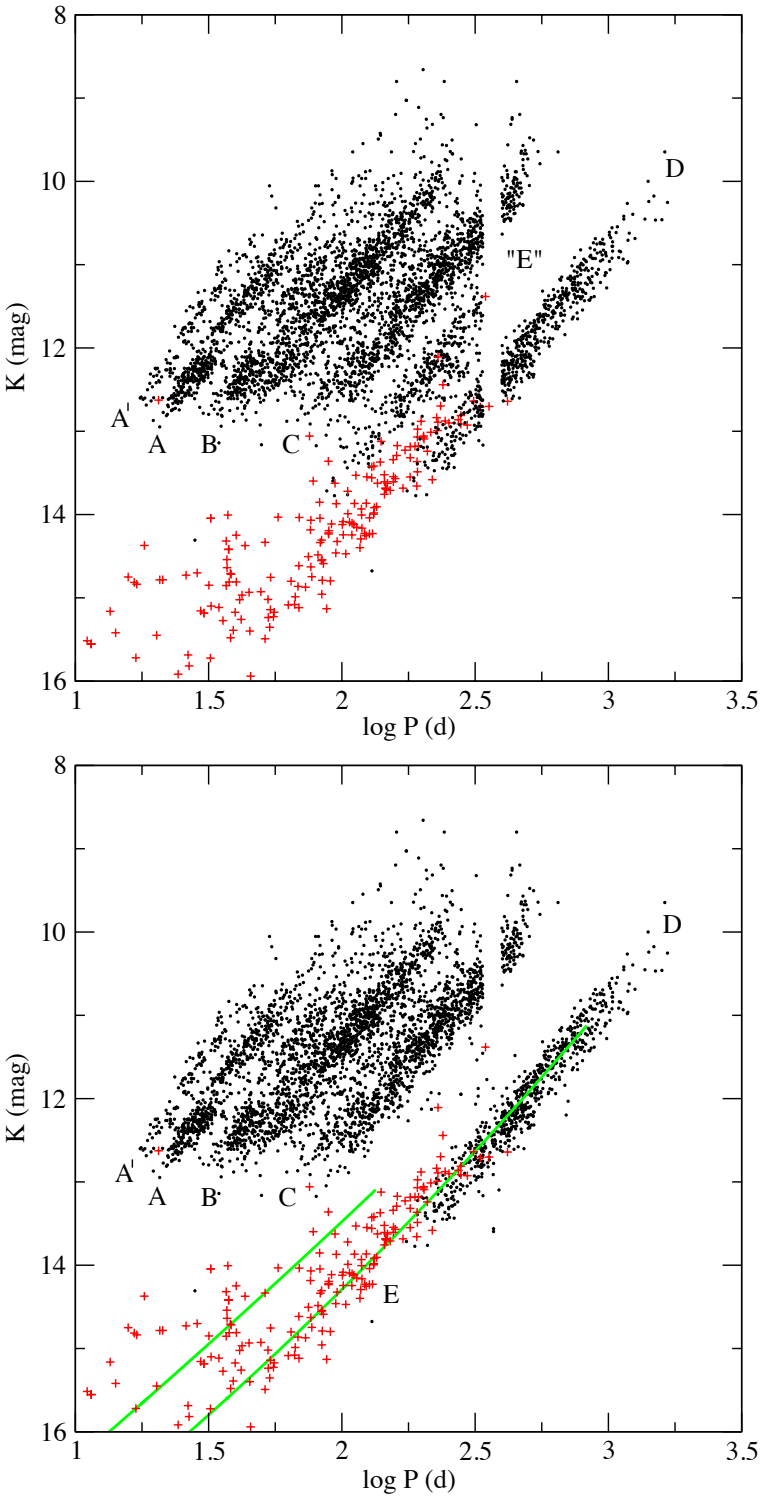

Figure 4.1 Period-Luminosity relations for red giant pulsators (black dots) before (top panel) and after (bottom panel) period correction of stars on Seq. E; 310 ellipsoidal and contact eclipsing binaries (red pluses) are shown with the correct periods in both plots. The solid lines in the bottom panel show model calculations using evolutionary tracks and assuming Roche-geometry (see text).

but practically none of them are eclipsing binaries. The majority turn out to be Mira stars that are very red ($J - K > 2$ mag) and are presumably carbon-rich Miras that are dimmed by circumstellar dust clouds (bottom panel of Fig. 4.2). We propose to retain the label E for the sequence of ellipsoidal variables in its corrected position (bottom panel of Fig. 4.1).

In the literature, only Soszyński et al. (2004b) plotted the eclipsing binary sequence at the correct (doubled) period. However, they did not discuss this issue and one can still find more recent studies where Seq. E was shown at the wrong period. Soszyński et al. (2004b) have, however, shown that Roche geometry gives a good fit to the OGLE ellipsoidal variables. We have also checked this on the MACHO sample. We calculated the theoretical orbital periods of systems at mass ratios of 1, where the components fill their Roche lobes. For this, we used evolutionary models of Castellani et al. (2003) and applied equations of Section 4 in Soszyński et al. (2004b). (Note, however, that the definition of $f(q)$ in their Eq. 1 actually gave $f(q)^{-1}$ as the filling factor.) For the calculations we took the evolutionary tracks of the 0.85 $\mathrm{M}_{\odot}$ and 2.5 $\mathrm{M}_{\odot}$ models, since theses masses represent the mass limits of stars that evolve through the RGB and AGB. The K magnitudes of the models were determined from $T_{\rm eff}$ vs. $(V - K)$ calibrations, combined from Houdashelt et al. (2000) and Kučinskas et al. (2006).

In the bottom panel of Fig. 4.1 we show these two limits (the shorter period line belongs to the higher mass). For any other mass ratios, the orbital periods shift towards smaller values. This simple approach with Roche geometry describes remarkably well the observed period-luminosity relation of ellipsoidal variables in the MACHO sample, in agreement with the study of Soszyński et al. (2004b). However, the OGLE sample contains a larger fraction of ellipsoidals and most of them have longer periods than are predicted by the models. Those stars do not entirely fill the Roche lobe (Soszyński et al., 2004b). It is also worth mentioning that the low fraction of ellipsoidal/eclipsing RGB stars in the MACHO data (1.5%) was used by Wood et al. (2004) as an argument against the binary origin of LSPs. However, the OGLE statistics clearly showed that there are at least 10 times more such RGB stars, and so that argument is no longer valid.

Since the lower mass model fits Seq. D quite well, the question arises: how similar are the ellipsoidal and LSP variables? To assess this, we examined the amplitudes of these stars. Soszyński et al. (2004b) mentioned that amplitudes of LSPs are positively correlated with the brightness of the star. Compared to OGLE data, the MACHO observations have the advantage of giving information on the colour variations. We ex-

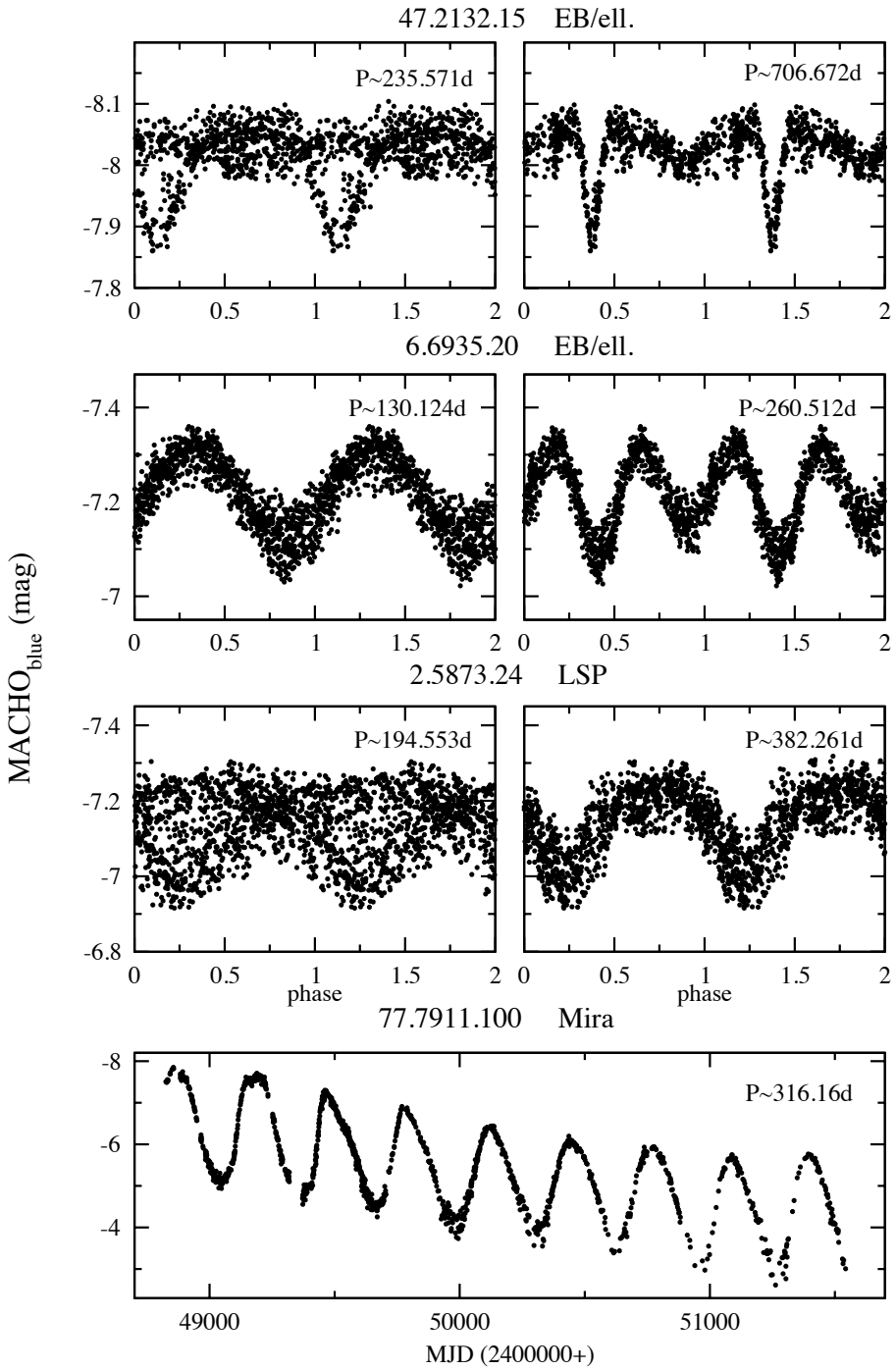

Figure 4.2 Example of phase diagrams before (left panels) and after (right panel) period correction. The first and the second star from the top show eclipsing binary and ellipsoidal variable light curve, while the third star has a typical LSP variation. The bottom panel shows the light curve of a Mira star that lies in the gap between Seqs. C and D and which faded ∼2 mags during 8 years of MACHO observations.

amined the amplitudes in the MACHO blue and red bands of the binary and LSP stars, and also included Seq. C stars, which allow a comparison with stars that we know to be pulsating.

The amplitudes were measured by fitting smooth spline functions to the phased light curves. The resulting blue peak-to-peak amplitudes are shown as a function of K magnitude in Fig. 4.3, where several features are apparent. Firstly, the amplitudes of ellipsoidal variables (circles in the upper panel) do not show any correlation with luminosity, as expected for variation caused by the geometry of a binary system. Secondly, the amplitudes of LSP variables (crosses in the upper panel) increase with luminosity, with their distribution forming a striking triangular envelope (the correlation coefficient is $r \sim 0.51$). It is also very interesting that the points below the well-defined upper envelope seem to show a flat distribution. Whatever the cause of the LSP phenomenon, there appears to be a maximum possible amplitude at each luminosity, with an apparently uniform distribution of amplitudes beneath this maximum value.

In comparison, stars on the pulsating P–L sequence C (lower panel in Fig. 4.3), show a very different distribution. To quantify the difference between the amplitude-luminosity distribution of Seqs. C and D, we performed the multivariate ε-test of Székely & Rizzo (2004), applied for two dimensions. In this test we measure the effects of random permutations of the initial distributions via changes in the "information energy" of the two distributions. In our case, 1000 random permutations showed that the difference between the C and D samples is highly significant. Therefore, we conclude that the physical mechanism causing the LSP phenomenon must be different from both the ellipsoidal variations of Seq. E and the radial fundamental-mode pulsations of Seq. C. Note, however, that for Seqs. A and B, there is a similar positive correlation between amplitude and luminosity (see the upper three panels in figs. 4 in Kiss & Bedding (2003) and Kiss & Bedding (2004)) than for Seq. D.

At the same time, comparing blue and red amplitudes for individual stars revealed further interesting information. In Fig. 4.4 we plot the blue-to-red amplitude ratios as function of period for Seqs. B, C, D and E stars. For the pulsating objects the median of the ratio is 1.40, indicating strong colour, thus temperature, changes during the pulsations. For ellipsoidal/eclipsing binaries, the median ratio is 1.13, while the LSPs have a median ratio of 1.29, being more similar to the pulsating stars (see also Huber et al., 2003). This behaviour agrees with the findings of Wood et al. (2004) who, based on colour-amplitude variations of single objects, argued for the pulsational origin of

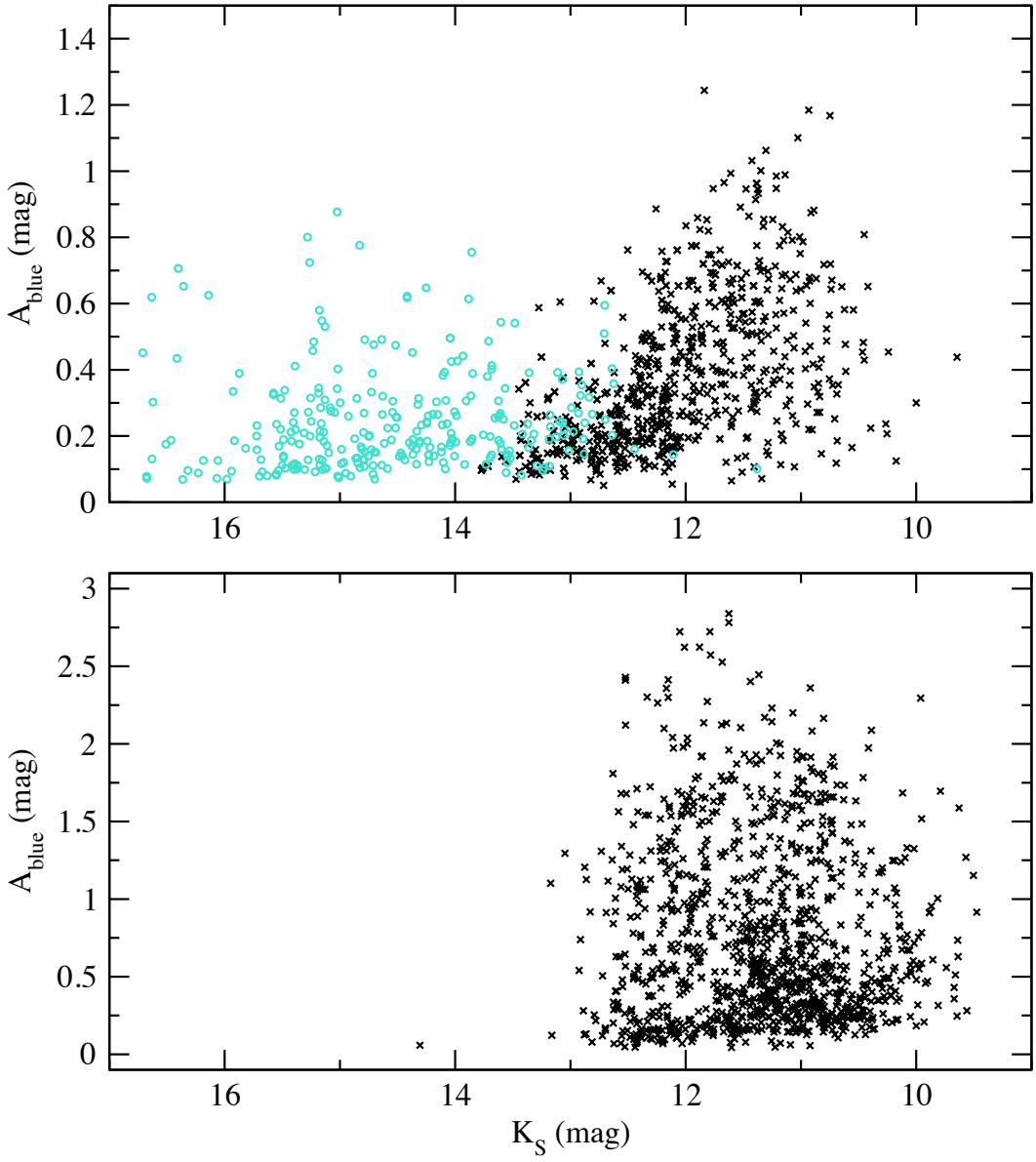

Figure 4.3 Luminosity-amplitude relation of stars on Seq. C, D and E. *Top panel:* Black crosses show the luminosity-amplitude relation for Seq. D stars, while turquoise circles the same for Seq. E stars, which contain ellipsoidal variables. The difference of the two sequence is very clear, e.g. amplitudes of Seq. D stars show moderately positive correlation with the luminosity. *Bottom panel:* Luminosity-amplitude relation for Seq. C stars, which are fundamental mode pulsators. This relation is significantly different from those of Seqs. D and E stars.

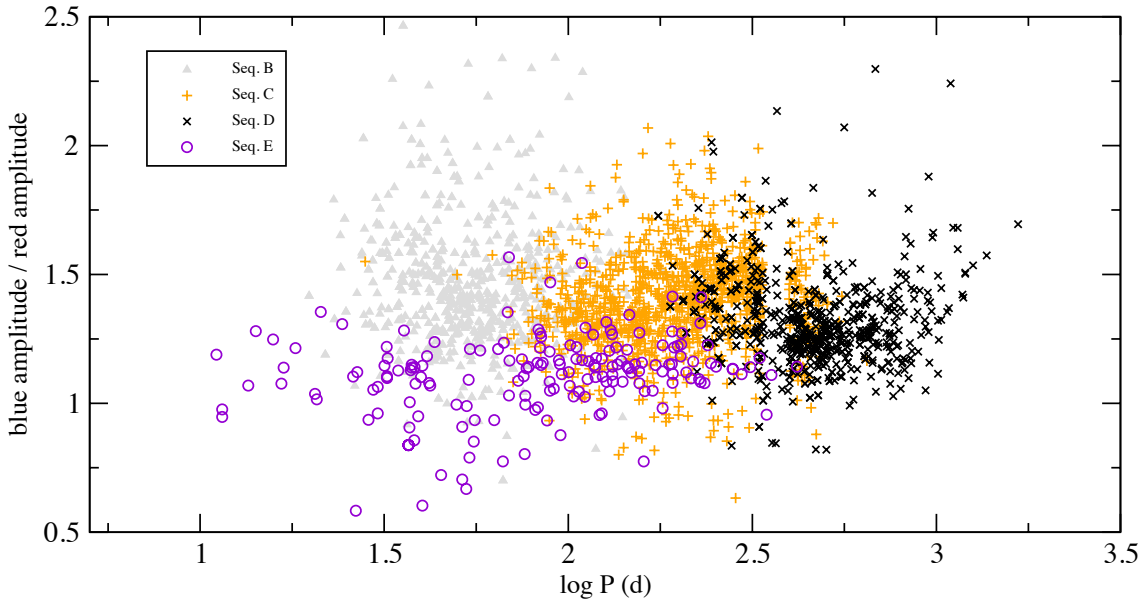

Figure 4.4 Blue-to-red amplitude ratios as function of period for stars on Seqs. B (grey triangles), C (orange pluses), D (black crosses) and E (purple circles). Grey triangles show those short period pulsations of Seq. D stars, which fall to Seq. B. The two clearly pulsating sequences, Seqs. B and C are the continuation of each other. Ellipsoidal variables (Seq. E) have lower amplitude ratio than pulsating stars. Amplitude ratios of Seq. D stars are more similar to those of pulsating stars.

LSPs. The overall statistics of more than 700 LSP variables favors this argument over the binary hypothesis, also agreeing with Hinkle et al. (2002), who concluded that the long-period velocity changes in their observed stars probably result from some kind of pulsation.

4.4 Summary

The main results of this paper can be summarised as follows:

- the period-luminosity relations of ∼6000 stars based on MACHO data confirm the existence of the short-period, small-amplitude P–L sequence at shortward of Seq. A, which belongs to a higher-overtone pulsation mode. We label this Seq. A′.
- the widely accepted sequence of eclipsing binaries between C and D, known as Seq. E, does not exist. The correct position for Seq. E, which comprises contact binaries and ellipsoidal variables, is at periods a factor of two greater. The true

Seq. E overlaps with the LSPs (Seq. D), which appears to suggest a binary origin for the LSP phenomenon (but see the last point).

- of the few stars that genuinely lie between Seq. C and D, most are under-luminous Mira variables, presumably enshrouded in dust.
- we confirmed that ellipsoidal variables have a similar P–L relation to LSP stars. Their P–L relation is well described by a simple model assuming Roche geometry.
- the amplitudes of LSPs have properties that are different from both the pulsations and the ellipsoidal variations, but they are more similar to the former than the latter, arguing for pulsation rather than binarity as the origin of the LSP phenomenon.

Chapter 5

Eclipsing binaries in the MACHO database: New periods and classifications for 3031 systems in the Large Magellanic Cloud

This chapter is reproduced from the paper *Eclipsing binaries in the MACHO database: New periods and classifications for 3031 systems in the Large Magellanic Cloud* by **A. Derekas**, L. L. Kiss, T. R. Bedding, 2007, Astrophysical Journal, 663, 249.

I downloaded and conducted the full analysis of the data. The code I used for period determination (PDM and string-length) was developed by László Kiss.

Abstract

Eclipsing binaries offer a unique opportunity to determine fundamental physical parameters of stars using the constraints on the geometry of the systems. Here we present a reanalysis of publicly available two-colour observations of about 6800 stars in the Large Magellanic Cloud, obtained by the MACHO project between 1992 and 2000 and classified as eclipsing variable stars. Of these, less than half are genuine eclipsing binaries. We determined new periods and classified the stars, 3031 in total, using the Fourier parameters of the phased light curves. The period distribution is clearly bimodal, reflecting refer to the separate groups of more massive blue main sequence objects and low mass red giants. The latter resemble contact binaries and

obey a period-luminosity relation. Using evolutionary models, we identified foreground stars. The presented database has been cleaned of artifacts and misclassified variables, thus allowing searches for apsidal motion, tertiary components, pulsating stars in binary systems and secular variations with time-scales of several years.

5.1 Introduction

The last decade witnessed the birth of a new research field, the large-scale study of variable stars in external galaxies. This has been made possible by the huge databases of microlensing observations in the Magellanic Clouds, such as the MACHO (Alcock et al., 1993), OGLE (Udalski et al., 1997) and EROS (Aubourg et al., 1995) projects. These programs (beyond their primary purpose) resulted in the discovery of thousands of eclipsing binaries and many other types of variable stars and gave an unprecedented homogenous coverage of their light curves. Recent all-sky surveys also give a good opportunity to study large numbers of stars (Paczyński et al., 2006). However, processing the huge amount of data can be quite challenging, even when looking at seemingly simple issues such as classification of variables, period determination, etc.

The astrophysical potential of large databases of eclipsing binaries has been explored by a number of authors, but we are still far from a full exploitation. Catalogs of eclipsing variables in the Magellanic Clouds have been published with an increasing completeness (Alcock et al., 1997a; Wyrzykowski et al., 2003, 2004). Attempts have been made to improve our understanding of the formation of contact binaries, especially those with giant components (Rucinski, 1997a,b, 1998; Maceroni & Rucinski, 1999; Rucinski & Maceroni , 2001). To help analyse large samples of stars, various automated pipelines have been developed (Devor, 2005; Tamuz et al., 2006; Mazeh et al., 2006), while the large-number statistics helped investigate orbital circularization over a broad range of stellar parameters (Faccioli et al., 2005). Another application is determining accurate distances using eclipsing binaries, which has been shown to offer the most accurate calibration of the local distance scale (e.g., Guinan et al., 1998; Ribas et al., 2000; Wyithe & Wilson, 2001; Salaris & Groenewegen, 2002; Fitzpatrick et al., 2002; Ribas et al., 2002; Michalska & Pigulski, 2005).

In contrast to these applications, the near-decade long time coverage of the available data has rarely been utilised. For example, Palen & Armstrong (2003) and Johnson et al. (2004) reported on searches for tertiary companions of eclipsing binaries in the MACHO

database, but no definite results have been published.

Here we present an analysis of the publicly available MACHO light curves of LMC variables classified as eclipsing binaries, which have been online since 2001. The main aim of this project is to measure period changes and search for eclipsing binaries with pulsating components. The period-luminosity (P–L) relations of contact binaries and their relation to pulsating red giants were already discussed in Derekas et al. (2006). In this paper we discuss the general properties of the sample, presenting a full reclassification, newly determined periods, the colour-magnitude diagram and period-luminosity distributions.

5.2 Period determination and classification

The MACHO observations were carried out between 1992 and 2000 with the 1.27m Great Melbourne telescope at Mount Stromlo Observatory, Australia. The telescope was equipped with a specificly designed camera, which gave a 0.5 square degree field of view. The observations were obtained in two non-standard bandpasses simultaneously: a 440–590 nm MACHO "blue" filter and a 590-780 nm MACHO "red" filter (Cook et al., 1995). Chapter 2 describes the methods of analysis in details.

For an initial period determination, we used the Phase Dispersion Minimization method (PDM, Stellingwerf, 1978). The method is based on a technique to minimize the sample variance of the phase diagram. It is calculated in the following way. The phase diagram for a given trial period is divided into m segments, each containing $\mathrm{n_j}$ $(\mathrm{j} = 1...\mathrm{m})$ points. The variance for each segment is defined as

$$s_j^2 = \sum_{i=1}^{n_j} \left(m_i - \overline{m}_j\right)^2 / \left(n_j - 1\right), \tag{5.1}$$

where m_i is the observed magnitude, $\overline{m}_j$ is the mean magnitude: $\overline{m}_j = \sum_{i=1}^{n_j} m_i/n_j$. The sample variance $s^2 = \sum_{j=1}^{m} s_j^2$ is minimized to get the best period. We calculated 600 000 trial phase diagrams for each star, covering a wide range of periods between 0.085 days and 1000 days (from 0.001 cycles/day to 12 cycles/day, with equidistant steps in frequency).

However, this was not enough for determining the true periods. As commonly happens in finding periods from light curves of eclipsing binaries, a significant fraction of

the PDM results were harmonics or subharmonics of the true period ($\mathrm{P_{PDM}}/\mathrm{P_{true}}$ was a ratio of small integers). To correct for this, we proceeded as follows. A visual inspection of every phase diagram showed whether the actual period was an alias or just slightly inaccurate. In the case of an alias, we multiplied the PDM period by different constants (in most cases by 2) until the shape of the curve was consistent with that of an eclipsing binary.

We next used the String-Length method (Lafler & Kinman, 1965; Clarke, 2002) to improve period determination. With this method, one calculates the total length of the phase diagram for any given period as the following sum:

$$SL^2 = \sum_{i=1}^{n-1} \left((m_{i+1} - m_i)^2 + (\varphi_{i+1} - \varphi_i)^2 \right), \tag{5.2}$$

where $\{\varphi_i, m_i\}_{i=1}^{n}$ is a folded dataset sorted in phase; φ_i and m_i are the phase and the magnitude of the observations taken at time t_i (so that $\varphi_i = [(t_i - t_0)/P]$, where t_0 was chosen as an epoch of the deeper minimum, P is the period, [ ] is the fractional part). The best period here was the one that minimized SL^2. In our case, we applied the SL method for 1000 periods within $\pm$1% of the best PDM period. An example of the period improvement is shown in Fig. 5.1. The typical period improvements resulted in a change in the 5-6th decimal place.

During the visual inspection of the phase diagrams we also made a rough classification of all 6833 variables. Based on the light curve shape, phased with the finally adopted periods, we placed each star into one of the following categories: Algol-type, β Lyrae-type, W UMa-type eclipsing binary, pulsating star (including RR Lyraes, Cepheids, Miras, etc.), non-periodic or multiply periodic, and unidentifiable. In cases of a pure sine-wave, which can be observed in a contact binary or a pulsating star, we compared the amplitudes of the MACHO blue and red phase diagrams. If there were noticeable colour variations exceeding a few hundredth of a magnitude, we considered the star as pulsating variable.

After the whole procedure, we ended up with 3031 genuine eclipsing or ellipsoidal binaries, the rest belonging to other type of variables. The identification numbers, J2000 coordinates, calibrated colours and magnitudes, periods and epochs of minimum light for the eclipsing variables are listed in Table 5.1 (available in full electronically). 12 of the 3031 systems have no periods because they showed signs of only one eclipse over the eight years of MACHO observations.

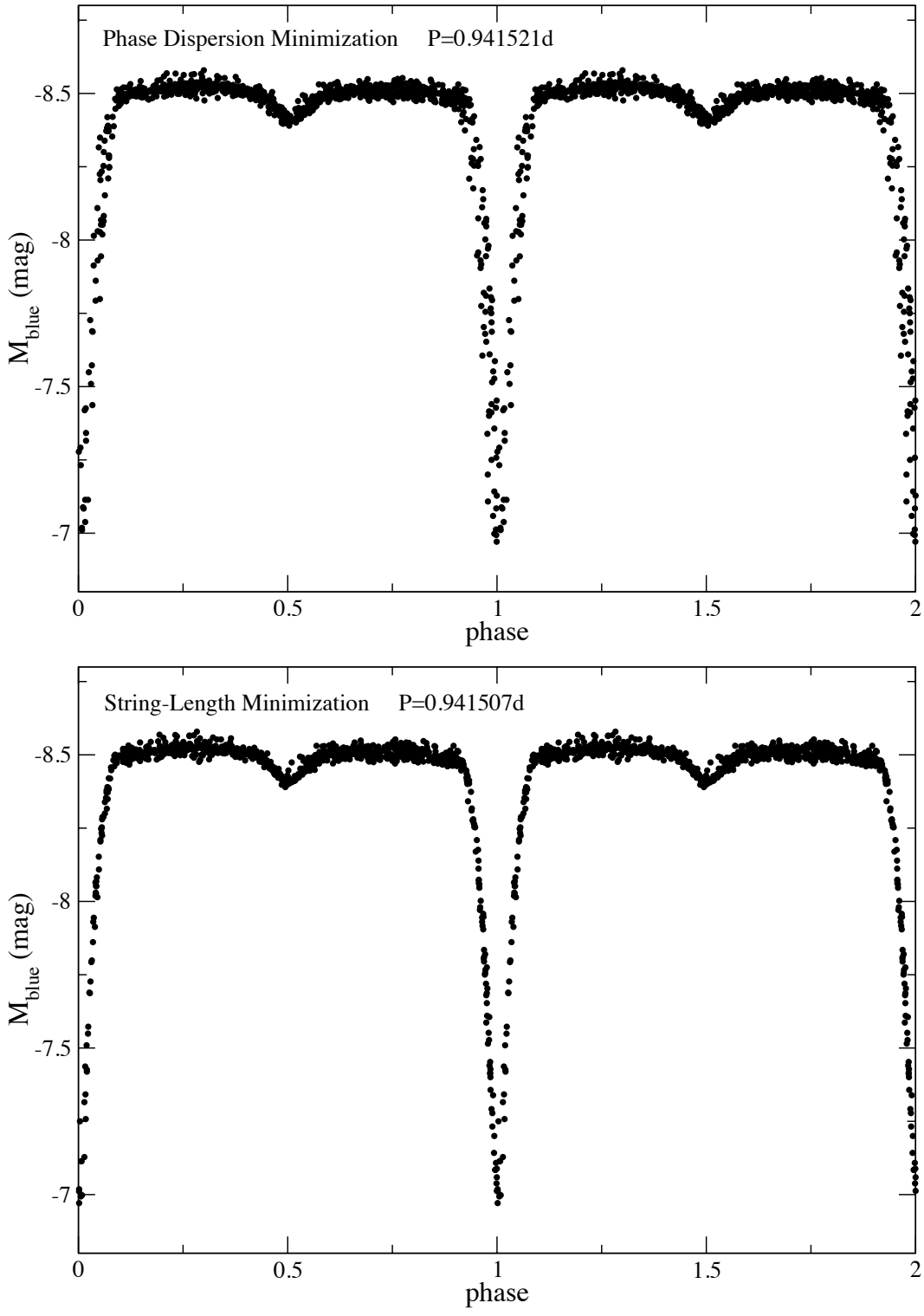

Figure 5.1 An example (81.9006.28) for improvement in period determination using PDM (top panel) and SL (bottom panel) methods.

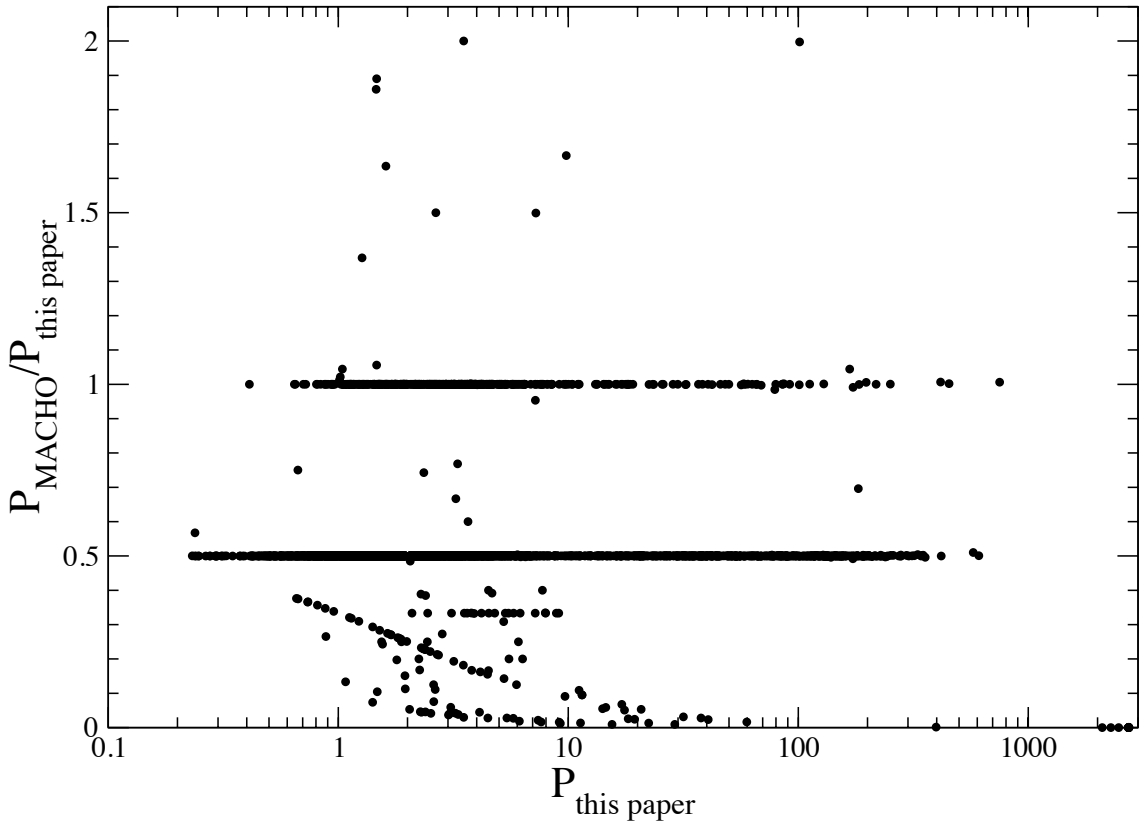

Figure 5.2 A comparison of periods presented in this study and those of the MACHO project.

A comparison of our periods with those in the online MACHO catalog shows that there is a major disagreement. A plot of the ratios of the periods (Fig. 5.2) reveals an interesting structure. A minor fraction of the period ratios are scattered around 1, while the majority are dominated by the cases when the MACHO period is half of ours. Also, we identified a number of stars with period ratios at 1/3, 1/4, 1/5, etc. The diagonal line in the lower part of the histogram corresponds to cases when the MACHO frequency ($1/\mathrm{P_{MACHO}}$) is ± 1 c/d offset from the true frequency or one of its integer harmonics.

To illustrate the improvement of periods in this paper compared to those in the online MACHO catalog, we performed the following statistical evaluation. For each star, we calculated the string-length using both our period and that of the MACHO online catalog. The ratio of the two lengths is plotted as a function of period in Fig. 5.3. We see a considerable improvement for all but a few stars; the points over 1.0 all refer to datasets with very few points, for which none of the statistics is well defined.

Ratios other than 0.5 occurred almost exclusively in stars with eccentric orbits, which

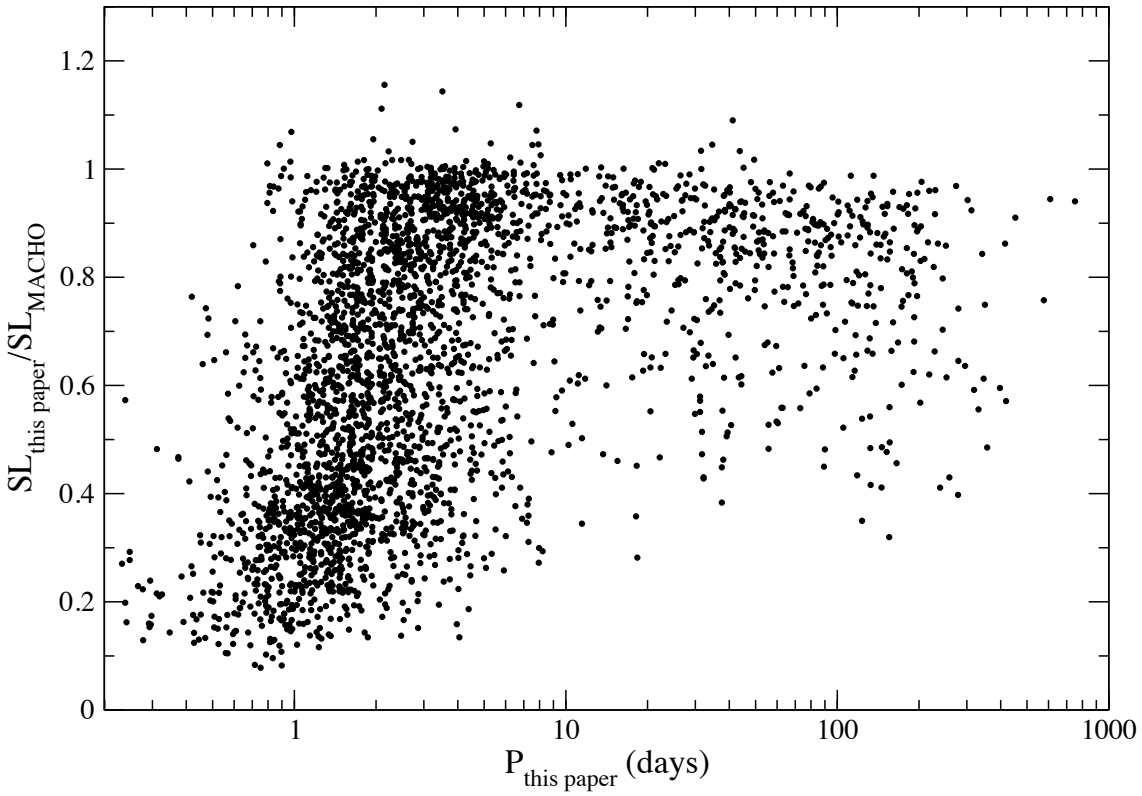

Figure 5.3 The ratio of the length of phase diagrams calculated with period in this paper to that using the MACHO period versus period of this paper.

causes a shift in the secondary minimum from 0.5 phase. These problems clearly illustrate that one has to be very careful when determining periods automatically for eclipsing binaries.

The histogram of the period ratios (Fig. 5.4) shows that roughly 16% of the periods agree. The true period turned out to be the double of the given MACHO period in about 78% of the binary sample, while the remaining 6% have other ratios. In Fig. 5.5 we show a few typical examples, plotting phase diagrams with the MACHO and our periods.

With the corrected phase diagrams, it became possible to re-classify the sample. As discussed above, pulsating and non-periodic variables were easily excluded, while eclipsing binaries were visually pre-classified as Algol (EA), β Lyrae (EB) and W UMa (EW) type stars. However, this kind of classification contains some subjectivity, so we decided to use a more objective method for this purpose. Rucinski (1993) showed that light curves of W UMa systems can be quantitatively described using only two

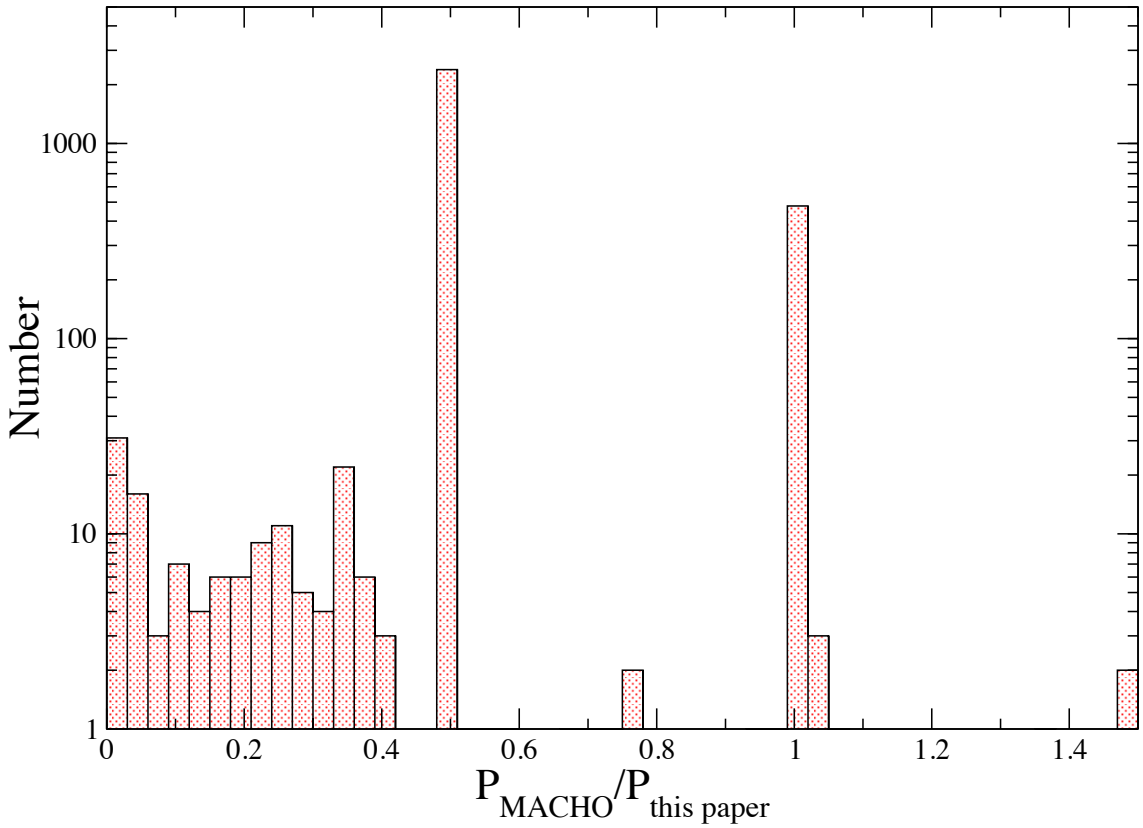

Figure 5.4 The histogram of period ratios presented in this study and by the MACHO project. Note the vertical axis is in logarithmic scale.

coefficients, a_2 and a_4, of the cosine decomposition $\sum \mathrm{a_i} \cos(2\pi \mathrm{i}\varphi)$. Pojmański (2002) tested the behaviour of semidetached and detached configurations in the $\mathrm{a}_2 - \mathrm{a}_4$ plane by decomposing theoretical light curves into Fourier coefficients. He found that in most cases contact, semi-detached and detached configurations can be distinguished quite accurately. We chose this method because it can be easily implemented for a large set of light curves.

Following the definitions by Pojmański (2002), we decomposed every light curve in the following form:

$$m(\varphi) = m_0 + \sum_{i=1}^{4} \left(a_i \cos\left(2\pi i\varphi\right) + b_i \sin\left(2\pi i\varphi\right)\right) \tag{5.3}$$

where $m(\varphi)$ is the phased light curve, m_0 is the mean magnitude, while the zero point of the phase corresponds to the primary minimum. The resulting distribution in the $\mathrm{a}_2 - \mathrm{a}_4$

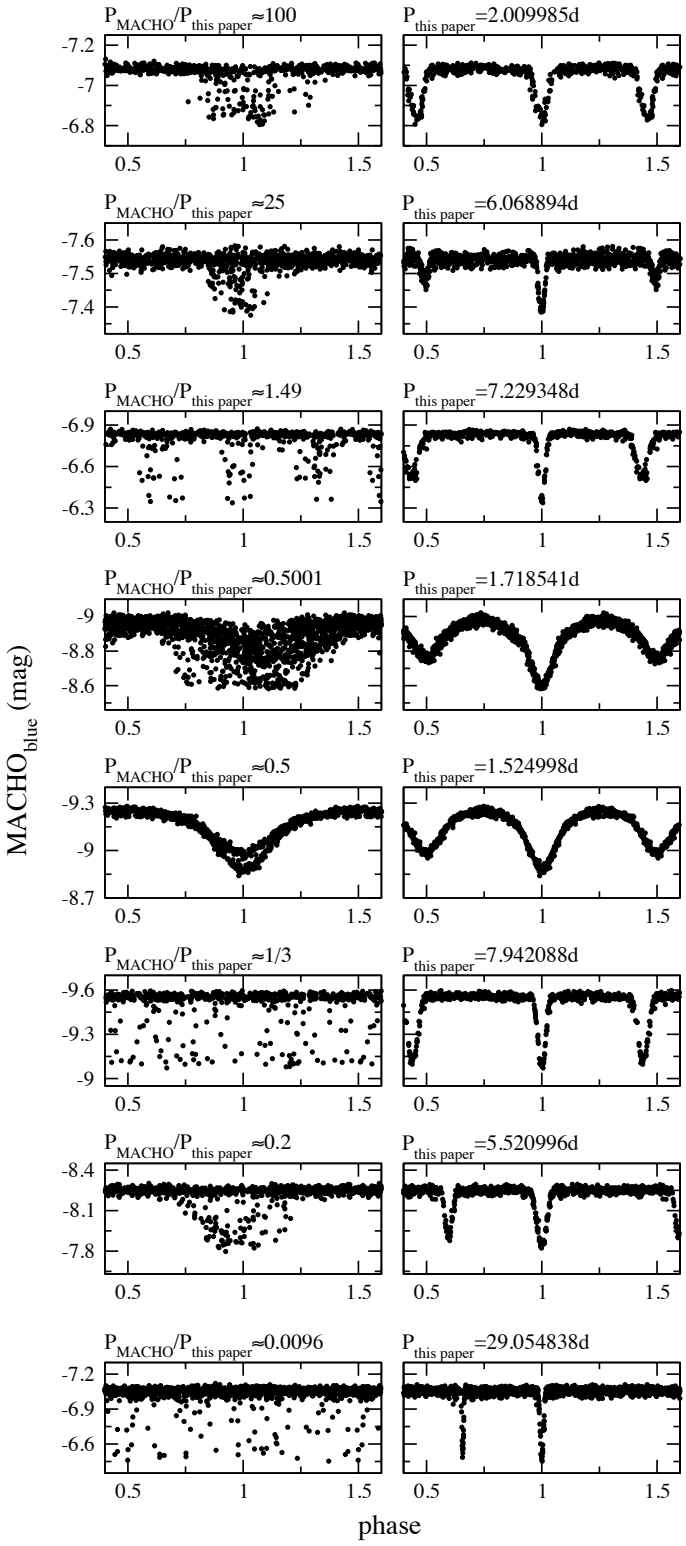

Figure 5.5 Examples of typical period ratios. In each case, the left panel shows the data phased with the MACHO period, while the right panel shows the final phase diagram with our period.

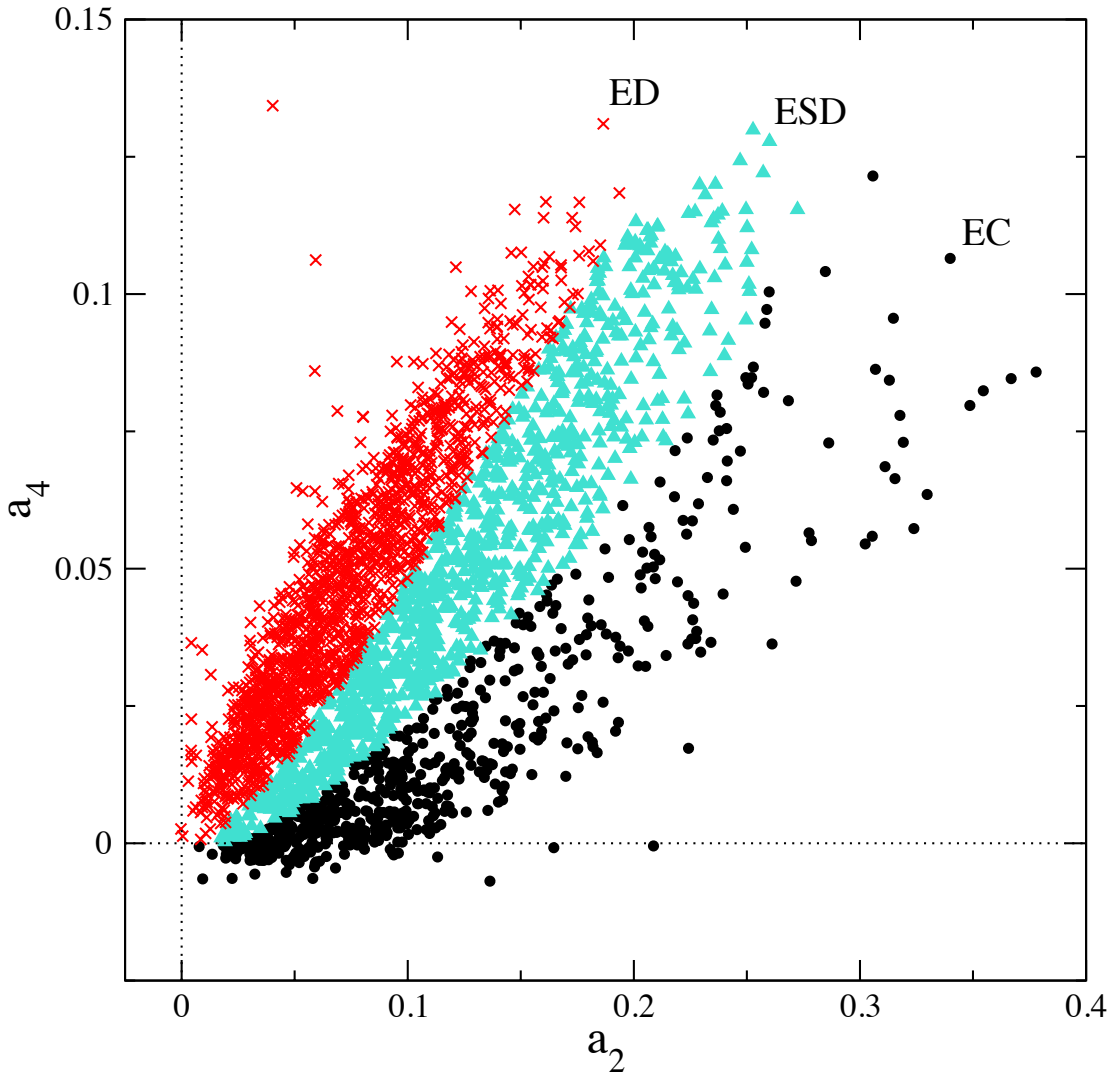

Figure 5.6 Classification of LMC eclipsing binaries in the Fourier coefficients plane $a_2 - a_4$.

plane, based on the MACHO blue data, is shown in Fig. 5.6. Using the boundary lines of Pojmański (2002), we marked the contact (EC), semi-detached (ESD) and detached (ED) configurations with different symbols.

The sample is dominated by bright main-sequence detached (1482 stars) and semidetached (937 stars) binaries, while a small fraction consist of contact systems (612 stars). Many of the latter are foreground Milky Way objects, as can be shown from their positions in the colour-magnitude diagram (Section 3.2). We list the EC/ESD/ED classification for each star in Table 5.1.

Table 5.1 Representative lines from the full Table 1 (available electronically). The (*) symbol in the Type column denotes foreground objects.

ID number	RA (J2000.0)	Dec. (J2000.0)	V (mag)	V–R (mag)	Period (days)	Epoch (2400000+)	Type
47.1402.116	04:49:21.544	−68:12:31.70	18.644	−0.034	1.761188	50249.7483	ESD
47.1527.178	04:49:28.952	−67:55:24.15	19.223	0.725	12.556414	50244.6082	EC
47.1528.41	04:49:34.577	−67:49:48.88	17.209	−0.179	5.024733	50249.8034	ED
47.1529.60	04:49:44.988	−67:48:57.28	18.005	0.574	112.073172	50252.7272	ED
47.1531.32	04:49:51.948	−67:41:38.13	16.842	−0.159	0.459804	50249.9699	EC
47.1530.30	04:49:52.060	−67:42:09.84	15.519	−0.249	1.633056	50249.3579	ED
47.1649.69	04:50:16.357	−67:53:06.87	17.396	−0.153	1.453116	50250.0195	ESD
47.1645.115	04:50:21.514	−68:07:37.01	18.048	−0.163	1.711124	50249.3182	ED
47.1647.143	04:50:33.106	−67:58:44.94	18.440	−0.186	1.620856	50250.1698	ED
47.1647.285	04:50:34.347	−67:59:24.49	19.653	0.082	1.387449	50249.4512	ESD
81.9248.127	05:37:00.635	−69:27:10.46	16.639	0.096	0.675994	50250.0858	EC(*)

5.3 General properties

After the visual inspection, we identified 3031 stars as eclipsing binaries, which is about 44% of the downloaded sample. We emphasize that our sample probably does not contain all LMC eclipsing binaries observed by the MACHO project. We assume that there might be eclipsing binaries classified as other variable types (such as RR Lyraes, Cepheids, Semiregulars, etc.). For example, Faccioli et al. (2005) studied orbital circularization of LMC eclipsing binaries presenting a new sample of 4576 stars; however, that sample is not available to us. With this caveat, we discuss the main properties of the sample.

5.3.1 Period distribution

One of the most fundamental parameters of binary stars is the orbital period, whose distribution can be of great aid in understanding formation and evolution of close binaries. Eclipse detection is highly influenced by the orbital period, because the wider the separation of components, the longer the orbital period gets, implying that eclipses will be seen in narrower range of the inclination angle. Hence the chances to detect eclipses are much higher for short orbital periods. Well before the microlensing projects, Farinella & Paolicchi (1978) and Giuricin et al. (1983) found a multi-modal period distribution

in the Milky Way. Recent studies of eclipsing binaries in the Small and the Large Magellanic Clouds revealed an overall similarity in the period distributions, peaking between 1 and 2 days (Alcock et al., 1997a; Wyrzykowski et al., 2003, 2004; Devor, 2005).

For a direct comparison with the OGLE sample for the LMC and the SMC, we downloaded periods of eclipsing binaries from the OGLE internet archive[1]. Our period distribution (Fig. 5.7) is in a good agreement with that of the OGLE sample of LMC and SMC stars (Wyrzykowski et al., 2003, 2004): the majority of systems have short periods, peaking between 1 and 2 days, and roughly 20% of stars have periods longer than 10 days, which is consistent for both the SMC and the LMC.

The distribution shown in the upper panel of Fig. 5.7 is also similar to that of Devor (2005), which was based on the OGLE observations of the Galactic Bulge. However, we do not confirm his conclusion that the peak at ~ 100 days is due to pulsating red giant stars. While Devor (2005) used single filtered I-band data of the OGLE project, thus having no information on the colour variations, the two-colour MACHO observations clearly showed that those long-period variables have only slight colour changes, which can be explained by the non-uniform temperature distribution on the surface of the non-spherical components.

The lower panel of Fig. 5.7 shows the histogram of all eclipsing binaries in the General Catalog of Variable Stars (Kholopov et al. (1985-1988) with all the recent updates available for download from the GCVS website[2]). Compared to the upper panel of Fig. 5.7, the distributions are different in two period ranges. For shorter periods, there is an excess of stars in the GCVS, which are all short-period main-sequence binaries that have fainter absolute magnitudes than the MACHO limit in the LMC. On the other hand, for periods longer than 40 days, there is a lack of stars in the GCVS, which we interpret as caused by a selection effect: these systems need years of observations before classification and period determination, which was hardly possible before the development of automatic all-sky survey projects like the All-Sky Automated Survey (ASAS, Pojmański, 2002). It also implies that there are considerable number of bright long-period eclipsing binaries waiting for discovery.

To make further comparison, we took detached and semi-detached binaries in the Galaxy observed by the ASAS project and compared their period distribution with detached and semi-detached binaries in the SMC and LMC. In the upper panel of Fig. 5.8

[1] http://bulge.astro.princeton.edu/ ogle
[2] http://www.sai.msu.su/groups/cluster/gcvs/gcvs/

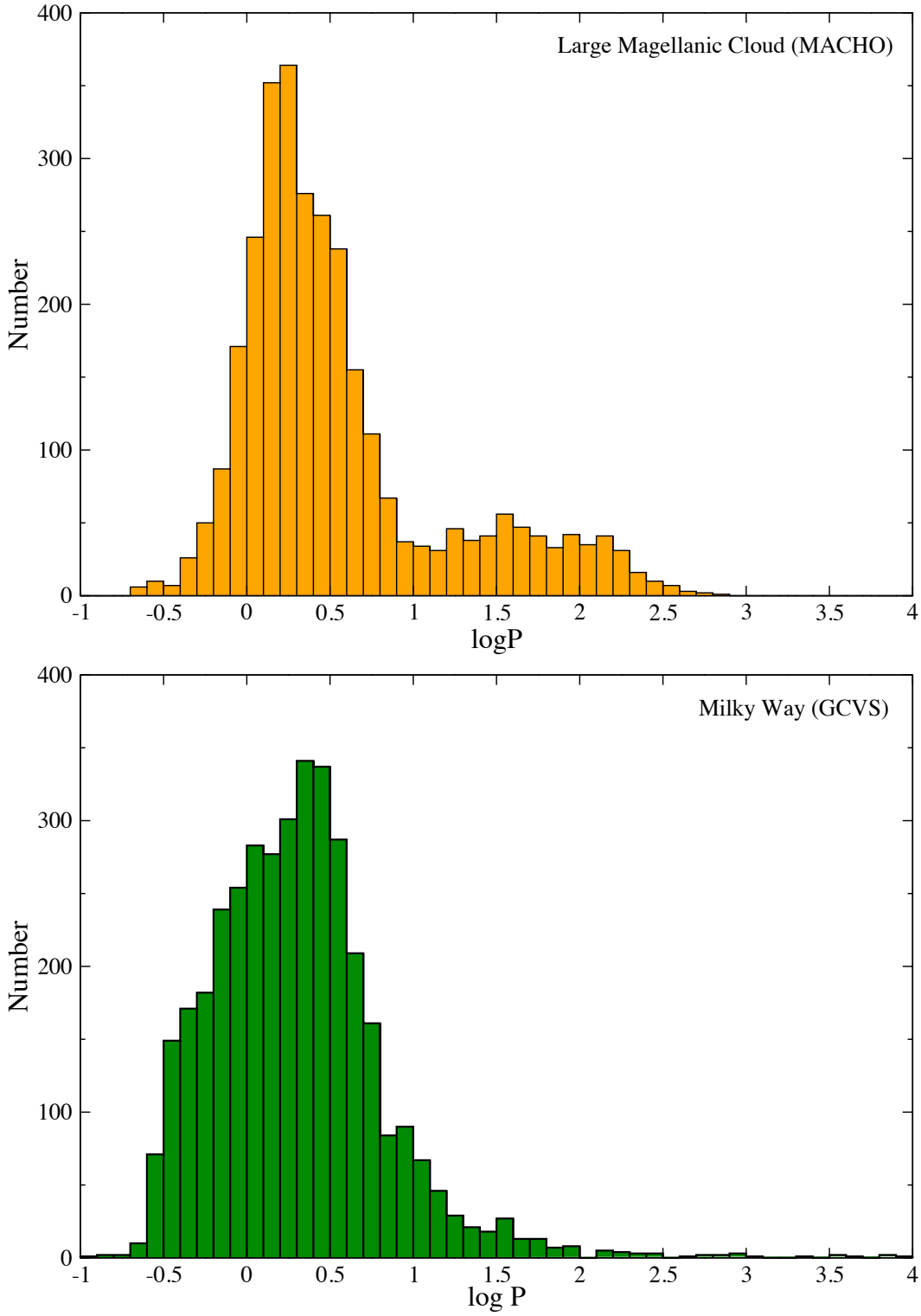

Figure 5.7 Upper panel: period distribution of eclipsing binaries in the MACHO database. Lower panel: histogram of orbital periods of eclipsing binaries in the General Catalog of Variable Stars.

we plotted the period distribution of orbital periods shorter than 10 days, which shows an overall similarity for the three galaxies. This diagram also shows the presence of a selection effect in the data: there is a noticeable dip at P=2d in the histograms of the MACHO and the ASAS data, which reveals that stars with exactly 1-d periods (i.e. the half of the true ones) were discarded during the initial analyses. For example, based on the shape of the histogram, about 50 MACHO eclipsing binaries with $\mathrm{P} \sim 2\mathrm{d}$ are missing from the sample, presumably due to deliberate exclusion from the data.

In the lower panel of Fig. 5.8 we plot the cumulative period distribution for the three samples. While the LMC and SMC samples have virtually indistinguishable distributions, the Milky Way shows an excess of stars around 10 days. A two-sample Kolmogorov-Smirnov test showed that the difference between the LMC and the SMC samples is insignificant, which confirms that the MACHO and OGLE selections of detached and semi-detached binaries were similarly complete. On the other hand the probability that the ASAS stars have the same distribution is only $10^{-11} percent$. This is a simple consequence of the different sampling: while MACHO and OGLE data represent magnitude-limited samples in absolute magnitudes, covering the brightest ~ 6 mag of the CMD, the ASAS database contains a broad mixture of stars in the Milky Way with a much wider range in absolute magnitude.

It is also apparent in Fig. 5.8 that, although the long-period tails of the ASAS and MACHO histograms overlap very well, the short-period peak in the LMC data is higher because of the different distributions of stars in the samples. Whereas the MACHO data cover the upper part of the Hertzsprung-Russell diagram with a relatively bright limit in absolute magnitude, the ASAS sample contains a broader mixture of stars in the galactic neighborhood, so that short-period B-type systems have a smaller relative contribution.

5.3.2 The Color-Magnitude Diagram and Period-Luminosity Relations

In order to construct the Color-Magnitude Diagram (CMD), we converted the observed MACHO blue and red magnitudes into Kron-Cousins V and R using the equations derived by Alcock et al. (1999). The resulting diagram, after translating apparent magnitudes outside the eclipses to absolute magnitudes using $\mu(\mathrm{LMC}) = 18.50$, is shown in Fig. 5.9. We also show stellar evolutionary tracks by Castellani et al. (2003). Most of the stars are moderately massive near-main sequence stars, while the red giant branch

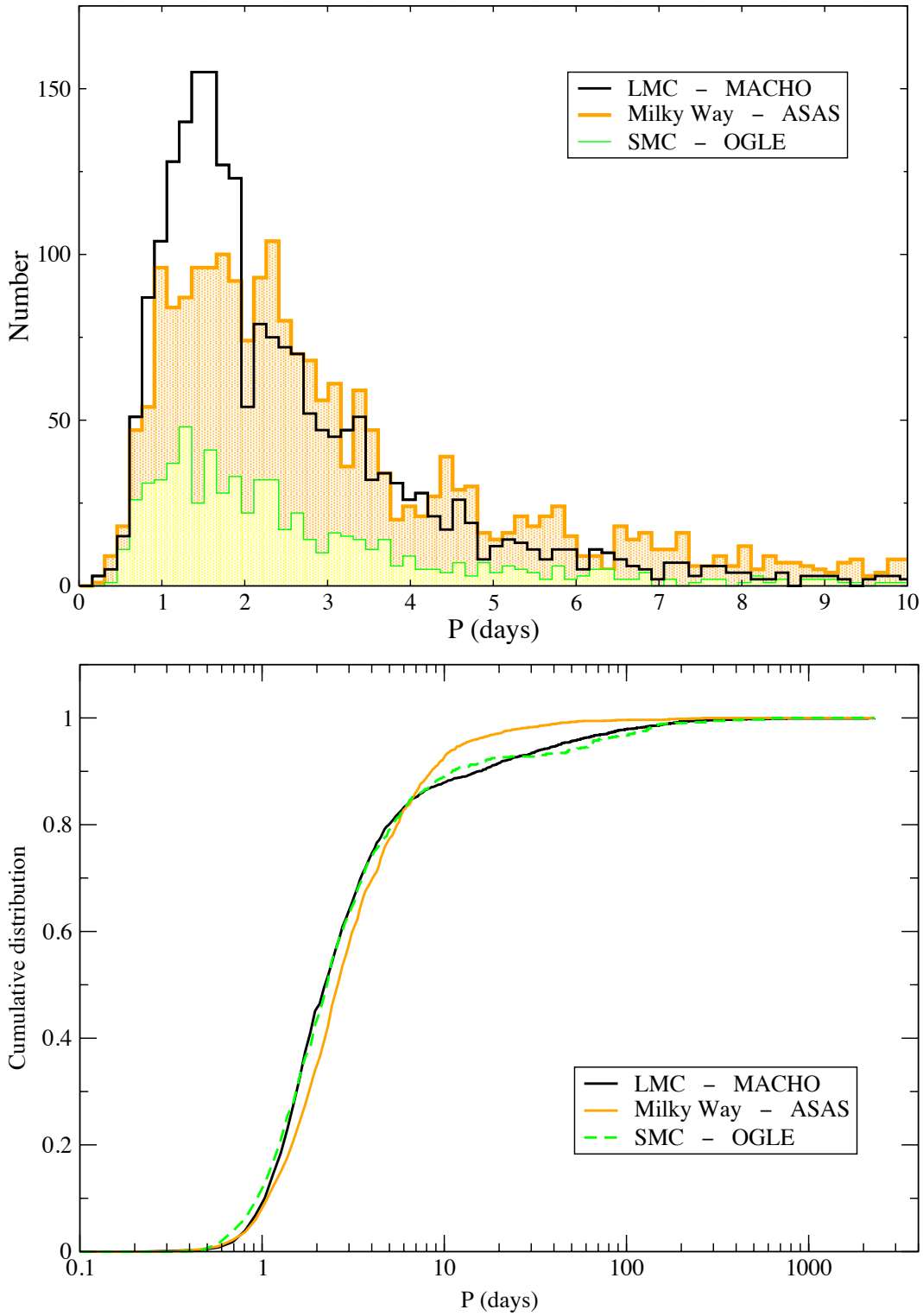

Figure 5.8 Upper panel: Orbital period distributions of detached and semi-detached eclipsing binaries in the Milky Way and the Magellanic Clouds. Lower panel: The normalized cumulative distributions.

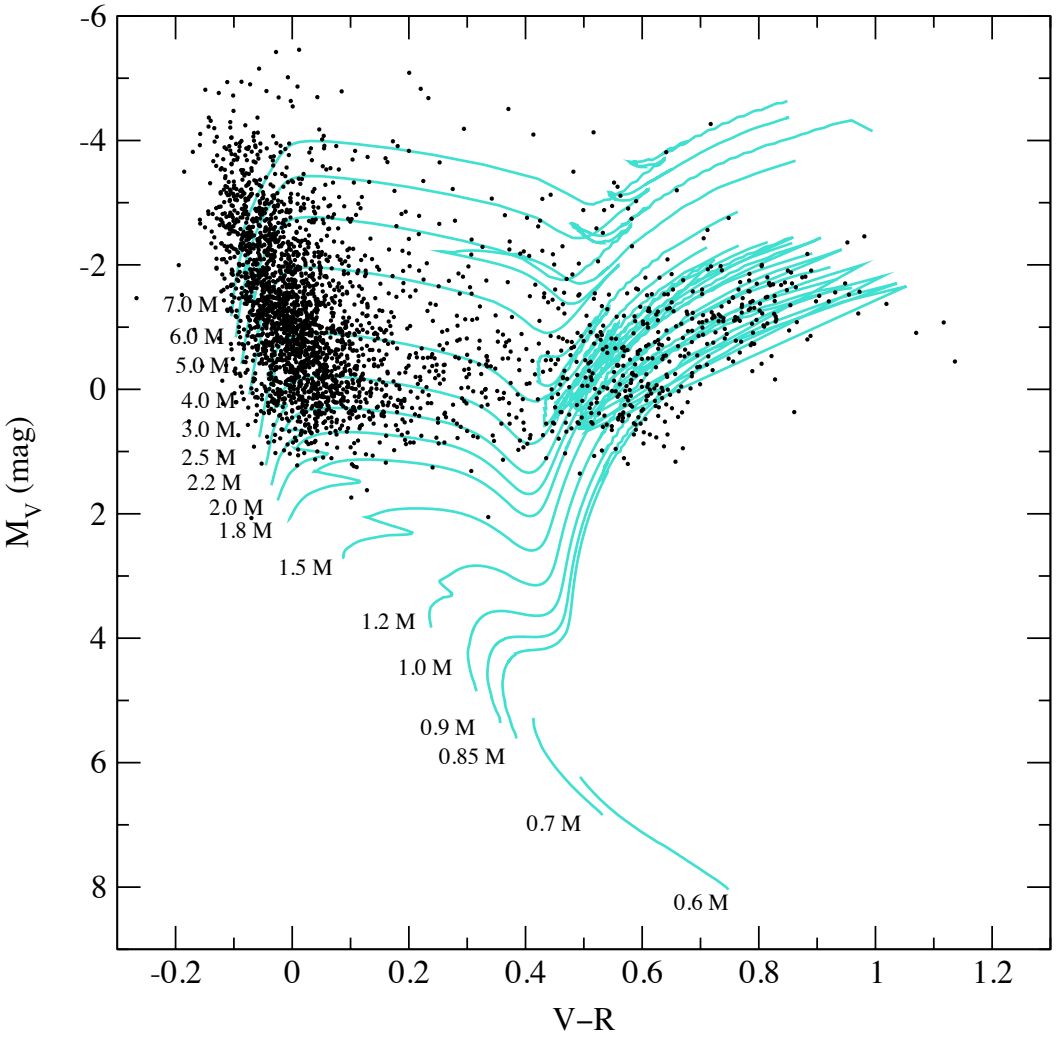

Figure 5.9 The colour-magnitude diagram of LMC eclipsing binaries with metal-poor evolutionary tracks of single stars overlaid (models taken from Castellani et al. (2003)).

of evolved stars is also clearly recognisable. The latter is dominated by first-ascent red giants and a few Asymptotic Giant Branch stars (Alcock et al., 2000a).

In Fig. 5.10 we plot the CMD for four orbital period ranges. These plots were used for cleaning the sample of the foreground objects, adopting the following simple considerations. First, the spread of distances of eclipsing binaries in the LMC is negligible compared to the distance to the LMC. This means that we can determine the absolute magnitude for any given object within ± 0.1 mag (e.g. Nikolaev et al., 2004; Lah et al., 2005). Second, we assumed that the mean position of a binary star in the CMD can be approximated by the location of the brighter component. In the case of two

identical components, this assumption means a 0.75 mag fainter absolute magnitude, however, as we proceeded, this was still a useful simplification in estimating foreground contamination.

Theoretical evolutionary tracks give the basic physical parameters of a single star, as well as colour and magnitude information. From the physical parameters we can calculate the minimum orbital period for any given mass, temperature and luminosity, applying simple relations. Combining the Stefan-Boltzmann law: $L/L_{\odot} = (R/R_{\odot})^2 (T/T_{\odot})^4$ and Kepler's third law: $a^3/P^2 = G(M_1 + M_2)/4 \cdot \pi^2$, we can calculate the minimum orbital period of a system for two extreme cases:

Case 1.: two identical components, for which the minimum orbital period occurs when $a = 2R$ and $M_1 + M_2 = 2M$; the minimal orbital period is

$$P_{\min}(1) = 4\pi\sqrt{\frac{R^3}{GM}} \tag{5.4}$$

Case 2.: a negligible secondary component, for which the minimum orbital period occurs when $a = R$ and $M_1 + M_2 = M$; the minimum orbital period is

$$P_{\min}(1) = 2\pi\sqrt{\frac{R^3}{GM}} \tag{5.5}$$

(M is the mass of a model point of the isochrone, while R is calculated from L and T).

Using Eq. (5.4) and Eq. (5.5) and theoretical stellar evolutionary tracks, we can determine contours in the CMD, on which the minimum orbital period has a given value. This is shown in the four panels of Fig. 5.10 by the thick solid lines (Case 1) and dashed lines (Case 2). As representative limits, we determined the locations where the minimum orbital period is 0.5, 1, 10 and 100 days.

We have selected the foreground objects as follows. As Fig. 5.10 shows, moving up and right in the CMD, the minimum orbital period gets longer. Therefore, if a star with $P_{\rm orb} \leq 0.5{\rm d}$ is located above the limiting line of $P_{\min} = 0.5{\rm d}$, it must be in the foreground of the LMC. This is shown in the upper left panel of Fig. 5.10. As expected, most of these short-period reddish eclipsing binaries are Galactic W UMa-type stars, many magnitudes above the calculated period lines (which means the adopted simplifications do not affect the conclusions).

For longer periods, only a few stars are clearly foreground objects (most notably in

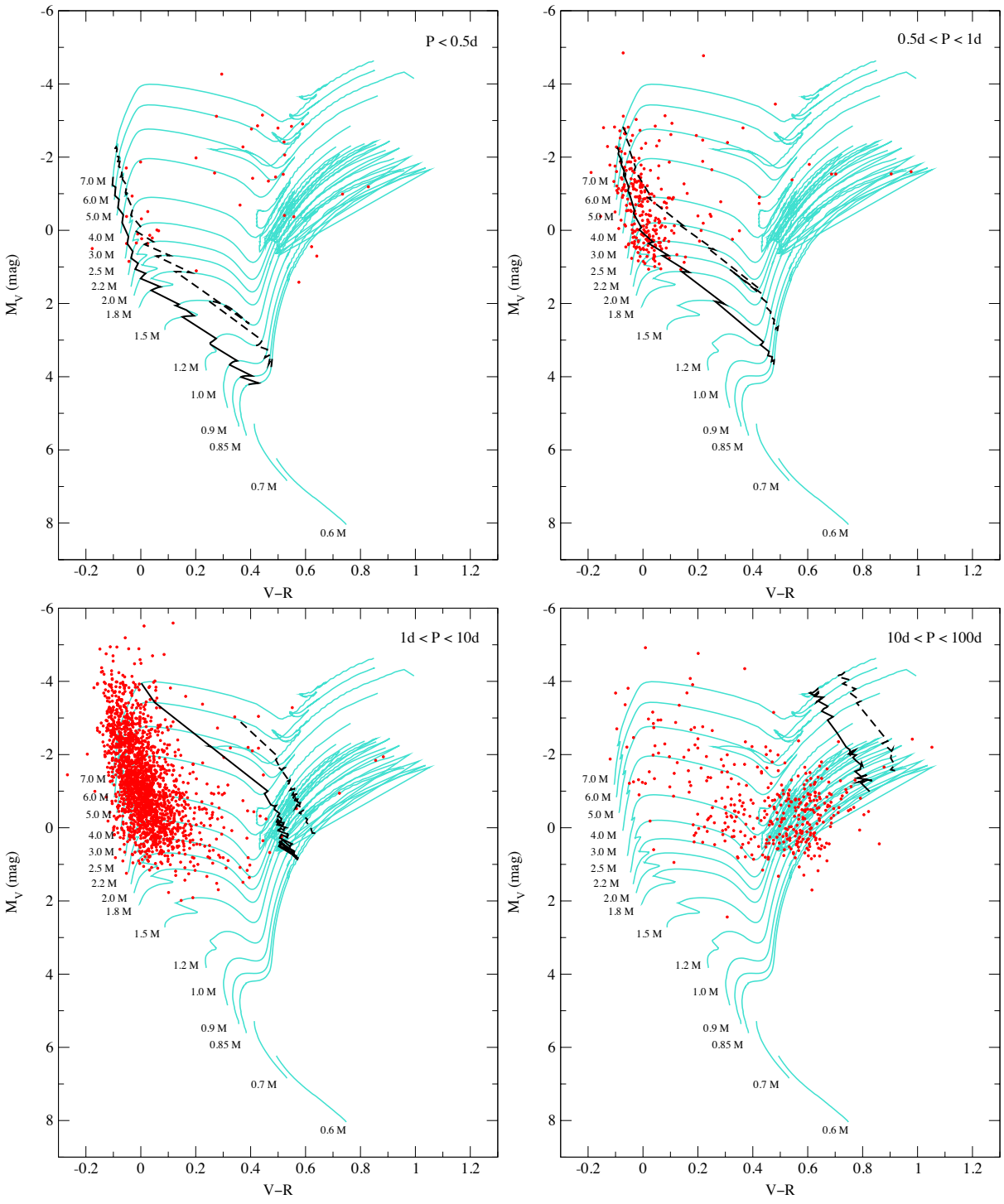

Figure 5.10 Eclipsing binaries in four period ranges and estimated locations of the minimum orbital periods. Stars upper and right of the dashed lines have positions that are not compatible with the LMC membership.

the upper right panel of Fig. 5.10), while for the majority, positions in the CMD are compatible with the LMC membership. We flagged all obvious foreground stars, being those located at least 1 mag above the dashed lines, in the last column of Table 5.1 (54 stars in total).

Finally, we briefly examine the period-luminosity (PL) relation of stars in the sample, for which we found near-infrared K-magnitudes in the 2MASS Point-Source Catalog. In Derekas et al. (2006) we already discussed how the red giant eclipsing binaries/ellipsoidal variables can be fitted with a simple model using Roche-lobe geometry. Here we examine the correlation between the period and the K-magnitude for the detached and semi-detached binaries. This is shown in Fig. 5.11, where the ED/ESD/EC classes are plotted with different symbols. As expected, detached binaries are spreaded uniformly, while longer period semi-detached systems may follow a loose correlation (the correlation coefficient for $\mathrm{P} > 10\mathrm{d}$ is ~ 0.58), but it is not as tight as for long-period contact binaries (whose correlation coefficient is ~ 0.86). Systems further away from the main correlation line might be foreground stars left unidentified as such in the CMD analysis.

5.4 Summary

In this paper we present the analysis of online light curves of eclipsing binaries in the Large Magellanic Cloud monitored by the MACHO project. We downloaded the data of all 6833 stars classified as eclipsing binaries from the Variable Star Catalog Retrieval form of the project.

We re-determined the periods for every star and reclassified all stars based on their light curve shape. As a result, 3031 stars remained as eclipsing binary, while the rest of the sample were RR Lyrae stars, Cepheids or long-period pulsators. For the binary sample, we showed that roughly 16% of the periods agreed with those given in the catalog. For almost three-quarter of the sample, the catalog periods turned out to be the half of the real ones.

We calculated the period histogram, which shows bimodal feature on logarithmic scale. The maximum of the distribution is at binaries with periods between 1 and 2 days, while roughly 20% of the sample (about 600 stars) have period between 10 and 200 days. We compared our period distribution for detached eclipsing binaries, with

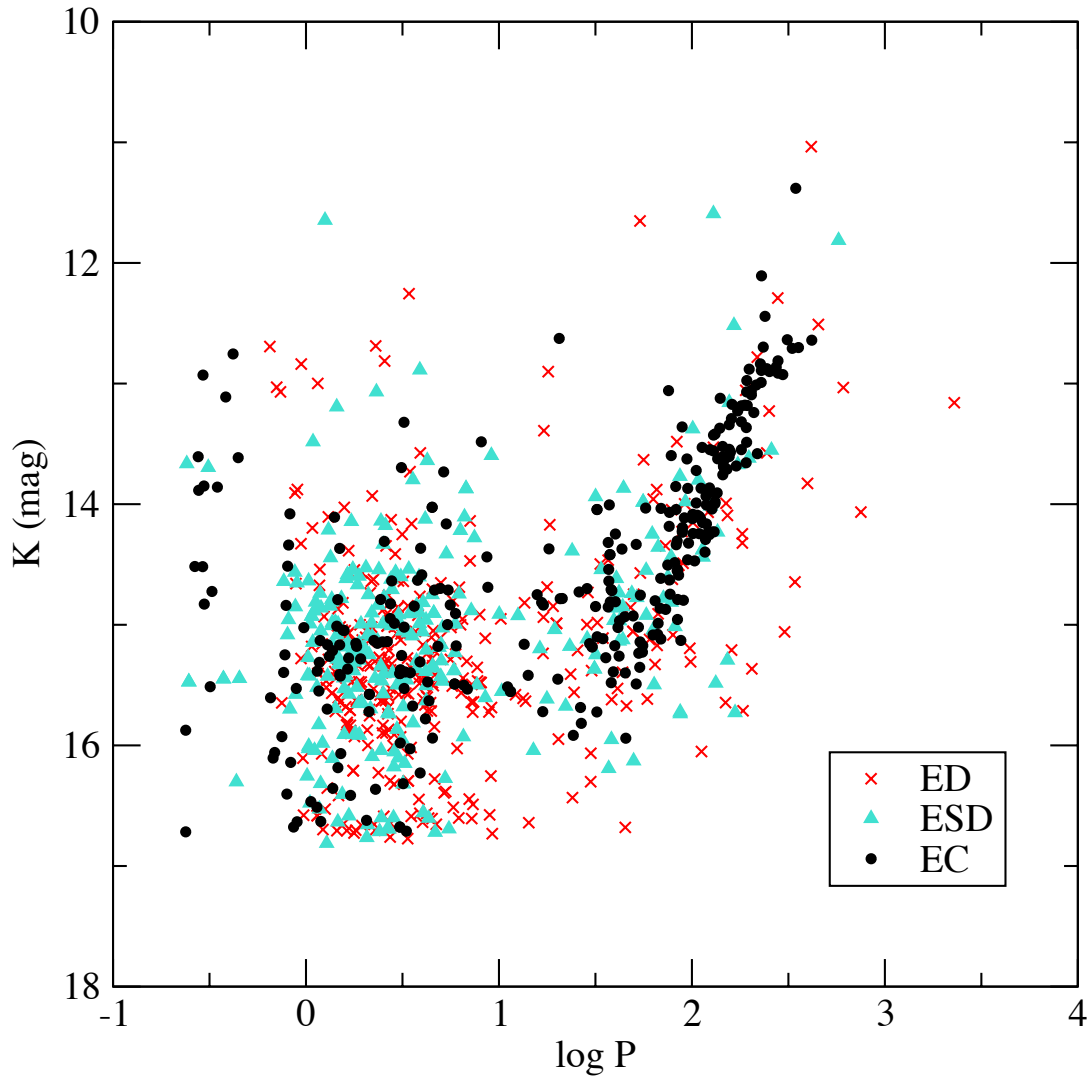

Figure 5.11 Period-K magnitude relation for eclipsing binaries in the LMC.

those of the SMC and the Milky Way and we found a good agreement in the most common periods in the studied galaxies.

For a more objective classification, we used cosine decomposition of the light curves into Fourier coefficients, where contact, semi-detached and detached configurations can be distinguished in $a_2 - a_4$ plane. The sample is dominated by bright main-sequence detached and semi-detached systems, while a small fraction consists of contact binaries. However, many of the latter are foreground Milky Way objects, which can be shown from their position in the colour-magnitude diagram. Most of the stars with periods shorter than 0.5 days are galactic W UMa systems. For longer period systems, we found

a few obviously foreground objects and they are flagged in the last column of Table 5.1.

The presented database opens up a new avenue into using the MACHO database for studying secular variations over a time-scale of a decade. This includes a search for systems with apsidal motion (recognizable through phase shifts of the primary and secondary minima in the opposite direction), tertiary components (indicated by cyclic phase shifts of the primary and secondary minima in the same direction) and eclipsing binaries with pulsating components (revealed by periodic secondary brightness fluctuations). The latter would be particularly interesting if evidence for tidally induced pulsations could be found in a larger sample of stars. With the OGLE-III project still taking data, after identifying these theoretically important test objects, it would become possible to extend the full time-coverage of observations up to 14-15 years. In a companion paper we will discuss the measured period changes for the whole sample of 3031 eclipsing binaries. To help the interested researchers, we have collected the original MACHO blue and red light curve data in a single compressed data file that can be accessed as an electronic appendix to this paper.

Chapter 6

Observations

For the first part of this thesis, I used publicly available data (MACHO dataset for the Large Magellanic Cloud) and performed various analyses on them, resulting in 3 papers that are described in the previous chapters (Chapters 3, 4 and 5). I also took photoelectric, CCD photometric and spectroscopic observations of δ Scuti and Cepheid variables and obtained service observations on two telescopes. I spent about 70 nights at Siding Spring Observatory between 2003 and 2007. The main aim of obtaining these data was to detect hidden binarity in pulsating stars in order to potentially allow the first fully dynamical mass determination for a star in these two classes. This chapter gives a basic description of the telescopes which were employed in the project and the data reduction and analyzing techniques I used during my postgraduate years.

6.1 Telescopes

The following telescopes and instrumentation were used to obtain photometric and spectroscopic data:

– *Szeged Observatory, 0.4 m (Hungary)*

  V-band CCD photometry was carried out with the 0.4 m Newtonian telescope at Szeged Observatory. The telescope has an $11' \times 17'$ field of view and the detector was an SBIG ST-7 CCD camera (765 $\times$ 510 pixels at 9 μm). Observations were taken for XX Cyg.

– *Siding Spring Observatory, 0.5 m (Australia)*

I obtained time-series I-band CCD photometry for RY Lep, BQ Ind and CY Aqr with the Automated Patrol Telescope (APT) at Siding Spring Observatory, which is owned and operated by the University of New South Wales (UNSW). The telescope was originally a Baker-Nunn design converted into CCD imaging (Carter et al., 1992) and has a three-element correcting lens and an f/1 spherical primary mirror. The camera has an EEV CCD05-20 chip with 770×1150 (22.5 μm) pixel to image a 2×3 deg^2 field of view.

– *Siding Spring Observatory, 24″/0.6 m (Australia)*

B, V, I photoelectric photometry of ZZ Mic, RS Gru and CY Aqr was obtained by me with the 0.6 m f/18 Cassegrain-reflector, on which a single-channel photometer was mounted. It had a computer-controlled 8-hole filter wheel, for which the dwell times on each filter can be varied. The detector was a thermoelectrically cooled Hamamatsu R647-4 photomultiplier tube with a 9 mm diameter bi-alkali (blue-sensitive) photocathode (Handler et al., 2000).

– *Piszkéstető Station, 0.6 m (Hungary)*

V-band CCD photometry was obtained on CY Aqr, XX Cyg, DY Her and DY Peg with the 60/90/180 cm Schmidt-telescope mounted at the Piszkéstető Station of the Konkoly Observatory. The detector was a Photometrics AT200 CCD camera (1536×1024 9 μm pixels, FOV=28′×19′).

– *Fred Lawrence Whipple Observatory, 1.5 m (USA)*

High resolution spectra were obtained on BE Lyn with the Tillinghast Reflection Echelle Spectrograph (TRES) and the 1.5 m telescope at the Fred Lawrence Whipple Observatory on Mt. Hopkins, Arizona during service time. TRES is a high-throughput fiber-fed echelle. It is cross-dispersed, yielding a passband of 380-920 nm over the 51 spectral orders. It accommodates 3 optical fiber pairs (science+sky) of different diameters, to offer a match for seeing conditions. Simultaneous ThAr calibration is also available via a separate fiber. The available resolutions are 64K, 35K and 31K, depending on the fiber size selected (1.5, 2.3 or 3.2 arcsec, respectively). The observations were taken as part of the instrument commissioning, using the small fiber and 300 s integration times. The 4.6k×2k detector was binned 2×2 in order to improve the duty cycle (15 s readout time), providing a slightly undersampled FWHM of 2.0 pixels.

– *Siding Spring Observatory, 2.3 m (Australia)*

I carried out spectroscopic observations for δ Scuti stars RY Lep, AD CMi, ZZ Mic, RS Gru and CY Aqr and for 40 Cepheid variables with the 2.3 m ANU telescope at the Siding Spring Observatory, Australia. All spectra were taken with the Double Beam Spectrograph using the 1200 mm^{-1} gratings in both arms of the spectrograph. The projected slit width was 2″ on the sky, which was about the median seeing during our observations. The spectra covered the wavelength ranges 4200–5200 Å in the blue arm and 5700–6700 Å in the red arm. The dispersion was 0.55 Å px^{-1}, leading to a nominal resolution of about 1 Å. The results are shown in Chapters 7 and 10.

– *Anglo-Australian Observatory, 3.9 m (Australia)*

We used the 3.9 m Anglo-Australian Telescope equipped with the UCLES spectrograph for 4.2 hours of high-resolution spectroscopy of RS Gru. The observations were taken by staff astronomers during service time. Our echelle spectra include 56 orders with a central wavelength of 6183 Å and a resolving power $\lambda/\Delta\lambda \approx$40 000.

From the above mentioned telescopes, I personally took data for my research with three telescopes located at the Siding Spring Observatory: I used the 0.5 m remotely for CCD time series photometry, the 24″ for obtaining photoelectric photometry, the 2.3 m telescope for spectroscopy. I have been granted service time on the Anglo-Australian Telescope and the TRES spectrograph at Fred Lawrence Whipple Observatory and obtained high-resolution spectroscopic data on two high-amplitude δ Scuti stars. The remaining telescopes were used by collaborators and their data were included in the results described in Chapter 7.

6.2 Data reduction

I reduced all the CCD photometric data taken with the UNSW APT 0.5 m telescope using IRAF[1] standard tasks. For bias removal and flat-field correction I used the task *ccdproc* utilizing sky-flat images taken during the evening or morning twillight. Differential magnitudes were calculated with aperture photometry using two comparison stars of

[1]IRAF is distributed by the National Optical Astronomy Observatories, which are operated by the Association of Universities for Research in Astronomy, Inc., under cooperative agreement with the National Science Foundation.

similar brightnesses. This was performed with the task *qphot* after determining the proper parameters for the aperture using *imexamine*.

I gained extensive experience in spectroscopy both in observations and reducing spectra. I granted 40 nights of telescope time on the 2.3 m telescope at Siding Spring Observatory where I have taken spectroscopic observations of mainly high-amplitude δ Scuti stars and Cepheids variables.

I reduced all of the spectroscopic data using standard tasks in IRAF. The reduction consisted of bias and flat field corrections (using *ccdproc*). The aperture extraction was done with tasks *apall* and *apsum* for the star spectra and the spectral lamps. For the wavelength calibration, I used the *identify* and *reidentify* tasks to indentify spectral lamp lines, then *refspectra* and *dispcor* tasks were used for the actual wavelength calibration of the observed star spectra. Continuum normalization was done with *continuum*. We checked the consistency of wavelength calibrations via the constant positions of strong telluric features, which verified the stability of the system.

Radial velocities were determined with the task *fxcor*, applying the cross-correlation method using a well-matching theoretical template spectrum from the extensive spectral library of Munari et al. (2005). I have also observed HD 187691 as a stable IAU velocity standard but extensive tests have shown that using model spectra from Munari et al. (2005) library produced more consistent results with the 2.3 m data. Depending on the signal-to-noise of the spectra, the estimated uncertainty of the radial velocities ranged from 1–5 km s^{-1} for the 2.3 m spectra. Radial velocities from the AAT and MH150 Echelle spectra have much better accuracy, $\leq$100 m s^{-1}.

For consistency, the radial velocities were all determined from a 50 Å region centered on the Hα line. The high-resolution spectra for BE Lyn and RS Gru allow us to compare hydrogen and metallic line velocities, which will be discussed in a future study.

The photoelectric photometry (ANU 24″ telescope) was reduced by Dr. L. L. Kiss and the transformation to the standard system using the coefficients from Berdnikov & Turner (2004) was calculated by me.

For the multiperiodic stars, we performed standard Fourier-analysis with prewhitening using Period04 (Lenz & Breger, 2005). Least-squares fitting of the parameters was also included and the S/N of each frequency was calculated following Breger et al. (1993).

Chapter 7

Binarity and multiperiodicity in high-amplitude δ Scuti stars

This chapter is reproduced from the paper *Binarity and multiperiodicity in high-amplitude δ Scuti stars* by **A. Derekas**, L. L. Kiss, T. R. Bedding, M. C. B. Ashley, B. Csák, A. Danos, J. M. Fernandez, G. Fűrész, Sz. Mészáros, Gy. M. Szabó, R. Szakáts, P. Székely, K. Szatmáry, 2009, Monthly Notices of the Royal Astronomical Society, in press

I wrote applications for telescope time and took about 90% of the observations (in total of about 60 nights). Other observations were made by Balázs Csák, José Fernandez, Szabolcs Mészáros, Gyula Szabó, Róbert Szakáts and Péter Székely. The reduction of the high-resolution spectroscopic data of RS Gru was done by Andrew Danos, while the BE Lyn data were reduced by Gábor Fűrész. Photoelectric observations with SSO60 were reduced with the code developed by László Kiss. All other photometric and spectroscopic data reductions were performed by me. I conducted all the analysis of the data.

Abstract

We have carried out a photometric and spectroscopic survey of bright high-amplitude δ Scuti (HADS) stars. The aim was to detect binarity and multiperiodicity (or both) in order to explore the possibility of combining binary star astrophysics with stellar oscillations. Here we present the first results for ten, predominantly southern, HADS variables. We detected the orbital motion of RS Gru with a semi-amplitude of $\sim$6.5 km s^{-1} and 11.5 days period. The companion is

inferred to be a low-mass dwarf star in a close orbit around RS Gru. We found multiperiodicity in RY Lep both from photometric and radial velocity data and detected orbital motion in the radial velocities with hints of a possible period of 500–700 days. The data also revealed that the amplitude of the secondary frequency is variable on the time-scale of a few years, whereas the dominant mode is stable. Radial velocities of AD CMi revealed cycle-to-cycle variations which might be due to non-radial pulsations. We confirmed the multiperiodic nature of BQ Ind, while we obtained the first radial velocity curves of ZZ Mic and BE Lyn. The radial velocity curve and the O–C diagram of CY Aqr are consistent with the long-period binary hypothesis. We took new time series photometry on XX Cyg, DY Her and DY Peg, with which we updated their O–C diagrams.

7.1 Introduction

δ Scuti stars are short-period pulsating variables of A-F spectral types, located at the intersection of the main sequence and the classical instability strip in the Hertzsprung-Russell diagram. Typical periods are in the order of a few hours with amplitudes less than 1 mag. A prominent group within the family comprises the high-amplitude δ Scuti stars (HADS), which have V-band amplitudes larger than 0.3 mag. Population II members of the group are also known as SX Phoenicis stars, often found in globular clusters (for a review of δ Scuti stars see e.g. Rodríguez & Breger (2001)).

HADS's are the short-period counterparts of the classical Cepheids, excited by the κ-mechanism and pulsating in one or two radial modes, usually in the fundamental and first-overtone modes (McNamara, 2000). The data in Rodríguez & Breger (2001) show that there is no rapidly rotating HADS ($v \sin i \leq 40$ km s^{-1}), suggesting an intimate relationship between the rotational state and the excitation of pulsations. In recent years, the number of HADS known with multimode oscillations has rapidly grown, hinting a new potential for asteroseismic studies of these objects (e.g. Poretti, 2003; Poretti et al., 2005). Several investigations suggested that some of the stars may have non-radial pulsation modes present (McNamara, 2000; Poretti et al., 2005). However, an important parameter in modeling stellar oscillations is the mass of the star, which is usually constrained from evolutionary models. This will inevitably lead to great uncertainties in any kind of modeling attempts, so that independent mass estimates could be of paramount importance. Thus, binary δ Scutis may play a key role in understanding oscillations of these stars.

There has been a great interest recently in δ Scuti stars that reside in eclipsing binary systems (e.g. Kim et al., 2003; Mkrtichian et al., 2006; Soydugan et al., 2006; Pigulski & Michalska, 2007; Christiansen et al., 2007). Currently, we know about 40 such δ Scutis, of which only one belongs to the HADS group (Christiansen et al., 2007). There are also a handful of non-eclipsing binary HADS (Rodríguez & Breger, 2001), usually deduced from the apparent cyclic period changes but with a few exceptions, like the single-lined spectroscopic binary SZ Lyn. The low number of binary δ Scutis suggests a strong observational bias, because one needs accurate observations with a long time span to detect multiplicity unambiguously (Rodríguez & Breger, 2001).

In this paper we present the results of our investigations into binarity and multiple periodicity in bright HADS variables. The sample was initially selected from the variable star catalogue of the Hipparcos satellite, which contains 21 "SX Phe" type stars (Perryman et al., 1997b). Of these, here we discuss 9 stars (and RY Lep in addition), i.e. our present sample contains almost half of all known bright HADS. Using a wide range of telescopes and instruments, we have been monitoring the target stars over the last five years, extending the earlier studies by our group (Kiss & Szatmáry, 1995; Kiss et al., 2002; Derekas et al., 2003; Szakáts, Szabó, & Szatmáry, 2008).

The paper is organized as follows. The observations and the data analysis are described in Sect. 2. The main discussion is in Sect. 3, in which the results for individual stars are presented. A brief summary is given in Sect. 4.

7.2 Observations and data reduction

The observed stars and their main observational properties are listed in Table 7.1. The full log of observations is given in Table A.1 in the Appendix. All data presented in this paper are available for download from the CDS, Strasbourg.

Observations were carried out using seven different instruments at five observatories in Australia, Hungary and the USA on a total of 65 nights between 2003 October and 2008 July. The telescopes and detectors used in this project are briefly described in Chapter 6.

Thanks to the dense sampling of the light curves, new times of maximum light for monoperiodic stars were easy to determine from the individual cycles. This was done by fitting fifth-order polynomials to the light curves around the maxima. We estimate

Table 7.1 The list of programme stars. The asterisks mark multiperiodic stars, for which this Table contains the dominant period only. References for the parameters are the following: (a) Rodríguez et al. (1996); (b) Rodríguez & Breger (2001); (c) Perryman et al. (1997b); (d) Kholopov et al. (1985-1988); (e) Szakáts, Szabó, & Szatmáry (2008); (f) Blake et al. (2003); (g) Rodríguez et al. (1995b); (h) Fu & Sterken (2003); (i) Derekas et al. (2003).

Star	Pop.[a]	V_{max}	V_{min}	P (days)	Obs.
RY Lep*	I	$8\overset{m}{.}20$	$9\overset{m}{.}10$	0.22514410[c]	$I/sp.$
AD CMi*	I	$9\overset{m}{.}21$	$9\overset{m}{.}51$	0.12297443[d]	$sp.$
BE Lyn	I	$8\overset{m}{.}60$	$9\overset{m}{.}00$	0.09586952[e]	$sp.$
DY Her	I	$10\overset{m}{.}15$	$10\overset{m}{.}66$	0.14863135[d]	V
XX Cyg	II	$11\overset{m}{.}28$	$12\overset{m}{.}13$	0.13486511[f]	V
BQ Ind*	II[b]	$9\overset{m}{.}78$	$10\overset{m}{.}05$	0.08200015[c]	I
ZZ Mic*	I	$9\overset{m}{.}27$	$9\overset{m}{.}69$	0.06718350[d]	$BV/sp.$
RS Gru	I	$7\overset{m}{.}92$	$8\overset{m}{.}51$	0.14701131[g]	$BVI/sp.$
CY Aqr	II	$10\overset{m}{.}42$	$11\overset{m}{.}16$	0.06103833[h]	$BVI/sp.$
DY Peg	II	$9\overset{m}{.}95$	$10\overset{m}{.}62$	0.07292630[i]	V

Table 7.2 New times of maximum (HJD-2400000).

Star	HJD_{max}	Filter	Star	HJD_{max}	Filter
RS Gru	52920.0196	V	CY Aqr	53334.9453	I
RS Gru	52921.9311	V	CY Aqr	53336.9592	I
RS Gru	52922.0772	V	CY Aqr	53337.9357	I
RS Gru	52923.9905	V	CY Aqr	54307.5293	V
RS Gru	52925.0188	V	CY Aqr	54308.5073	V
CY Aqr	52920.9223	V	XX Cyg	54307.4294	V
CY Aqr	52920.9827	V	XX Cyg	54309.4515	V
CY Aqr	52921.0439	V	XX Cyg	54677.3633	V
CY Aqr	52923.0587	V	DY Her	54304.4772	V
CY Aqr	52926.9643	V	DY Peg	54305.4731	V
CY Aqr	52927.0258	V			

the typical uncertainty to be about $\pm$0.0003 d. The new times of maximum light are listed in Table 7.2.

7.3 Results

7.3.1 RS Gruis

RS Gru (HD 206379; HIP 107231) is a monoperiodic HADS with a pulsation period of 0.147 d and a mean magnitude of $\sim$7.9 mag. Its light variation was first detected by Hoffmeister (1956) and studied later by Eggen (1956) and Oosterhoff & Walraven (1966). Kinman (1961) took photometric and spectroscopic observations and measured a mean velocity of 81 km s^{-1} with a velocity amplitude of $\sim$45 km s^{-1}. McNamara & Feltz (1976) obtained *uvby*β photometry and spectrographic data and determined physical parameters. van Citters (1976) acquired photoelectric radial velocity curves on two nights, while further photometric observations were taken by Dean et al. (1977). New radial velocity measurements taken by Balona & Martin (1978a) showed unambiguously the variation of the center-of-mass velocity, indicating the binary nature of RS Gru but the orbital period was not determined for nearly three decades. Further investigations were done by Breger (1980); Andreasen (1983); McNamara (1985); Antonello et al. (1986); Garrido, Garcia-Lobo, & Rodríguez (1990); Claret, Rodríguez, & Garcia (1990); Rodríguez et al. (1990). Period decrease was found by Rodríguez et al. (1995a,b) and physical parameters were also calculated by Rodríguez et al. (1995b). Joner & Laney (2004) took high-quality spectroscopic measurements and determined the radius and the absolute magnitude for RS Gru. They again showed unambiguously that RS Gru is a spectroscopic binary with an orbital period of approximately two weeks but no exact period was given.

We obtained standard BVI photoelectric photometry using SSO60 on 4 nights in 2003 and 1 night in 2004. For differential magnitudes we used two comparison stars: comp=HD 207193 ($V = 6.79$ mag, $B - V = 0.35$ mag) and check=HD 207615 ($V = 8.53$ mag, $B - V = 0.08$ mag). The full log of observations is given in Table A.1 and the light and colour variation are plotted in Fig. 7.1.

To measure the orbital period of the system, we obtained medium-resolution spectroscopy on 16 nights between 2003 and 2005 using the SSO230 instrument. In addition, we observed the star with the AAT on 1 night in 2006. The whole phased dataset

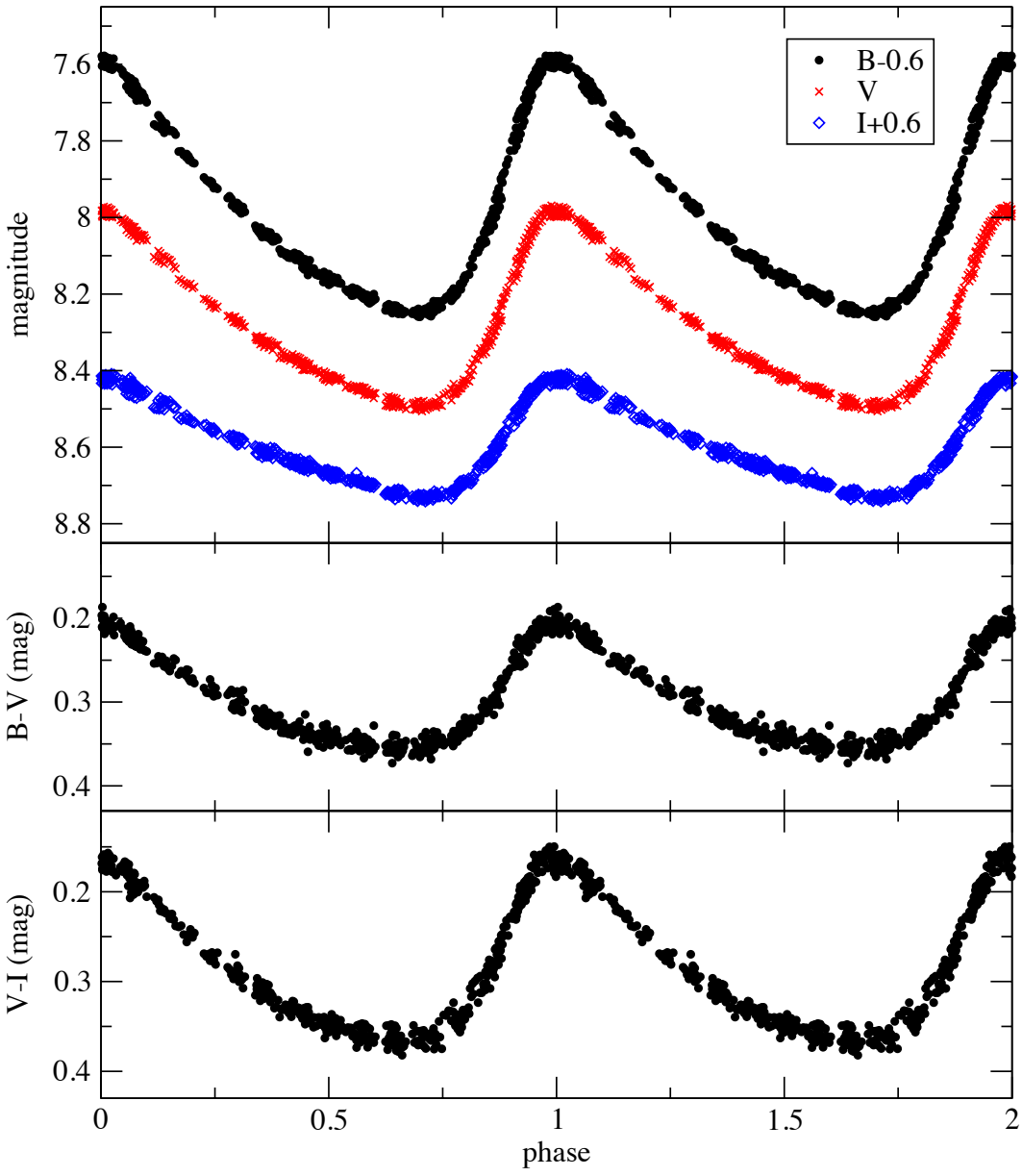

Figure 7.1 Standard light and colour variations of RS Gru (E_0=2452920.0196; P=0.14701131 d).

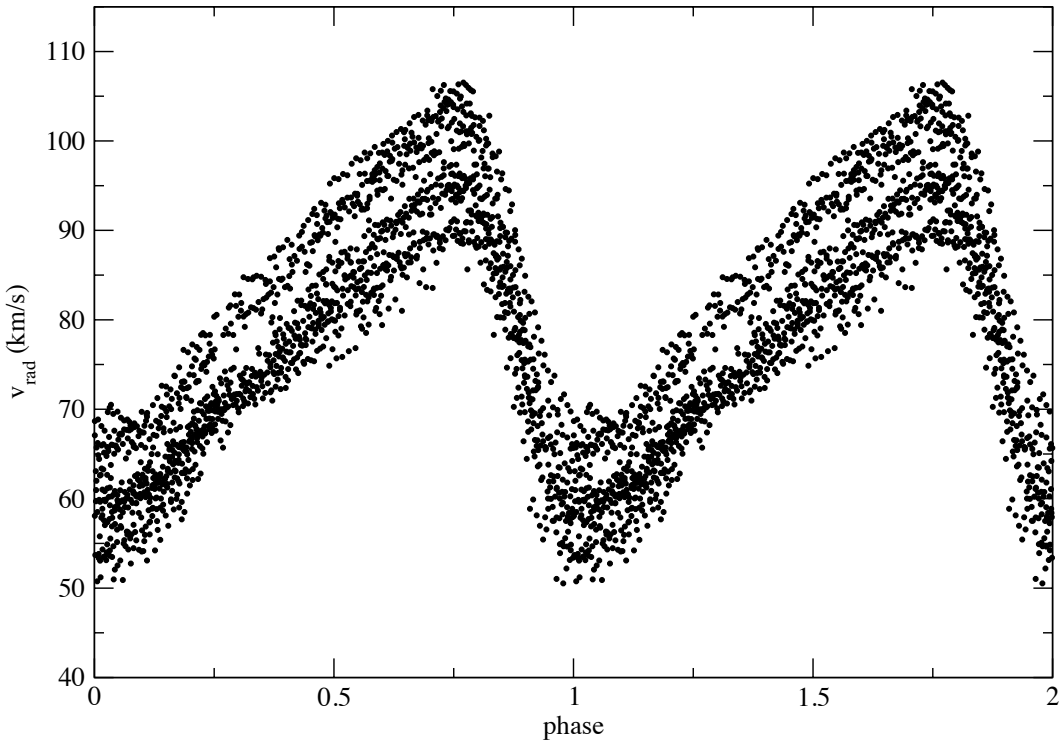

Figure 7.2 Radial velocities of RS Gru, phased with the pulsation period.

is shown in Fig. 7.2, where the continuously changing shift in the systemic velocity is evident.

We performed a period analysis of the radial velocities, which revealed the main pulsation frequency at f_1=6.802 c/d, its integer harmonics ($2f_1$, $3f_1$), and a low frequency component at about $\sim$0.11 c/d, corresponding to a period of 9 days. However, we did not accept this as the orbital period because the high-amplitude pulsation and random sampling may interplay and thus render the results unreliable. Therefore, we determined the orbital period as follows. First, we selected the best-defined single-night radial velocity curve to fit a smooth trigonometric polynomial to the phased RV data. Then we used the fixed polynomial to determine individual γ-velocities for each night by fitting the zero-point only. This way we could determine the center-of-mass velocity on 15 nights (listed in Table 7.3). The Fourier spectrum of the data (Fig. 7.3) shows a broad hump of peaks around 0.1 c/d with the highest peak at 0.087 c/d, which we identify as the most likely orbital frequency. The phased γ-velocities (Fig. 7.4) show a reasonably convincing sine-wave, for which the best-fit curve (solid line in Fig. 7.4) indicates a velocity amplitude of K=6.5 km s^{-1}.

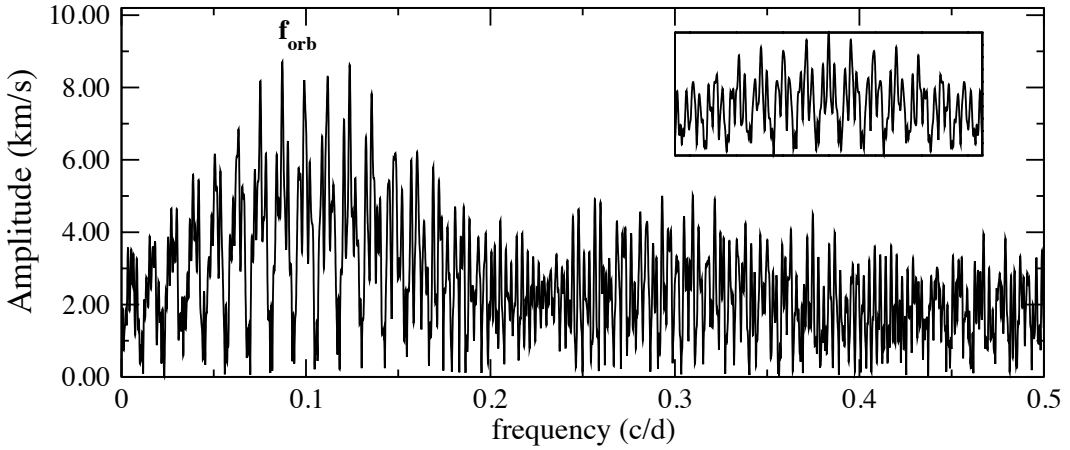

Figure 7.3 Fourier spectrum of the γ-velocities of RS Gru. Inset shows the spectral window.

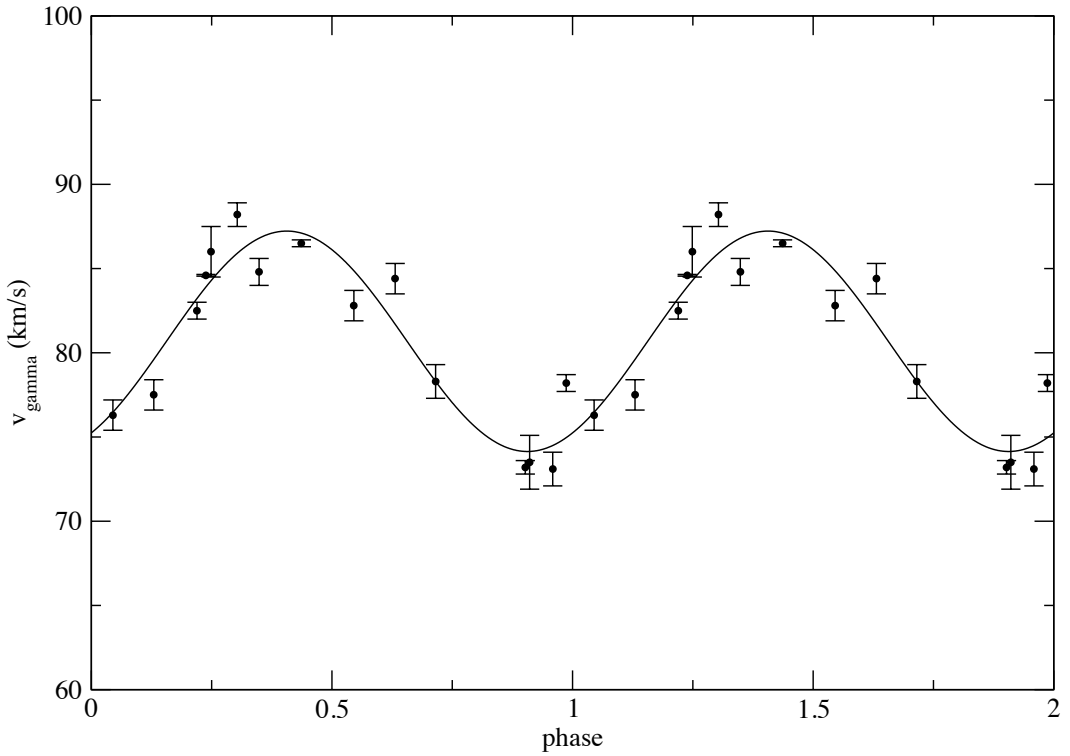

Figure 7.4 γ-velocity variation of RS Gru phased with $\mathrm{P_{orb}} = 11.5$ d.

Table 7.3 Center of mass velocities of RS Gru.

HJD-2 400 000 (d)	v_γ (km s^{-1})	HJD -2 400 000 (d)	v_γ (km s^{-1})
52922.0214	73.5±0.2	53524.2197	88.2±0.3
53274.1377	82.8±0.2	53600.0627	73.2±0.2
53275.1222	84.4±0.2	53601.0413	78.2±0.2
53276.0892	78.3±0.2	53604.0516	86.0±0.8
53520.2614	73.1±0.2	53605.1980	84.8±0.3
53521.2482	76.3±0.2	53606.2073	86.5±0.1
53522.2248	77.5±0.2	53937.2552	84.6±0.05
53523.2573	82.5±0.2		

Table 7.4 Estimated mass (M_2) for the companion of RS Gru.

	$M_1 = 1.5\ M_\odot$	$M_1 = 2\ M_\odot$	$M_1 = 2.5\ M_\odot$
Inclination (°)	M_2 ($M_\odot$)	M_2 ($M_\odot$)	M_2 ($M_\odot$)
90	0.09	0.11	0.13
70	0.10	0.12	0.14
50	0.12	0.15	0.17
30	0.20	0.24	0.27
10	0.66	0.78	0.89

From these, we can estimate the mass of the companion from the mass function (Hilditch, 2001): $f(M) = (1.0361 \times 10^{-7})(1-e^2)^{3/2}K^3P = M_2^3 \sin^3 i/(M_1+M_2)^2 = 3.3 \times 10^{-4} M_\odot$. Assuming that the δ Scuti mass is about 1.5–2.5 $M_\odot$, the calculated minimum mass for the companion at different inclinations is shown in Table 7.4. The derived masses show that the companion of the RS Gru is most likely a low-mass star. We can also estimate the semimajor axis of the system, which is about ∼0.1 AU ($a = 0.11$ AU at $M_2 = 0.09\ M_\odot$ and $a = 0.13$ AU at $M_2 = 0.89\ M_\odot$).

There is an interesting possibility to determine the pulsation constant, which is most useful for pulsating stars in eclipsing binaries, where the radius of the stars can be determined accurately (Jørgensen & Grønbech, 1978). Combining Kepler's third law and the pulsation constant formula:

$$\frac{a^3}{P_{\rm orb}^2} = \frac{G}{4\pi^2}\left(M_1 + M_2\right) \quad \text{and} \quad Q = P_{\rm pul}\left(\frac{M_1}{R_1^3}\right)^{\frac{1}{2}} \tag{7.1}$$

results in (using the same units):

$$Q = 0.1159\frac{P_{\rm pul}}{P_{\rm orb}}\left(\frac{R_1}{a}\right)^{-\frac{3}{2}}\left(1+\frac{M_2}{M_1}\right)^{-\frac{1}{2}} \tag{7.2}$$

Adopting $R_1 = 2.9 \pm 0.1 R_\odot$ (Balona & Martin, 1978a), $P_{\rm pul} = 0.147$ d, $P_{\rm orb} = 11.5$ d, $a = 0.12 \pm 0.01$AU, $M_1 = 2.0 \pm 0.1 M_\odot$ (Rodríguez et al., 1995b), $M_2 = 0.2 \pm 0.02 M_\odot$, the resulting $Q = 0.037 \pm 0.013$ d is consistent with pulsations in the radial fundamental mode. The dominant sources of error are the radius, the unknown inclination and the orbital semi-major axis, which pose a significant limitation at this stage. It is nevertheless reassuring that the given orbital period and size yield a consistent picture of RS Gru being a fundamental mode pulsator.

7.3.2 RY Leporis

The light variation of RY Lep (HD 38882; HIP 27400; V=8.2 mag; I=8.3 mag) was discovered by Strohmeier (1964) and the star was thought to be an eclipsing binary with an unknown period for more than two decades. The SIMBAD database still lists it as an eclipsing binary. Diethelm (1985) obtained five nights of observations which revealed the real HADS nature of this star. He determined the pulsation period as 0.2254 d and also noted small cycle-to-cycle variations, but the data were not sufficient to draw a firm conclusion. Rodríguez et al. (1995b) determined physical parameters based on one night of $uvby\beta$ observations, covering one pulsation cycle. Laney et al. (2002) found aperiodic or possibly multiperiodic variations and detected binary motion in the radial velocities with a period more than 500 days. Finally, Rodríguez et al. (2004) has shown unambiguously the multiperiodic nature of RY Lep (f_1=4.4416 c/d, f_2=6.60 c/d) and its binarity was also suggested from an analysis of the O–C diagram (details have not yet been published).

To study RY Lep photometrically, we obtained I-band CCD images on 20 nights between October 2004 and January 2005 using the APT50 instrument. We obtained more than 5000 data points with 10 s exposures. The full log of observations is given in Table A.1. For the aperture photometry we used two comparison stars: comp=GSC 05926-

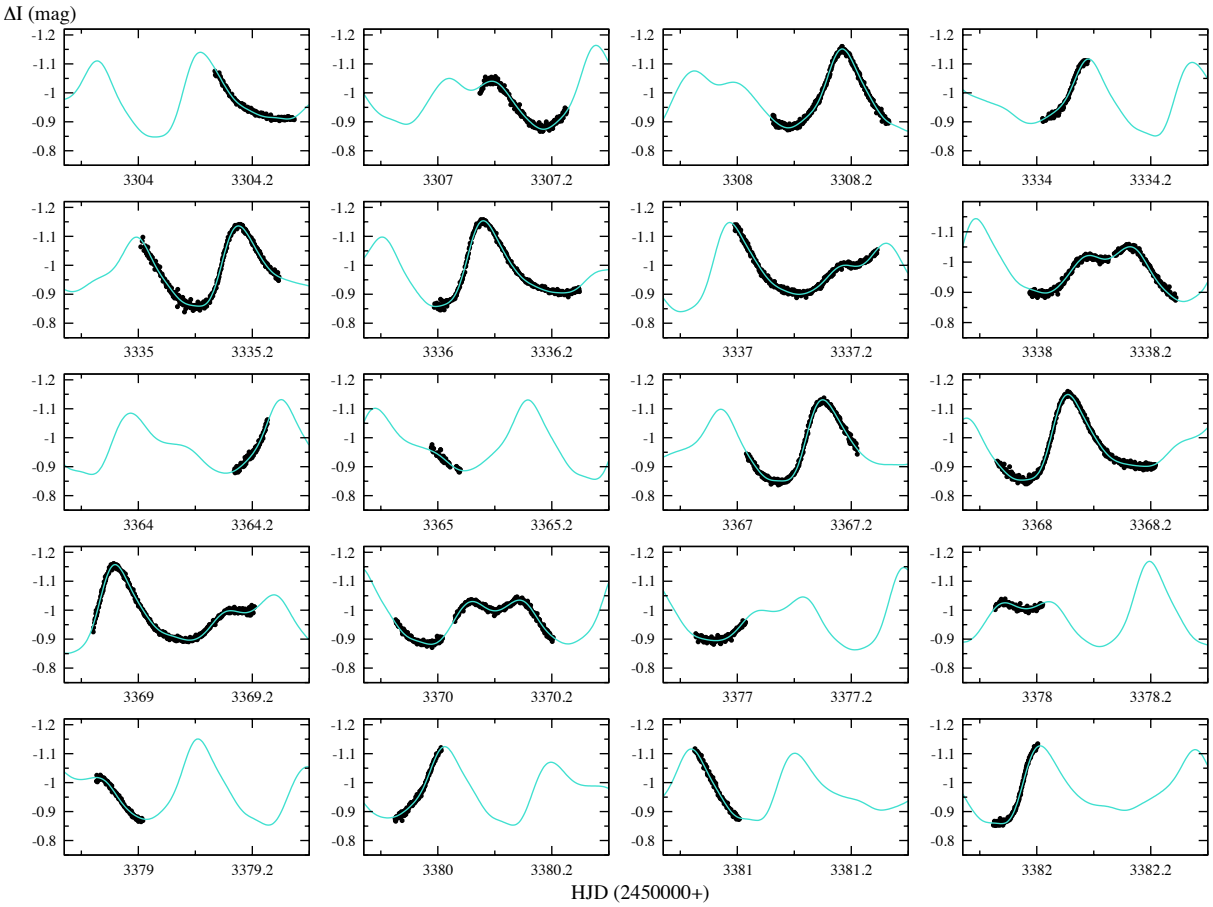

Figure 7.5 Individual light curves of RY Lep (small dots) with the light curve fit (continuous line).

01037 ($V = 9.98$ mag, $I = 9.34$ mag $B - V = 1.2$ mag), check=HD 39036 ($V = 8.21$ mag, $I = 8.72$ mag $B - V = 1.06$ mag).

We performed standard Fourier analysis of the data. Fig. 7.6 shows the results of the frequency search. We identified the two main pulsational frequencies at f_1=4.4415 c/d and f_2=6.5987 c/d. A further 14 statistically significant peaks were found in the data, which are mainly the various linear combinations of the two pulsation modes, and thereupon validating the pulsational nature of f_2. The results of the period analysis are summarised in Table 7.5. The final light curve fit is shown in Fig. 7.5.

The resulting frequencies (f_1, f_2) are in very good agreement with those by Rodríguez et al. (2004). We have two low-amplitude peaks that seem to be significant and may be related to pulsations (f_{14} and f_{15}), similarly to V743 Cen, AI Vel and VW Ari, where 3, 4 and 7 frequencies were detected, respectively (McAlary & Wehlau, 1979; Walraven,

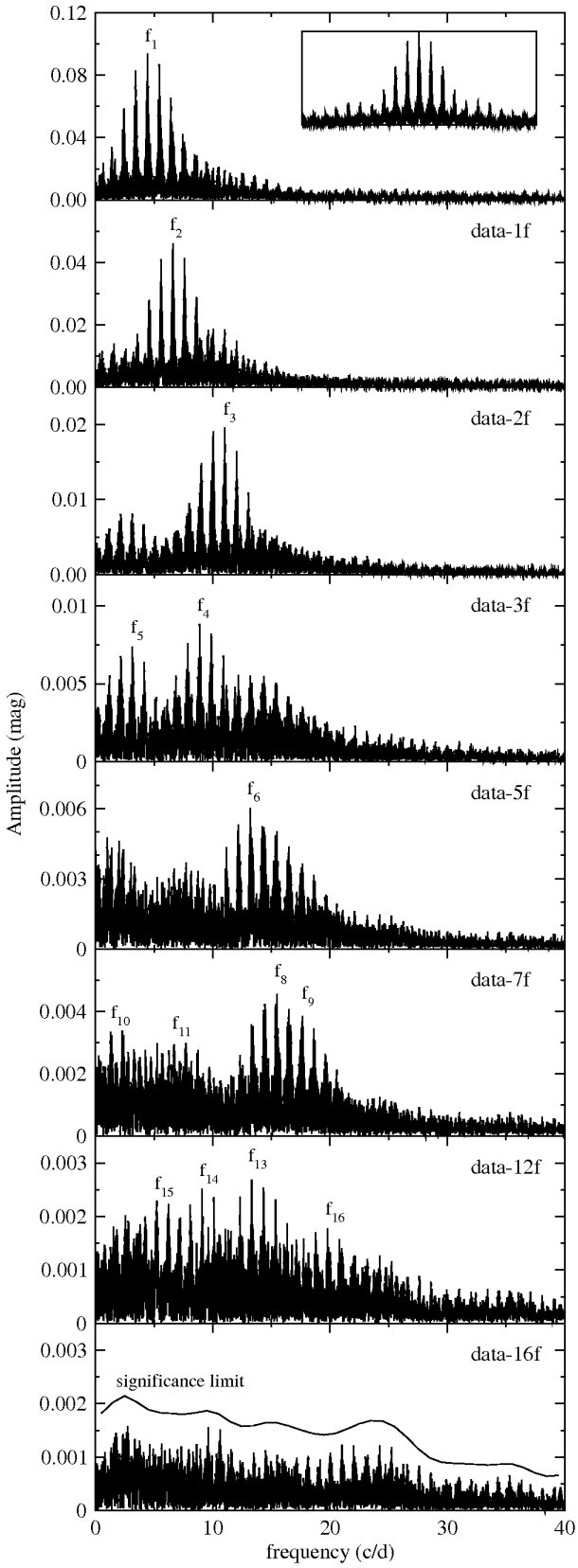

Figure 7.6 Amplitude spectra of 20 nights of I-band data for RY Lep. The insert shows the window function. From top to bottom, every panel shows an amplitude spectrum prewhitened with all frequencies marked in the panels above. 16 frequencies can be identified with S/N larger than 4.

Table 7.5 The result of the period analysis for RY Lep. f_1 and f_2 are the two pulsation modes, the remaining peaks are predominantly the harmonics or linear combinations of these two frequencies.

No.	Frequency (d^{-1})	Amplitude (mmag)	S/N	Frequency identification
		$\pm$0.4		
f_1	4.4415	96.8	204	
f_2	6.5987	46.6	103	
f_3	11.0402	19.3	42	$f_1 + f_2$
f_4	8.8830	10.5	24	$2f_1$
f_5	3.1600	10.2	20	$f_2 - f_1 + 1.0$
f_6	13.1978	5.3	14	$2f_2$
f_7	0.0046	5.0	12	?
f_8	15.4833	4.0	10	$2f_1 + f_2$
f_9	17.6382	3.7	10	$f_1 + 2f_2$
f_{10}	1.3962	5.6	12	?
f_{11}	6.7237	3.6	8	$3f_1 - f_2$
f_{12}	0.2379	3.4	8	?
f_{13}	13.3228	3.2	8	$3f_1$
f_{14}	9.0885	2.9	8	?
f_{15}	5.2661	3.5	8	?
f_{16}	19.7970	1.9	5	$3f_2$

Walraven & Balona, 1992; Liu et al., 1996). Three low-frequency components are presumably artifacts (f_7, f_{10} and f_{12}). The frequency ratio of f_1 and f_2 is 0.6731 which is not compatible with the usual scenario of fundamental and first overtone radial modes ($\mathrm{FU}/1\mathrm{O} \approx 0.77$). Rodríguez et al. (2004) identified f_1 with the fundamental mode and f_2 with a non-radial p_2 mode. The frequency ratio could also indicate first and third overtone radial modes, for which theoretical models predict $1\mathrm{O}/3\mathrm{O} \approx 0.68$ (Santolamazza et al., 2001), but the physical parameters of the star, such as temperature, luminosity and evolutionary mass, are not compatible with that possibility (Rodríguez et al., 1995b, 2004).

Looking at the pulsational amplitudes of RY Lep, one can notice some interesting features. In our data the amplitude ratio of the f_2 and f_1 frequencies is about 0.5. Contrary to this, observations by Rodríguez et al. (2004) implied a significantly lower amplitude ratio of about 0.1. If we use a transformation factor F$\approx$1.7 between the I-band and the V-band amplitudes (see fig. 2 of Balona & Evers (1999)), numbers in

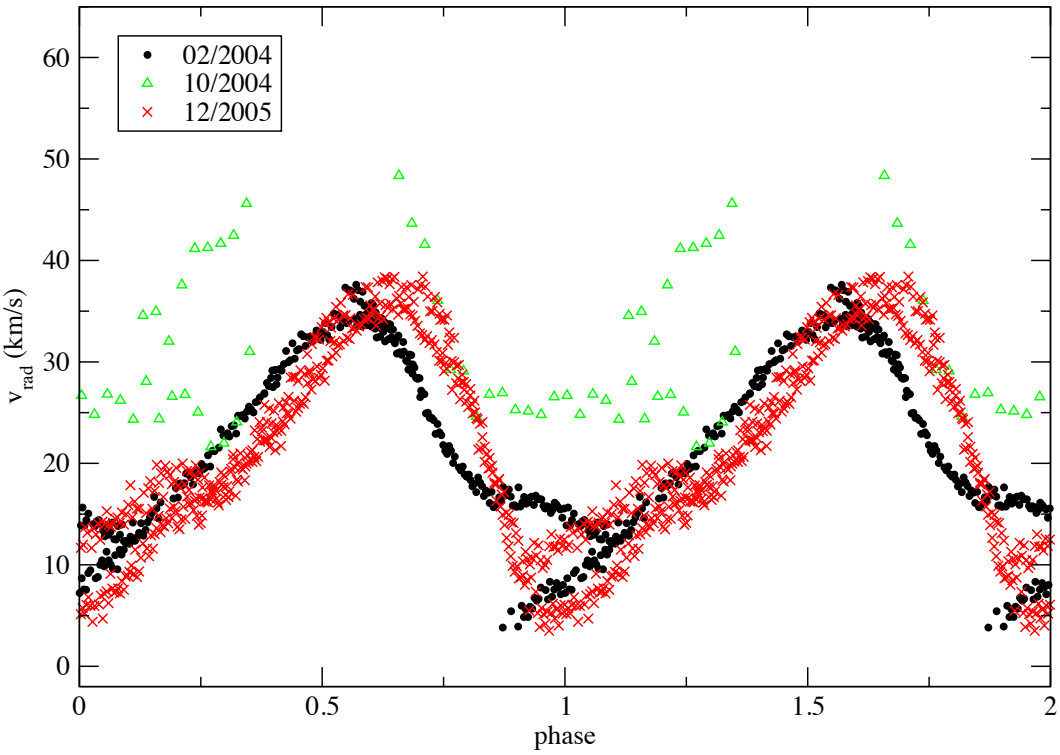

Figure 7.7 The RV curve of RY Lep phased with P=0.225 d. The data of 6 nights in 2004 and 2005 clearly show the ~ 25 km s^{-1} of γ-velocity shift between the two sets of observations. Note that the October 2004 dataset is binned.

Table 7.5 imply $\Delta V(f_1) = 164.6$ mmag and $\Delta V(f_2) = 79.2$ mmag. In comparison, the data in Rodríguez et al. (2004), obtained between 1998 and 2002, revealed $\Delta V(f_1) = 164.8$ mmag and $\Delta V(f_2) = 11.1$ mmag (Rodríguez, 2008, personal communication). We conclude that f_1 seems to be very stable in amplitude, whereas f_2 shows strong amplitude variations, with recent data implying an 8-times larger amplitude.

The first spectroscopic measurement of RY Lep was presented by Popper (1966), where the spectral type was determined as F0. Recently, Laney et al. (2002) found clear evidence for binary motion using radial velocity measurements but the data did not allow them to determine the orbital period which appeared to be longer than 500 days.

We obtained radial velocity measurements on four nights in 2004 and two in 2005. The RV curves of the seasonal datasets (February 2004, October 2004 and December 2005) phased with the main period (f_1) are presented in Fig. 7.7 with three different symbols.

The pulsation amplitude of RY Lep is about 30 km s^{-1} and its multiperiodic nature

causes cycle-to-cycle variations in the RV curves. The February 2004 and December 2005 datasets have basically the same γ-velocity values but the October 2004 dataset has a higher value by about 25-30 km s^{-1}. This leads to the conclusion that the orbital motion is clearly detected in the almost 700 day long dataset, which is in agreement with Laney et al. (2002) but still does not allow us to determine the orbital period. To estimate the approximate nature of the companion, we assumed that the orbital period is about 730 d (Laney, Joner, & Rodríguez, 2003) and took the full range of 25 km s^{-1} in v_γ as an estimate of the 2K$_1$ velocity amplitude. Repeating the same calculations as for RS Gru, the companion's mass is about 1.1$\pm$0.15 M$_\odot$ and the orbital semi-major axis is 2.3 AU, i.e. the companion is comparable to RY Lep in mass. The lack of noticeable spectral lines from the secondary may suggest a white dwarf but a firm conclusion would require spectra with broader coverage.

7.3.3 AD Canis Minoris

One of the best studied HADS is AD CMi (HD 64191; HIP 38473; V=9.38 mag), whose light variation was discovered by Hoffmeister (1934) and classified as an eclipsing binary by Zessewitch (1950). The first detailed study of the star was done by Abhyankar (1959) who took photometric and spectroscopic observations but the data were not sufficient to determine the radius using the Wesselink method. Further observations were obtained by Anderson & McNamara (1960); Epstein & Abraham de Epstein (1973); Dean et al. (1977); Balona & Stobie (1983). Breger (1975) used *uvby*β photometry to determine radius, mass and variations of physical parameters during the pulsation cycle, while McNamara (1985) found that the rotational velocity is smaller than 20 km s^{-1}. Fourier decomposition of the light curve (Antonello et al., 1986) showed a surprisingly high ϕ_{21} value, suggestive of overtone pulsation. However, the star seems to pulsate in fundamental mode as other monoperiodic HADS stars do (Kilambi & Rahman, 1993). There has been no explanation for this phenomenon. Kim (1990) and Kim & Joner (1994) determined the radius of AD CMi, using the visual surface brightness method and found a very good agreement with angular diameters from theoretical and empirical relationships. Kilambi & Rahman (1993) analysed 8 nights of $UBVR$ photometry and calculated physical parameters that agree well with Breger (1975) and suggested the star is lying on the cool-edge of the instability strip of the Population I stars. Jiang (1987) reported a continuous period increase at the star, which was confirmed by Rodríguez, Rolland, & Lopez de Coca (1988, 1990). The stability of light

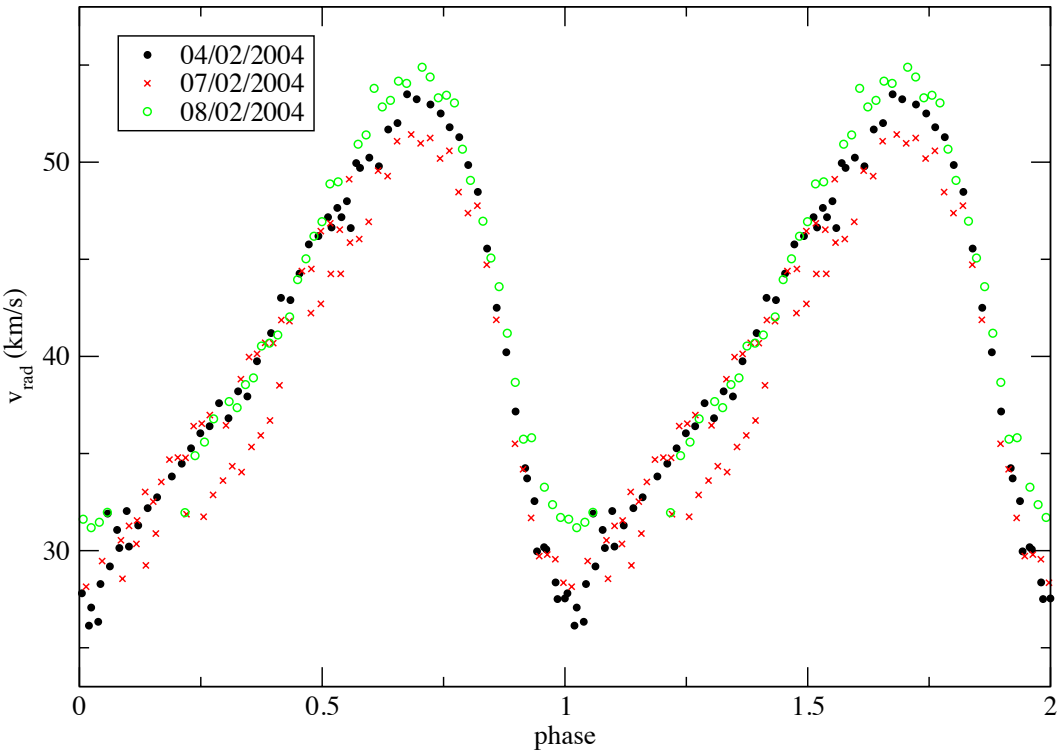

Figure 7.8 RV curve of AD CMi phased with the pulsation period (E_0=2449401.1320 d; P=0.12297443 d).

curve was studied by Rodríguez (1999) who found no significant long-term changes in amplitude. The first suggestion for binarity for AD CMi was presented by Fu & Jiang (1996), who found a possible orbital period of 30 years from the O–C diagram. Most recently, Hurta et al. (2007) and Khokhuntod et al. (2007) have studied the period variations of AD CMi using published and new data. They deduced the presence of light-time effect due to binarity and a slow period increase due to evolutionary effect. In addition, Khokhuntod et al. (2007) detected an extra low-frequency component in the photometric data, which provides a possible explanation for the large scatter of the O−C diagram.

We performed spectroscopic measurements on 3 nights in February 2004 (see Table A.1). The phased RV data (Fig. 7.8) have a mean amplitude of ∼25 km s^{-1}, while showing significant cycle-to-cycle variation. The mean velocity is about 40 km s^{-1}. Two radial velocity measurements are available in the literature (Abhyankar, 1959; Balona & Stobie, 1983). They determined γ-velocities at 34.5 km s^{-1} and 38.8 km s^{-1}, respectively. Hurta et al. (2007) interpreted the current O–C diagram as a combination of the

a continuous period increase and light-time effect. The amplitude of the orbital motion is expected to be about 1.1 km s^{-1} (Hurta et al., 2007). Considering this orbital amplitude, our data are in good agreement with Balona & Stobie (1983). The Abhyankar (1959) data, six points in total, are of lower quality and have poor phase coverage, so that the larger difference is still compatible with our result.

Petersen & Hog (1998) were the first to notice that AD CMi may be peculiar in terms of luminosity because the Hipparcos parallax indicated that the star, among five others, was situated approximately 3 mag below the standard P–L relation. They even suggested the possible existence of an "AD CMi group". We have checked the new reduction of the Hipparcos data (van Leeuwen, 2007). The updated parallax $\pi = 6.20 \pm 1.47$ mas differs by about 1-σ from the original value at $\pi_{\rm old} = 8.40 \pm 1.73$ mas. While the new value pushes the absolute magnitude of AD CMi about 1 mag brighter, there is still a significant shift left unexplained. Studies of HADS/SX Phe variables in clusters and nearby galaxies (e.g. Poretti et al., 2006) do not indicate this large spread in absolute magnitude, so that we suspect that there might be a yet-to-identify source of systematic error in some of the Hipparcos HADSs.

Our data also shows cycle-to-cycle variations in the shape of RV curve that are within a range of a 2-3 km s^{-1} as shown in the phase diagram in Fig. 7.8. This might be due to the presence of an additional pulsation mode but our data are not extensive enough to resolve multiple modes. If this secondary mode is the same one reported by Khokhuntod et al. (2007), its amplitude must change in time, because the very low amplitude in the Khokhuntod et al. (2007) data is hardly compatible with the $2-3$ km s^{-1} cycle-to-cycle RV change we find in the spectroscopic measurements. It is interesting to add that the Abhyankar (1959) data showed a larger peak-to-peak amplitude of about 35 km s^{-1}, which may also be due to cycle-to-cycle variations caused by a second excited mode.

7.3.4 BQ Indi

BQ Ind (HD 198830; HIP 103290) was discovered to be a variable by the Hipparcos satellite and has a mean magnitude V=9.8 mag, I=9.7 mag and a period of 0.0819877 d (Perryman et al., 1997a). The multiperiodic nature of the star first discovered by Sterken, Fu, & Brogt (2003), who determined two frequencies (f_1=12.1951 c/d, f_2=15.7686 c/d), corresponding to the fundamental and first overtone modes. Since then, no further observations have been reported in the literature.

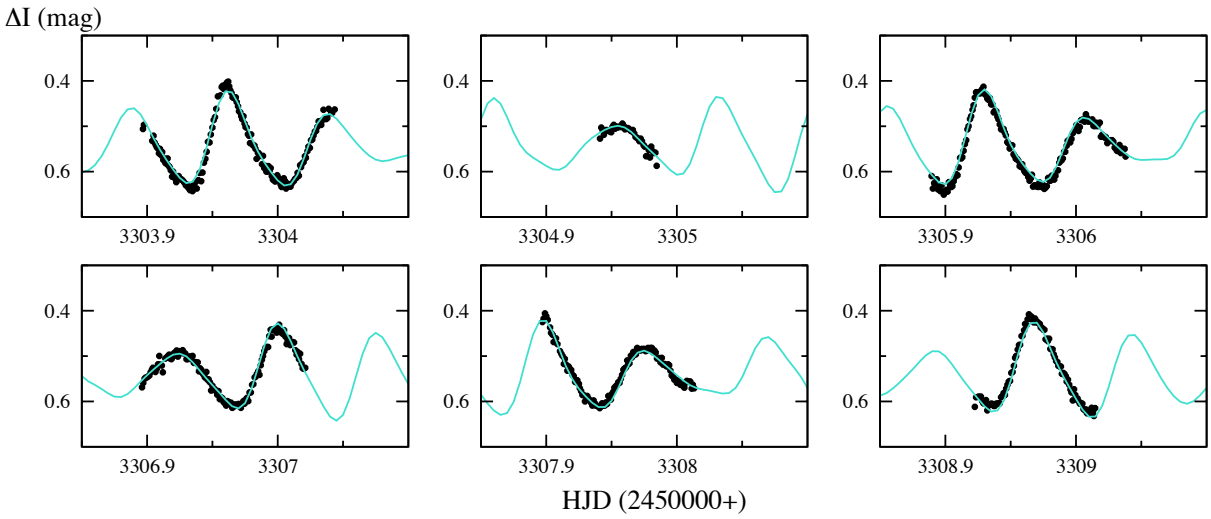

Figure 7.9 Individual light curves of BQ Ind (small dots) with the five-component fit.

We performed CCD photometry on BQ Ind on six consecutive nights in 2004 with APT50. More than 700 data points were obtained with 30-40 s exposure time in I-band; a log of observations is given in Table A.1. For the aperture photometry we used two comparison stars: comp=GSC 08800-00069 ($V = 10.6$ mag, $I = 9.51$ mag, $B - V = 1.28$ mag), check=PPM 774605 ($V = 10.5$ mag, $I = 9.34$ mag, $B - V = 1.38$ mag).

The amplitude spectrum is shown in Fig. 7.10. The primary peak was found at $f_1 = 12.1961\ d^{-1}$ and the next prewhitening step yielded the secondary frequency at $f_2 = 15.7593\ d^{-1}$. After subtracting the two main frequencies we ended up at their linear combination and then the integer harmonics ($2f_1$, $3f_1$) of the primary frequency. Their parameters are summarised in Table 7.6.

The resulting two frequencies (f_1, f_2) confirm the double-mode nature of BQ Ind, and are in very good agreement (within 1%) with the frequencies determined by Sterken, Fu, & Brogt (2003), with no further frequencies in the residuals. The period ratio is $f_1/f_2 = 0.7739$, which suggests fundamental (f_1) and first-overtone (f_2) mode pulsation. The Fourier-fit of the individual light curves is presented in Fig. 7.9.

7.3.5 ZZ Microscopii

The short-period variability of ZZ Mic (HD 199757; HIP 103684) was discovered by Churms and Evans (1961). Its average V magnitude is 9.43 mag and the pulsation pe-

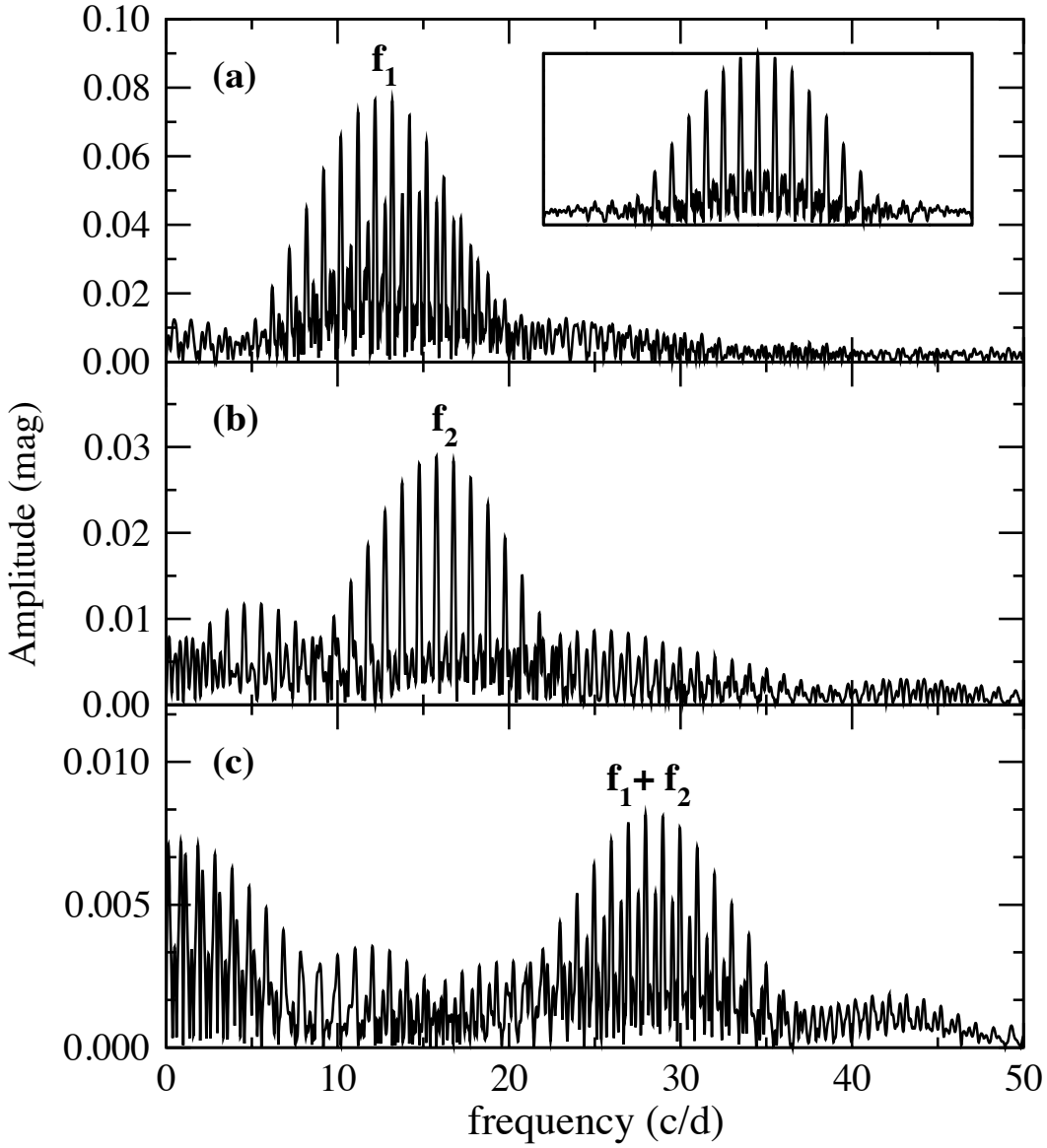

Figure 7.10 Fourier analysis of BQ Ind. Panel **a:** Amplitude spectrum of the complete dataset. The insert shows the window function. Panel **b:** After removal of the main period and its harmonics, the secondary period is clearly seen. Panel **c:** After removal of the secondary period, the next peak is the linear combination of the two frequencies.

Table 7.6 The result of the period analysis for BQ Ind.

No.	Frequency (d^{-1})	Amplitude (mmag)	S/N	Mode combination
		$\pm$1.1		
f_1	12.1961	71.1	54	
f_2	15.7593	30.2	29	
f_3	27.9580	9.0	6	$f_1 + f_2$
f_4	24.3903	10.4	7	$2f_1$
f_5	36.5671	2.9	5	$3f_1$

riod is 0.0654 d. The first detailed analysis of this star was done by Leung (1968), who found cycle-to-cycle variation in ultraviolet light and also detected a period decrease. Later the photoelectric observations and data analysis (Chambliss, 1971; Rodríguez, 1999) did not confirm any change in the light curve shape. Percy (1976) reanalysed Leung's observations and deduced two periods: 0.0654 d and 0.0513 d, suggesting fundamental and first overtone pulsations (Balona & Martin, 1978b). Previously, Bessell (1969) analysed spectrophotometric and spectroscopic observations and determined the pulsation constant, masses and absolute magnitudes, concluding the first-overtone pulsating nature of ZZ Mic. The first radius determination of the star was carried out by Balona & Martin (1978b). The last analysis of the star was done by Rodríguez (1999), who studied the stability of the light curve and did not find any significant long-term amplitude change.

We took three nights of photoelectric observations in 2004 using B, V filters on SSO60. For the calculations of differential magnitudes we used the following two comparison stars: comp=HD 199639 ($V = 7.28$ mag, $B - V = 0.16$ mag) and check= HD 200320 ($V = 8.96$ mag, $B - V = 0.51$ mag). The phase diagrams are shown in Fig. 7.11.

Since the discovery of ZZ Mic, it has been controversial in terms of changing light curve shape and being multiperiodic. In order to study the question, we performed a period analysis of our admittedly meagre V-band data. The pre-whitening steps are plotted in Fig. 7.12, while the resulting parameters are listed in Table 7.7. The Fourier spectrum is dominated by the main pulsational period (f_1 =14.896 c/d) and its harmonic. With a much lower amplitude (A_3 =14 mmag compared to A_1 =147.3 mmag) we detected a secondary period at f_3 =19.15 c/d which is a reasonably good agreement

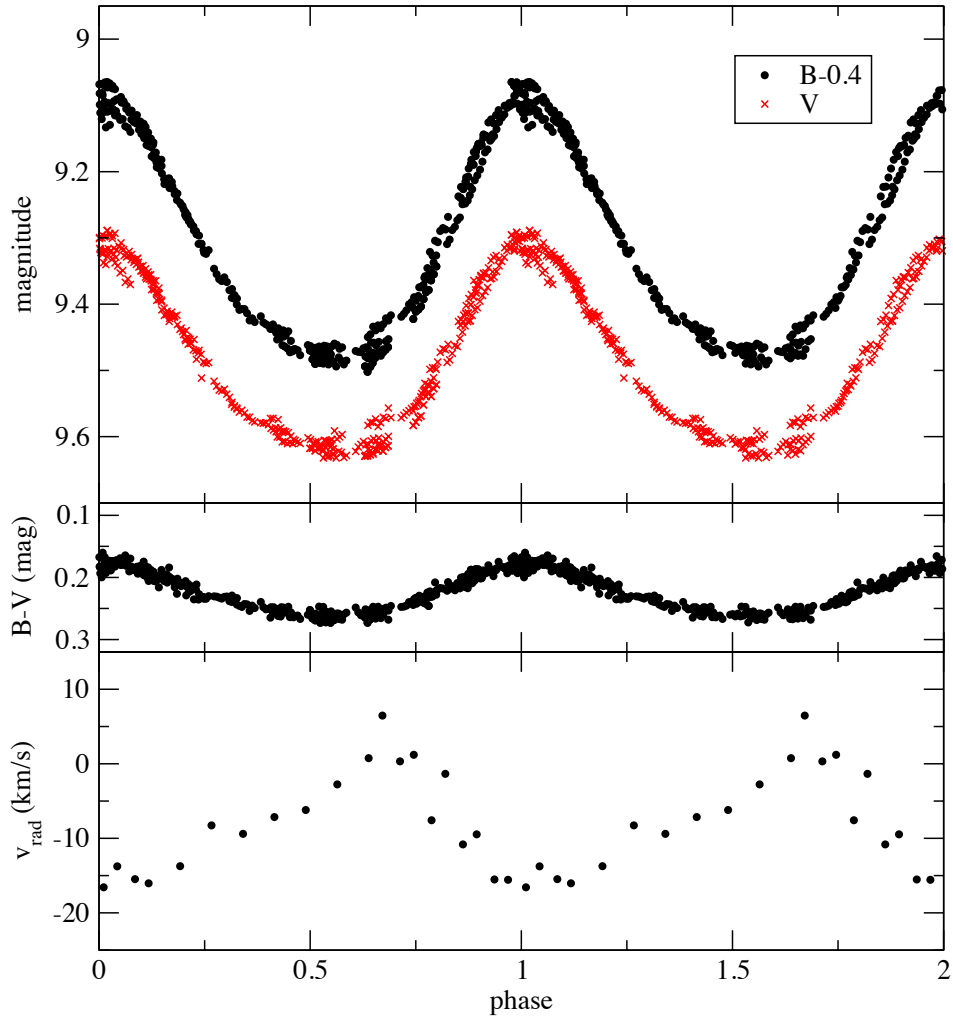

Figure 7.11 Standard light, colour and radial velocity variations of ZZ Mic (E_0=2453305.9819 d; P=0.0671835 d).

with that of Percy (1976) (f_1 =15.3 c/d, f_2 =19.5 c/d). The S/N ratio of this frequency is 8, which is quite low compared to f_1 and $2f_1$ but still above the significance limit.

Because of the limited data we have, we tried to detect the secondary frequency in other publicly available data. We analysed the data from the All Sky Automated Survey (ASAS) project (Pojmański, 2002). The Fourier spectrum of this data (Fig. 7.13) clearly shows the main pulsational period at f_1 =14.885 c/d but the noise level in the dataset (∼23 mmag) is too high compared to the amplitude of the secondary frequency (∼14 mmag), which prevents any detection in the ASAS data.

If we accept f_3 as an independent mode, the ratio of the two modes is f_1/f_3 =

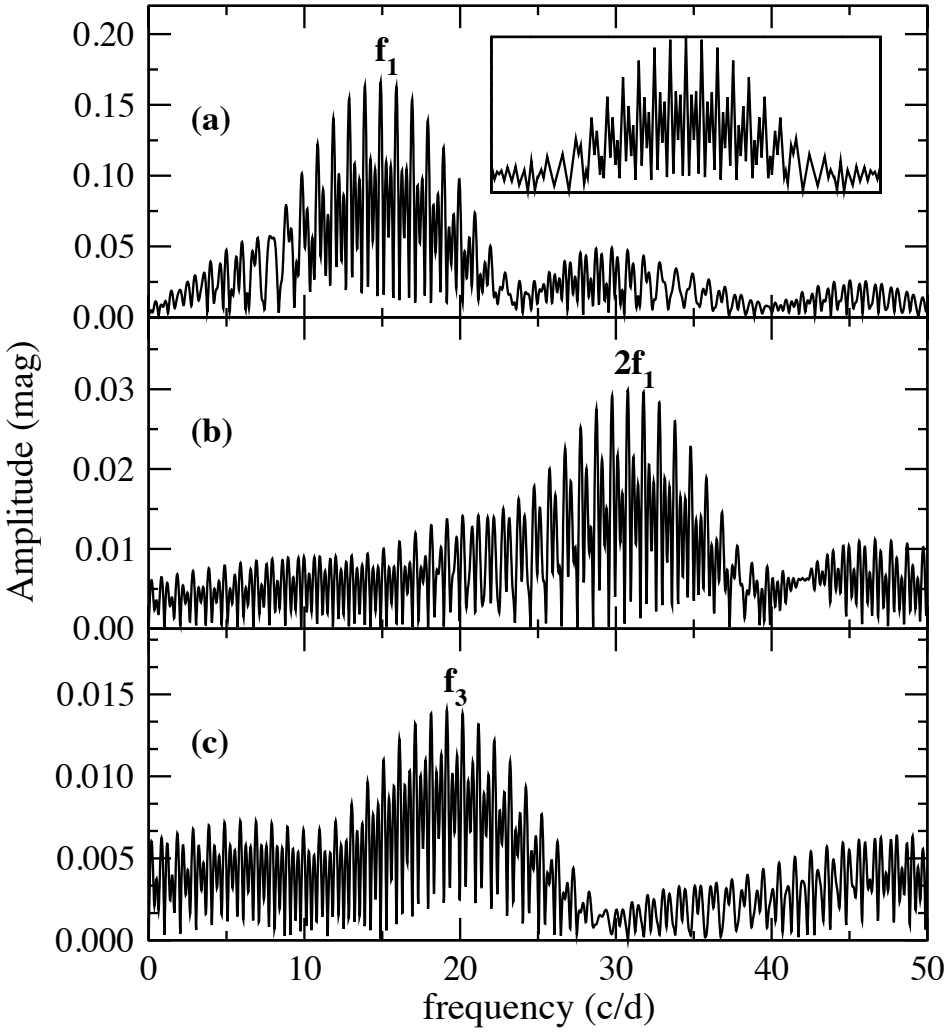

Figure 7.12 Fourier spectra of ZZ Mic with the pre-whitening steps. The insert shows the spectral window.

Table 7.7 The result of the period analysis for the ZZ Mic.

No.	Frequency (d^{-1})	Amplitude (mmag)	S/N	Mode combination
		$\pm$1.4		
f_1	14.896	147.3	85	
f_2	30.77	29.7	42	$2f_1$
f_3	19.15	14	8	

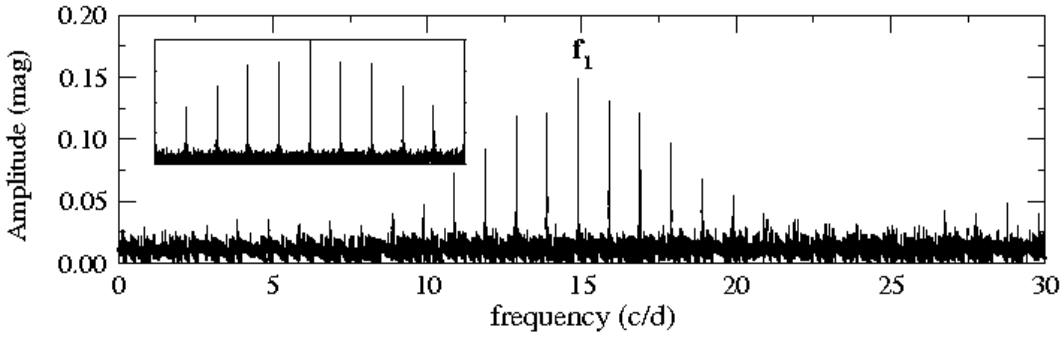

Figure 7.13 The Fourier spectrum of ZZ Mic using the ASAS data. The insert shows the spectral window.

0.778. This suggests f_1 is the fundamental mode and f_3 is the first overtone mode. The fundamental mode identification for f_1 is strongly supported by the $ubvy\beta$ photometry of Rodríguez, Lopez-González, & Lopez de Coca (2000). Moreover, f_1 must be a radial mode which was suggested from the phase shifts in BV photometry by Rodríguez et al. (1996).

Moreover, a period ratio of 0.778 seems to be too large for a normal Pop. I HADS (Poretti et al., 2005; Petersen & Christensen-Dalsgaard, 1996) which suggests that ZZ Mic is a Pop. II star. However, the value of f_3 is not too reliable, so the period ratio might be slightly different. Studies on metal abundances and space motions (Breger, 1980) suggest that ZZ Mic is a normal Pop. I HADS, which is also supported by Rodríguez, Lopez-González, & Lopez de Coca (2000).

We obtained spectra simultaneously with BV light curves on one night using SSO230. The resulted RV curve is shown in the bottom panel of Fig. 7.11, which is the first radial velocity curve obtained of ZZ Mic. The full amplitude of the RV curve is 22 km s^{-1}.

7.3.6 CY Aquarii

CY Aqr (HIP 111719; V=10.7 mag, I=10.3 mag) is one of the shortest period HADS in the galactic field, with a pulsation period of 0.061038d, and has been subject to many investigations. It was discovered by Hoffmeister (1935). A number of early studies on the star are listed by Hardie & Tolbert (1961), who estimated physical parameters and found that the shape of the light curve varies. The period stability was studied by Ashbrook (1954), who found no change in period but noticed a phase jump that seemed to

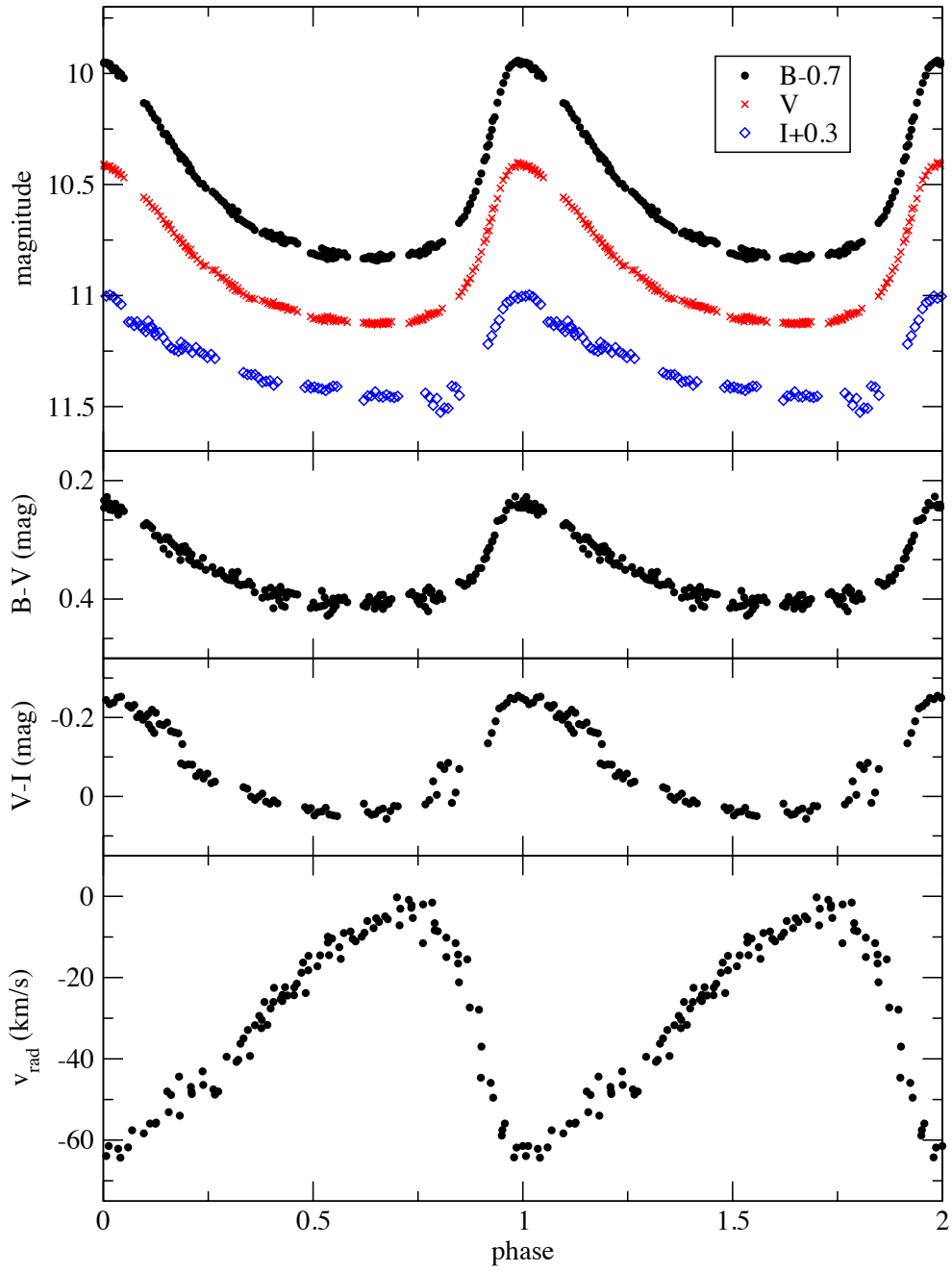

Figure 7.14 Standard light, colour and radial velocity variations of CY Aqr (E_0=2452920.9223 d; P=0.061038328 d).

be attributed to the star. Further studies were made by Zissell (1968); Nather & Warner (1972); Bohusz & Udalski (1980). Changes in light curve shape and the possibility of another period were also investigated in several papers, e.g. Elst (1972); Fitch (1973); Figer (1978) but both phenomena were discounted later by Geyer & Hoffmann (1975); Percy (1975); Purgathofer & Schnell (1984); Hintz & Joner (1997). Finally, Coates et al. (1994) set a definite upper limit of 1.5 mmag in V for the amplitude of any long-lived secondary period.

Kämper (1985) made a thorough period study and his results indicated the presence of random fluctuations in pulsation frequency that cannot be explained by considering only evolution. Other period change studies were performed by Rolland et al. (1986); Mahdy et al. (1988); Powell, Joner & McNamara (1995). McNamara, Powell, & Joner (1996) determined physical properties. Fu, Jiang, & Liu (1994) suggested that the period changes due to the presence of an unseen companion with an orbital period of around 50 years. Zhou, Fu, & Jiang (1999) and Fu & Sterken (2003) studied the O–C diagram to characterize long-term period evolution. They found a long-term cyclic component, and both suggested possible binarity for CY Aqr with an orbital period of $\sim$62.4 yr and $\sim$52.5 yr, respectively.

We obtained 3 nights of standard BVI photoelectric, 5 nights I-band and 2 nights CCD V-band photometry with SSO60, APT50 and P60 between 2003 and 2007. The integration time was 15s with SSO60 and 50s with the APT50. The full log of observations is given in Table A.1. Differential magnitudes were calculated using the following comparison stars: comp=GSC 00567-02242 ($V = 9.8$ mag, $I = 8.96$ mag, $B-V = 1.38$ mag) and check=GSC 00567-01242 ($V = 10.6$ mag, $I = 9.62$ mag, $B - V = 1.14$ mag). The resulting light and colour curves are plotted in the top three panels of Fig. 7.14. We determined new times of maximum that are listed in Table 7.2. The O–C diagram (not shown) is in a very good agreement with light-time solution determined by Fu & Sterken (2003).

We obtained spectroscopic observations on two nights in 2003 and 2004. The mean radial velocity is –38 km s^{-1}. This value is in a good agreement with previous data by Struve (1949) and Fernley et al. (1987), who measured –32 km s^{-1} and –40 km s^{-1}, respectively. The predicted amplitude of mean velocity change due to the binarity is $\sim$1.4 km s^{-1} (Zhou, Fu, & Jiang, 1999) which is comparable to the accuracy of our observation. Furthermore, due to the high eccentricity and long period of the binary system, the mean velocity changed only slightly in the last 10 years, which is far beyond

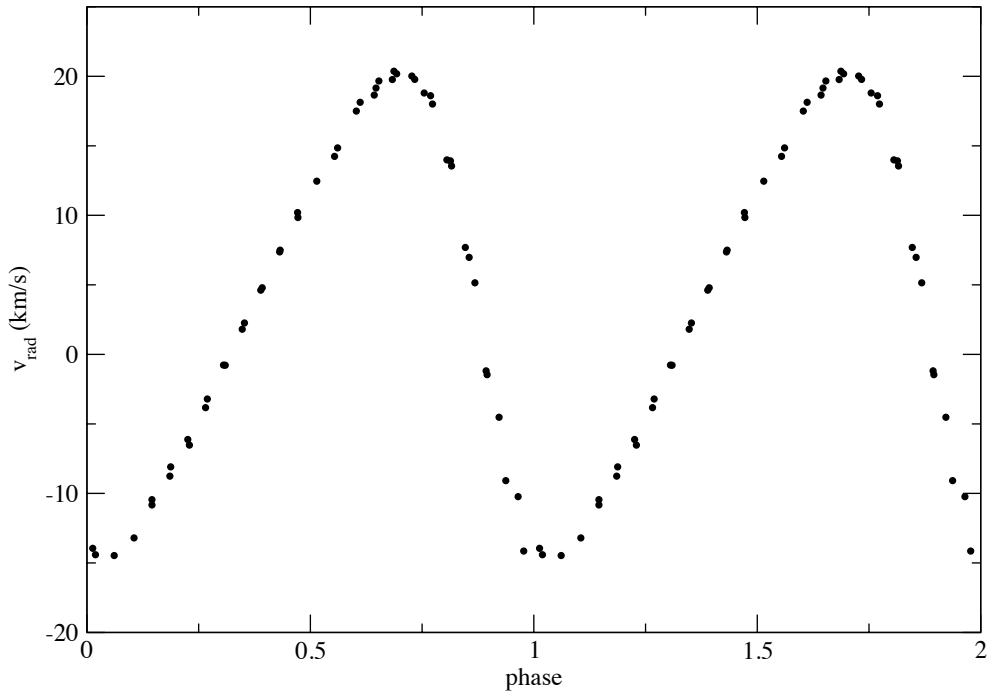

Figure 7.15 Phased RV curve of BE Lyn (HJD=2449749.4651 d, P=0.09586952 d).

our detection limit. In conclusion, our radial velocity observations do not contradict the current understanding of the nature of CY Aqr.

7.3.7 BE Lyncis

We obtained high-resolution spectroscopy of BE Lyn on three nights with MH150 in order to detect possible binarity or additional pulsational frequencies. The period change of this star inspired a series of studies by our group (Kiss & Szatmáry, 1995; Derekas et al., 2003; Szakáts, Szabó, & Szatmáry, 2008) and, while the initial orbital elements of the suspected binary system were ruled out and hence leaving the binarity unconfirmed, the lack of spectroscopic data in the literature has kept this star in our focus.

To our knowledge, our radial velocity measurements are the first obtained for BE Lyn. The phased RV curve is shown in Fig. 7.15, where we see characteristic shape and velocity amplitude for fundamental mode pulsation. The center-of-mass velocity is measured at 3.4 km s^{-1}, while the amplitude of the variation is $\sim$34 km s^{-1}. There is no sign of gamma velocity change during the three nights of observation and we also could not detect any non-radial mode pulsation in the RV curve. Further study of the

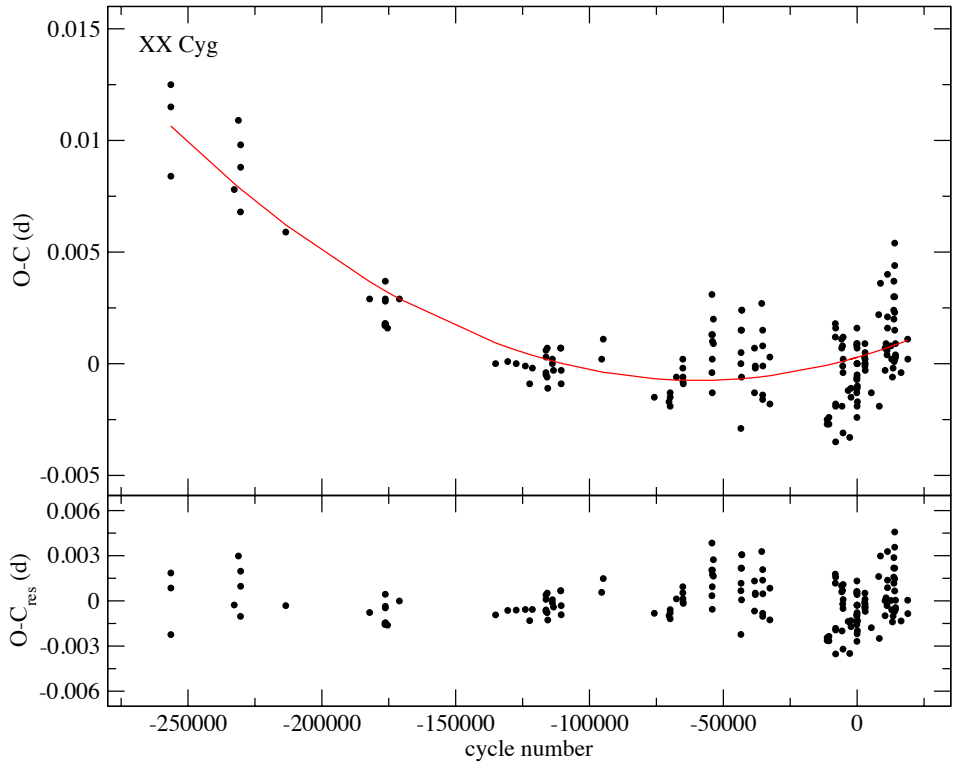

Figure 7.16 O–C diagram of XX Cyg.

data in terms of velocity gradient within the stellar atmosphere is in progress.

7.3.8 Period updates for XX Cygni, DY Pegasi and DY Herculis

We performed times-series photometry on XX Cyg, DY Peg and DY Her. Previous studies of these stars are listed in Derekas et al. (2003). Since then, only DY Peg was studied by Hintz et al. (2004), who explained the period change of the star with two period breaks rather than continuously decreasing rate, as was previously thought.

We obtained 3 nights of V-band CCD photometry on XX Cyg with P60 and Sz40 and 1-1 night on DY Her and DY Peg with P60 during 2007 and 2008. The journal of observations is given in Table A.1. We determined new times of maximum that are listed in Table 7.2. The updated O–C diagrams contain these and recently published data collected from the literature (Agerer & Hübscher, 2003; Hübscher, 2005; Hübscher, Paschke & Walter, 2005; Bíró et al., 2006; Hübscher, Paschke & Walter, 2006; Klingenberg, Dvorak, & Robertson, 2006; Hübscher, 2007; Hübscher & Walter, 2007).

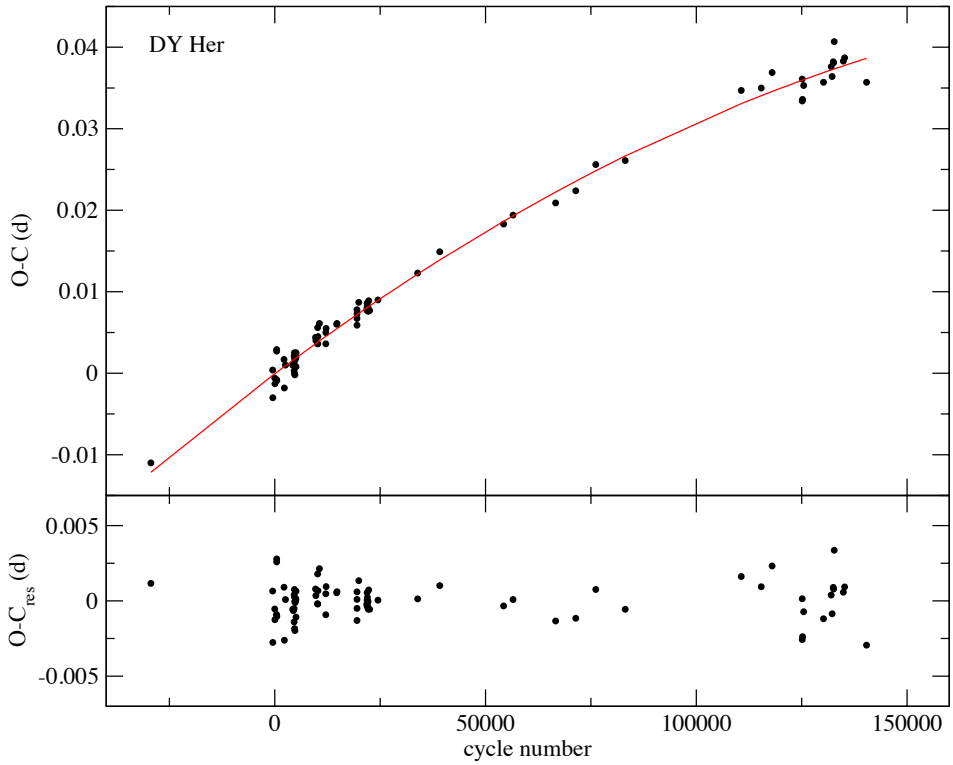

Figure 7.17 O–C diagram of DY Her.

We calculated the O–C diagram of XX Cyg using the following ephemeris (Derekas et al., 2003):

$$\mathrm{HJD}_{\max} = 2451757.3984 + 0.13486513 \times E \tag{7.3}$$

and the resulting diagram is shown in Fig. 7.16. The parabolic fit form of the O–C diagram is:

$$\mathrm{HJD}_{\max} = 0.0003 + 3.49 \times 10^{-8} E + 2.93 \times 10^{-13} E^2 \tag{7.4}$$

with an rms of 0.00152 d. The second-order coefficient corresponds to a relative rate of period change $\frac{1}{P}\frac{dP}{dt} = 1.17 \times 10^{-8}\mathrm{yr}^{-1}$, which is only slightly different from the value of $1.13 \times 10^{-8}\mathrm{yr}^{-1}$ given by Blake et al. (2003). Therefore, we can conclude that the period of XX Cyg has been increasing at a same rate of the last few years. The residuals have no signs of any other change.

The O–C diagram of DY Her was calculated with the following ephemeris (Derekas et al., 2003):

$$\mathrm{HJD}_{\max} = 2433439.4871 + 0.1486309 \times E. \tag{7.5}$$

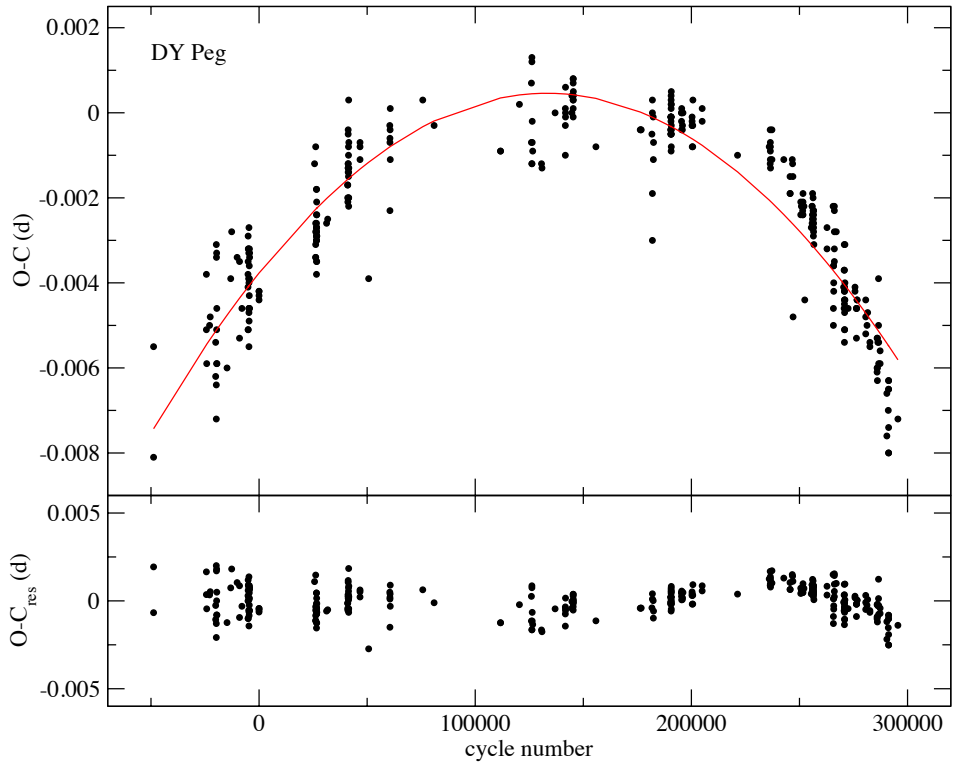

Figure 7.18 O–C diagram of DY Peg.

The diagram is shown in Fig. 7.17. The O–C diagram was fitted with a parabolic form of

$$\mathrm{HJD}_{\mathrm{max}} = -0.001(3) + 3.98 \times 10^{-7} E - 8.98 \times 10^{-13} E^2 \tag{7.6}$$

with an rms of 0.0013 d, which gives $\frac{1}{P}\frac{dP}{dt} = -2.96 \times 10^{-8}\mathrm{yr}^{-1}$. This is 6% difference in the rate of period change previously given by Derekas et al. (2003). The residuals do not show any other period change, so we can conclude that the present results in period change is very well agreed with the previous studies of DY Her and the star is showing continuous slow period decrease.

Finally, we also updated the O–C diagram of DY Peg using the following ephemeris (Mahdy, 1987):

$$\mathrm{HJD}_{\mathrm{max}} = 2432751.9655 + 0.072926302 \times E \tag{7.7}$$

and shown the final O–C diagram in the bottom panel of Fig. 7.18. We performed a parabolic fit of the diagram that resulted in the following form:

$$\mathrm{HJD}_{\mathrm{max}} = -0.003(8) + 6.34 \times 10^{-8} E - 2.38 \times 10^{-13} E^2 \tag{7.8}$$

with an rms of 0.0008 d. From this, we derived $\frac{1}{P}\frac{dP}{dt} = -3.27 \times 10^{-8}\mathrm{yr}^{-1}$ which is in a good agreement with Mahdy (1987), Peña, González & Hobart (1987) and Derekas et al. (2003). The residuals of the O–C diagram show some signs of cyclic change over 100 000 cycles but the present data are insufficient to draw a firm conclusion.

7.4 Summary

We have carried out multicolour photometry and medium- and high-resolution spectroscopy of ten bright high-amplitude δ Scuti stars over 5 years. Our aim was to detect binarity and/or multiperiodicity in HADS variables in order to deepen our knowledge of interaction between oscillations and binarity.

To put our binary targets in a broader context, we have compiled a complete list of binary HADS variables, presented in Table 7.8. How do RS Gru and RY Lep, the two newly confirmed spectroscopic binaries, compare with other known systems? Looking at the 8 stars in Table 7.8, we can see three distinct groups with markedly different orbital periods. RS Gru is one of the shortest-period binary and it is interesting to note that neither UNSW-V-500 nor RS Gru show evidence of multimode pulsations. RY Lep is similar to SZ Lyn both in the orbital period and the reasonably large mass of the companion. These intermediate-period systems are also promising for detecting spectral features of the companion in the ultraviolet or infrared region, thus allowing a full dynamical mass determination. To be able to detect spectroscopically the binary nature of the long-period systems, will require very high-precision spectroscopy, since the expected v_γ change is in the range of 1 km s^{-1}.

To summarise, the main results of this paper are the follows:

1. We monitored RS Gru spectroscopically on 17 nights in order to measure the orbital period. We derived the orbital period as 11.5 days.
2. We confirmed the multimode pulsation of RY Lep from CCD photometry, detecting and refining the frequencies of two independent modes. Spectroscopic measurements also show the multimode pulsation. We detected the orbital motion in the radial velocity curve, confirming the preliminary results of Laney et al. (2002) on the binary nature of RY Lep. Our 700 day-long dataset is in good qualitative agreement with Laney et al. (2002). The limits on the orbital period and RV amplitude suggest a binary companion of about 1 $M_\odot$, possibly a white dwarf star.

Table 7.8 Summary of the estimated masses of the companions in the known HADS binary systems. Sources for $P_{\rm orb}$ and masses are: (1) Christiansen et al. (2007), (2) Moffett et al. (1988), (3) Fu et. al (2008) (4) Fu & Jiang (1999), (5) Hurta et al. (2007), (6) Fu, Sterken & Barrera (2004).

Star	$P_{\rm orb}$	$m_{\rm comp}(M_\odot)$	Refs.
UNSW-V-500	5.35 d	$\sim$0.3	1
RS Gru	11.5 d	0.1–0.2	present paper
RY Lep	730 d:	$\sim$1.1	present paper
SZ Lyn	3.2 yr	0.7–1.6	2
KZ Hya	26.8 yr	0.83–3.4	3
BS Aqr	31.7 yr	0.1–0.33	4
AD CMi	42.9 yr	0.15–1.0	5
CY Aqr	52.5 yr	0.1–0.76	6

3. The radial velocity curve of AD CMi shows cycle-to-cycle variations that support the presence of a low frequency mode pulsation reported by Khokhuntod et al. (2007). The center-of-mass velocity is in good agreement with the previous measurement by Balona & Stobie (1983) and does not contradict the binary hypothesis of the star, since the predicted γ-velocity change is around 1 km s^{-1}.

4. We obtained the first spectroscopic measurements for BE Lyn. The RV curve has an amplitude of $\sim$34 km s^{-1} and the center-of-mass velocity is 3.4 km s^{-1}.

5. We confirmed the double-mode nature of BQ Ind, corresponding to the fundamental and first overtone modes.

6. We detected a low-amplitude secondary period in the photometry of ZZ Mic but further observations are needed to confirm its validity. The RV curve has a full amplitude of 22 km s^{-1}.

7. We updated the O–C diagram for CY Aqr, corroborating binarity found by Zhou, Fu, & Jiang (1999) and Fu & Sterken (2003). Our radial velocity data are in a good agreement with previous observations by Struve (1949) and Fernley et al. (1987) but have better accuracy.

8. We obtained new time series photometry on XX Cyg, DY Her and DY Peg and updated their O–C diagrams with new times of maximum. DY Her and DY Peg show continuous period decrease, while XX Cyg has continuous period increase.

Further analysis of the photometric and spectroscopic observations (e.g. determination of physical parameters) will be presented in a subsequent paper.

Chapter 8

"HH Nor": a pulsating star and an eclipsing binary

The first part of this chapter is reproduced from the paper *"HH Nor": a double star with two variable components* by L. L. Kiss and **A. Derekas**, 2004, Information Bulletin on Variable Stars, No. 5555. Section 8.2.3 was added to the text as a result of follow-up spectroscopy of the system.

I carried out all the spectroscopic observations for the system, reduced and analysed the spectroscopic data.

8.1 Introduction

In a recent paper Dvorak (2004) listed several misidentified and missing southern eclipsing binaries. He compared ASAS-3 observations (Pojmański, 2002) with the available information in the GCVS catalogue (Kholopov, 2003) and checked their consistency. One of the "incorrectly classified variable stars" was HH Nor, listed as an Algol-type eclipsing binary in the GCVS (period: 8.58313 d). Contrary to this, Dvorak (2004) reclassified the star as an RR Lyrae type variable and determined a period of 0.598275 days. The wild disagreement with the GCVS and the apparent scatter of the phased ASAS-3 data in Dvorak (2004) caught our attention and this note summarises our findings.

8.2 Discussion

8.2.1 CCD image of HH Nor

The DSS image (Fig. 8.1) shows that the star is actually a visual double star of two comparable components. The first (and to our knowledge, the only) period determination was made by Alden (1935), who was fully aware of the double nature of the eclipsing binary named later as HH Nor. He referred to it as the fainter component of h 4794, a double star with similar components ($\Delta m \approx 1$ mag) separated by $12\farcs6$ in position angle 148°. The same parameters are also listed in the CCDM catalogue (Dommanget & Nys, 2002), which also gives the proper motions of the components. Since their separation is smaller than the confusion radius of the ASAS observations (about 20 arcsec, Pojmański (2002), the system remained unresolved, so that the measured magnitudes contain light from both components. Therefore, our first conclusion is that the brighter component of the system is a newly discovered RR Lyrae type variable that outshone the eclipsing component (=HH Nor) in the blended images. However, the predominantly downward scatter in Fig. 8.2 of Dvorak (2004) shows that besides the RR Lyrae variations there is also information on HH Nor itself.

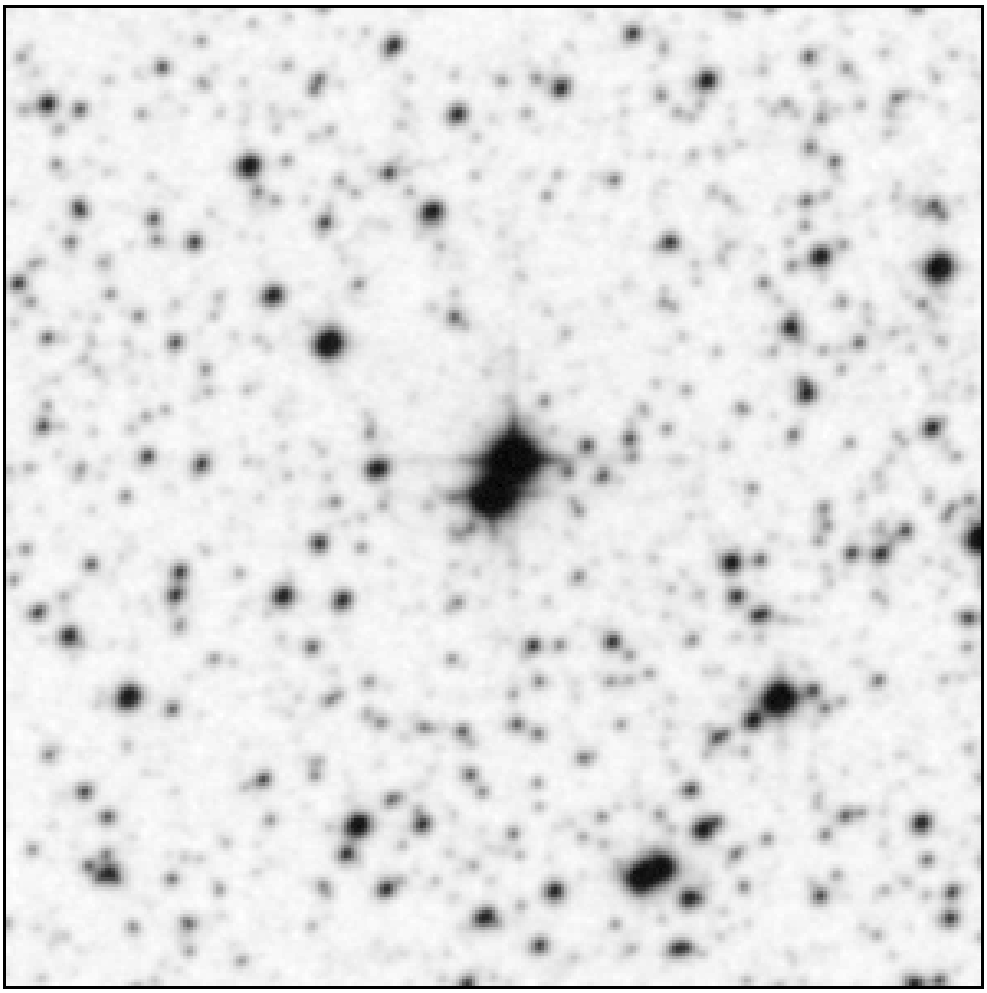

Figure 8.1 A $5' \times 5'$ DSS field centered on HH Nor. North is up, east is to the left.

8.2.2 Light curve analysis

To extract this further information, we downloaded V-band ASAS-3 observations [1] and performed a secondary light removal in two steps. We adopted $V = 10.3$ mag for the outside-eclipse brightness of HH Nor (as given by Alden (1935); after converting all magnitude values to fluxes, we subtracted HH Nor's light from the measured brightnesses and converted the results back to magnitudes. The remaining outlying points (mostly caused by the eclipses) were removed manually from the phased data, using the RR Lyr ephemeris in Dvorak (2004). This way we arrived to the corrected mean light curve of the RR Lyr component (left panel in Fig. 8.2).

[1] `http://archive.princeton.edu/~asas/`

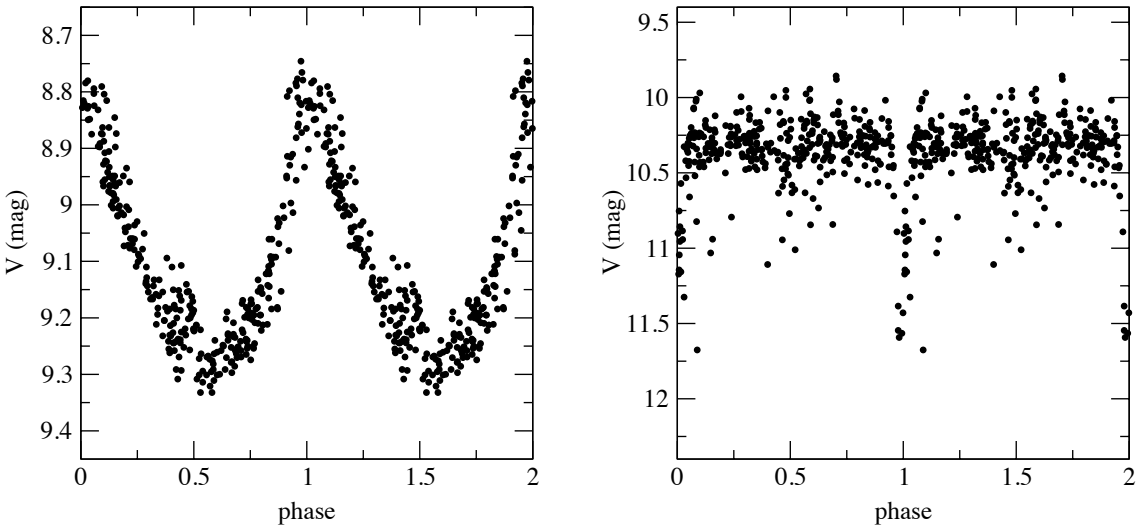

Figure 8.2 Corrected phase diagrams of the RR Lyrae component (left) and HH Nor (right).

In the next step we fitted this mean light curve with a third-order Fourier-polynomial, with which we corrected the initial data for the variations of the brighter star. The residuals were then analysed by a combination of the Phase Dispersion Minimization (Stellingwerf, 1978) and the String Length method (Lafler & Kinman, 1965). As a result, we derived a period of 8.5835(2) days, which is in very good agreement with that of by Alden (1935). The measured eclipse depth of the primary minimum (about 1.2 mag) is also in good agreement with the unblended observations of Alden (1935), which supports the consistency of the secondary light removal. We plot the final phase diagram of HH Nor in the right panel of Fig. 8.2. We summarise the main parameters for both variables in Table 8.1.

8.2.3 Spectroscopy

We obtained medium-resolution spectroscopic observations with the 2.3 m telescope at Siding Spring Observatory, Australia on 12 nights in 2005. The main aim of these observations was to decide whether the RR Lyrae star and the eclipsing binary compose a real physical system. For this we took 19 and 334 spectra for the binary and the pulsating star, respectively. The data were reduced with standard tasks of IRAF, as described in Section 6. The radial velocities were determined with the task *fxcor*, applying the cross-correlation method using a well-matched theoretical template spectrum from the extensive spectral library of Munari et al. (2005). The velocities were measured from

Table 8.1 Main parameters of "HH Nor" (=h 4794). E_0 is the epoch of minimum and maximum for the eclipsing and the pulsating component, respectively.

parameter	eclipsing component	RR Lyr component
RA(2000)[a]	15 43 30.17	15 43 29.37
Dec(2000)[a]	−51 50 48.9	−51 50 37.5
μ(RA) (mas/yr)[a]	2	−3
μ(Dec) (mas/yr)[a]	−23	−14
V (mag)[b]	10.3–11.5	8.8–9.3
period (d)	8.5835(2)[b]	0.598275[c]
E_0 (−2400000)	52503.348[b]	52093.53[c]

Data sources:[a] the CCDM catalogue; [b] this paper; [c] Dvorak (2004).

the 50 Å region centered on the Hα line. The resulting radial velocity curves for the eclipsing binary and the pulsating star are shown in Fig. 8.3 and 8.5, respectively.

The spectra of HH Nor showed the presence of the secondary component that was extracted by the cross-correlating function. The radial velocity curves of the two components are shown in Fig. 8.3. The amplitudes of the radial velocity curves of the components are ∼130 km s^{-1} and ∼170 km s^{-1} at $v_\gamma \approx -25$ km s^{-1}. The cooler primary component shows emission in the Hα that was revealed after subtracting the best-fit model spectrum from the observed spectra (Fig. 8.4).

The pulsating component has a radial velocity amplitude of ∼27 km s^{-1} at $v_\gamma \approx -10$ km s^{-1}. Using the best-fit spectrum, the light curve and the radial velocity curve we got the following parameters of the star: $\mathrm{T_{eff}} \approx 6200$ K, $\log \mathrm{g} \approx 1.3$ that indicates this star is an ultrashort-period Cepheid rather than an RR Lyrae star (analysis still in progress).

The difference of the two components' γ-velocity is about 15 km s^{-1} which indicates unambiguously that there is no physical connection between HH Nor and the Cepheid.

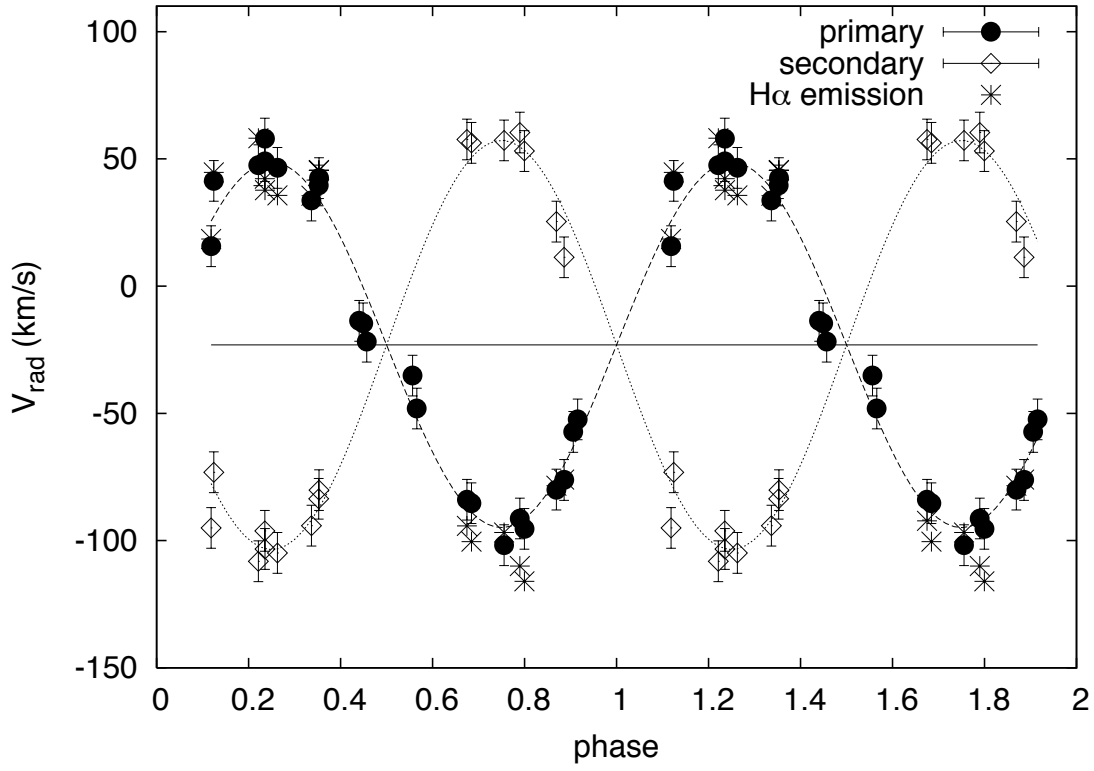

Figure 8.3 Radial velocity curves of the two components of HH Nor and the Hα emission.

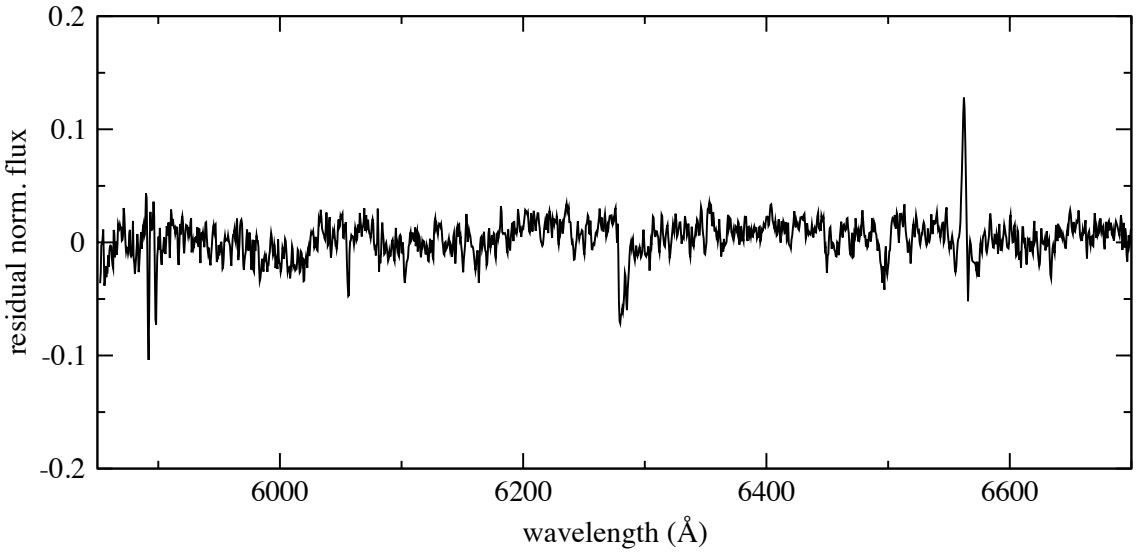

Figure 8.4 Subtracting the best-fit model spectrum reveals the Hα emission of the cool primary component.

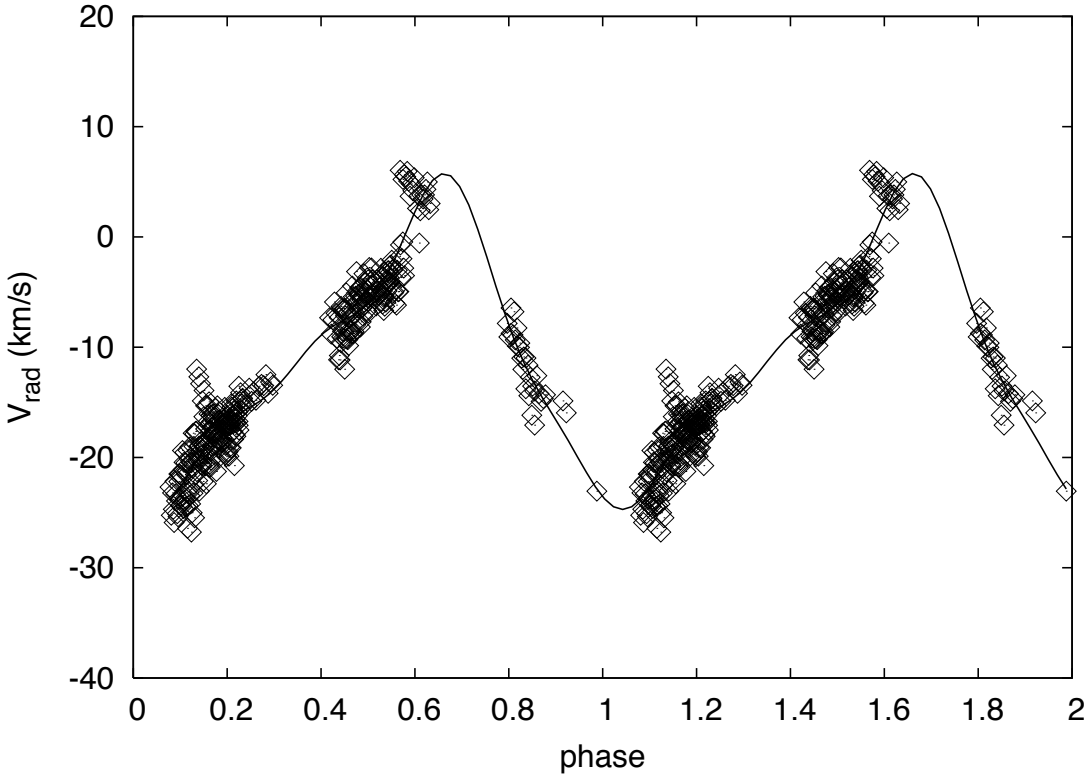

Figure 8.5 Radial velocity curves of the pulsating companion. The solid line shows a four-component Fourier fit.

Chapter 9

A radial velocity survey of candidate binary Cepheids

This chapter contains preliminary results of the radial velocity survey performed on southern binary candidate Cepheid variables.

I carried out and reduced all the spectroscopic observations. The analysis was done in close collaboration with László Szabados (Konkoly Observatory, Hungary), who kindly provided data from the literature.

9.1 Introduction

Cepheids are radially pulsating supergiant stars in the helium-burning stage and have spectral types of F5–G5 and large luminosities. Pulsation periods range from a few days to more than hundred days. They are high-mass stars (5-30 $M_{\odot}$) and the more massive the star, the higher luminosity and the longer the pulsation period. There are Cepheids in both populations, where Pop. II Cepheids are also known as W Virginis stars.

It is well known that Cepheid variables are key objects in establishing the cosmic distance scale because they serve as standard candles via the period–luminosity relationship, discovered by Henrietta Swan Leavitt in 1912 (Leavitt & Pickering, 1912). Due to the regularity of their pulsation, various relationships exist between the physical properties of these variables, e.g. period-radius, surface-brightness colour, period-projection factor etc. (Kervella et al., 2004; Groenewegen, 2007; Nardetto et al., 2007).

Binarity is quite common among Cepheids. Most known binary Cepheids are brighter than 8 mag but it is expected that at least half of all Cepheid variables should have companions. The detection of physical companions to classical Cepheids is important for several reasons. Binary systems are useful for determining mass and luminosity of the Cepheid involved. Moreover, unrecognized companions may contaminate photometric observations, thus affect luminosity, radius, temperature, and other properties inferred from photometry. In addition, binarity among Cepheids can be used for testing the current models on stellar evolution, such as the role of convective overshoot (Evans, 1994).

There are various methods for detecting binarity of Cepheids. Study of Cepheids in the ultraviolet region by the IUE led to the discovery of blue companions in a number of cases (Evans, 1990, 1992). However, such methods are not decisive as to the physical relation of the companion and the Cepheid. Spectroscopic radial velocity data can give the definitive proof if the orbital motion superimposed on the radial velocity variation due to atmospheric pulsation can be revealed. There are more than a hundred Cepheids whose binarity has been detected in this way (Szabados, 2003). However, these observations are very time consuming, since the orbital periods range from months to years. It is not surprising that such observations of Cepheid variables have been a neglected field (many stars have not been observed for ten or more years).

For these reasons, we decided to monitor spectroscopically 40 suspected binary Cepheids in order to detect γ-velocity changes by comparing our observation with pre-

vious data in the literature. Since the current observational technique results in much more precise radial velocity data than several decades ago, the resulting radial velocity phase curve is more reliable than those based on the data taken from the early literature. These more precise data can be used to study the amplitudes and amplitude ratios of the individual Cepheids. The ratio of the photometric and radial velocity amplitudes for a pulsational cycle is indicative of the mode of pulsation (Balona & Stobie, 1979). In addition, other properties of the pulsation can be studied through the differences between the photospheric (from metallic lines) and upper atmospheric (from hydrogen lines) velocities (Vinkó et al., 1998; Kiss & Vinkó, 2000; Petterson et al., 2005).

Most of the observed stars have been amply observed photometrically, so a precise value of the pulsation period can be reliably determined from those data. Knowledge of the period as accurately as possible is indispensable for the proper phasing of radial velocity phase curves from different epochs.

In this chapter we present preliminary results of our radial velocity survey of 40 Cepheids. The sample was selected from bright southern, spectroscopically neglected Cepheids. All programme stars are Type I Cepheids, and 13 are small-amplitude pulsators. We have monitored them over three observing seasons.

9.2 Observations

Observations were carried out at the Siding Spring Observatory, Australia, using the 2.3 m telescope with the Double Beam Spectrograph over two years between 2004 and 2006 on a total of 34 nights (9 nights in 2004, 18 nights in 2005 and 7 nights in 2006). The telescope and the data reduction are described in more detail in Chapter 6. Currently all the data taken with the red arm are reduced and used in this analysis. The blue arm data will be used in a further analysis of the sample, such as searching for direct evidence for blue companions or determining spectroscopic reddenings using specific spectral lines that are sensitive to interstellar matter (e.g. sodium D, calcium H and K, strong DIBs).

The observed stars and the their main observational properties are listed in Table 9.1 and the phased velocity curves are shown in Figs. 9.6-9.10.

Table 9.1 The list of programme stars.

Star	⟨V⟩ (mag)	Period (days)	Number of data points	Star	⟨V⟩ (mag)	Period (days)	Number of data points
MY Pup	5.7	5.695	36	AZ Cen	8.6	3.211	26
VZ Pup	9.0	23.171	40	V419 Cen	8.2	5.507	26
WX Pup	9.1	8.937	36	SU Cru	9.5	12.848	26
AD Pup	10.0	13.594	33	R Cru	6.9	5.826	28
AP Pup	7.4	5.084	33	VW Cru	9.6	5.826	26
AQ Pup	8.5	30.104	33	V378 Cen	8.4	6.459	29
AT Pup	8.1	6.665	32	V659 Cen	6.7	5.622	28
RZ Vel	7.1	20.398	30	V737 Cen	6.8	7.066	30
SW Vel	8.3	23.441	30	BP Cir	7.5	2.398	17
SX Vel	8.3	9.550	27	AV Cir	7.4	3.065	24
ST Vel	9.6	5.858	27	LR TrA	7.8	2.428	9
BG Vel	7.7	6.924	27	QZ Nor	8.9	3.786	24
AE Vel	10.4	7.134	26	V340 Ara	10.2	20.811	25
V397 Car	8.3	2.064	33	V500 Sco	8.8	9.317	17
SV Vel	8.8	14.097	26	V482 Sco	7.9	4.528	17
WZ Car	9.4	23.013	21	RV Sco	6.7	6.061	18
FO Car	10.7	10.357	21	AV Sgr	11.3	15.415	18
GH Car	9.1	5.726	27	AY Sgr	10.1	6.57	22
V898 Cen	8.0	3.527	28	BB Sgr	6.9	6.637	16
GI Car	8.3	4.431	24	YZ Sgr	7.4	9.554	16

9.3 Results of the binarity survey

Binarity was studied on the sample by comparing our data with those in the literature. If a Cepheid is in a binary system, the components are orbiting around the barycentre and the orbital motion can be revealed in the pulsational radial velocity curve as the systemic velocity shifts. Therefore, the main aim of this project was to detect these shifts in the γ-velocity.

The first results reveal 6 new spectroscopic binary Cepheids. In the following, I discuss these new discoveries. In some cases, a γ-velocity shift can already be detected within our data. For this, we divided the datasets into at least two subsets. One subset contains data taken in the end of 2004 and the beginning of 2005 (hereafter referred as 2004/2005), the other subset has data obtained in 2006.

9.3.1 V898 Centauri

V898 Cen (HD 97317; HIP 54659) is a Type I Cepheid with a pulsation period of $\sim$3.527 d and a mean magnitude of V$\sim$8.0 mag. Its light variation was discovered by Strohmeier et al. (1964). The first photometric study was done by Berdnikov et al. (1999) who took BVI_C photometry and determined new elements. Zakrzewski et al. (2000) computed Fourier parameters of the Hipparcos data and identified V898 Cen as a Pop. I overtone Cepheid, while Berdnikov et al. (2001) took new photoelectric observations. Moskalik & Gorynya (2005) predicted the mean angular diameter and the amplitudes of angular diameter variations. Gontcharov (2006) presented a single epoch radial velocity as –2.3 km s^{-1}.

We obtained medium resolution spectroscopy on 28 nights between 2004 and 2006. The radial velocity curve of the whole dataset is shown in Fig. 9.1, while the phased radial velocities are plotted in Fig. 9.6. The data clearly reveal that the γ-velocity is changing between –25 km s^{-1} and +17 km s^{-1} over 450 day observing period. This suggest a reasonably massive companion with an orbital period longer than 450 days.

9.3.2 AD Puppis

AD Pup (HD 63446; HIP 38063) is a Type I Cepheid with pulsation period of $\sim$13.6 days and a mean magnitude of V$\sim$10.0 mag. Its variability was discovered by Hoffmeister (1933). It has been observed photometrically by Walraven, Muller & Oosterhoff (1958); Irwin (1961); Schaltenbrand & Tammann (1971); Madore (1975); Eggen (1983); Schechter et al. (1992); Groenewegen (1999); Berdnikov et al. (2001). The radius of the star was calculated by Sollazzo et al. (1981) using the Walraven system. Antonello & Morelli (1996) has studied the light curves in order to find resonances between pulsation modes. Detailed chemical composition was determined by Lemasle et al. (2007). The only radial velocity measurement of AD Pup was taken by Joy (1937) who determined v$_\gamma$=58 km s^{-1}.

The phased radial velocities are plotted in Fig. 9.9. From the data obtained on 33 nights, we could determine that v$_\gamma$ $\approx$75 km s^{-1}. Comparing it to the results of Joy (1937), we can conclude a definite γ-velocity shift of about 17 km s^{-1}.

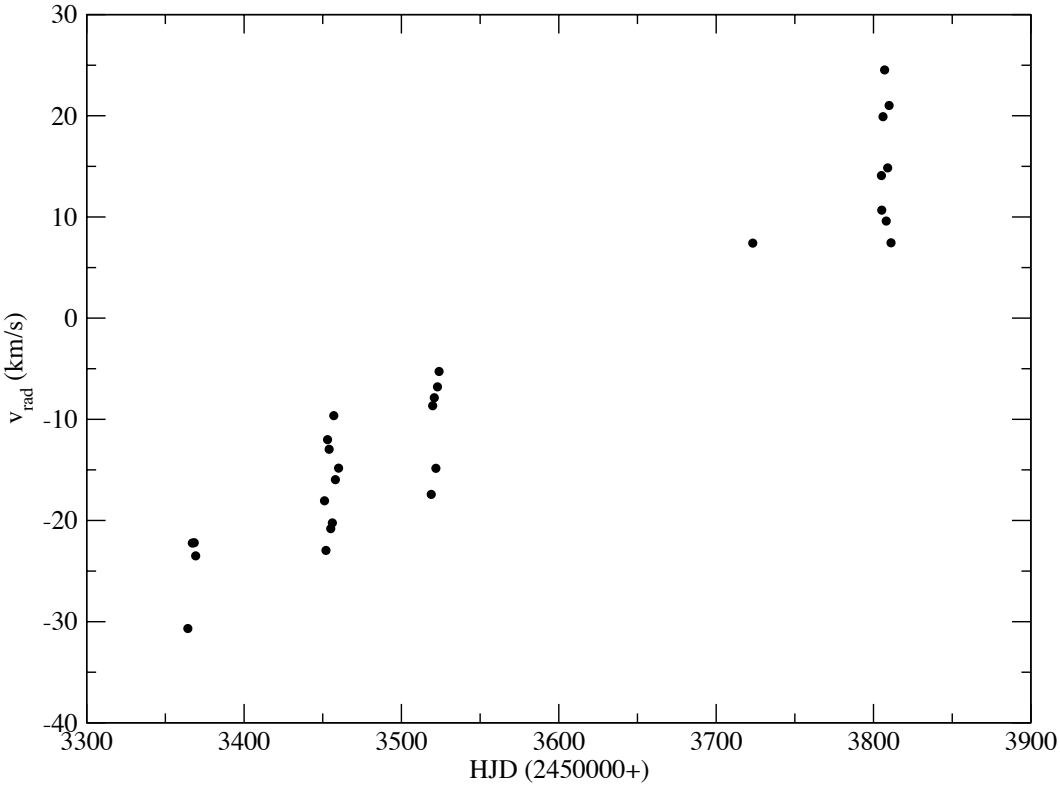

Figure 9.1 Radial velocity curve of V898 Cen. The data clearly reveal the systemic velocity shift, indicating an orbital period longer than 450 days.

9.3.3 GH Carinae

GH Car (HD 306077; HIP 54621) is a Type I Cepheid with a pulsation period of $\sim$5.726 days and a mean magnitude of V$\sim$9.0 mag. It has been the object of a number of photometric studies, such as Walraven, Muller & Oosterhoff (1958); Irwin (1961); Makarenko (1971); Schaltenbrand & Tammann (1971); Opolski (1984); Antonello & Poretti (1986); Berdnikov et al. (2001); Caldwell et al. (2001). The star is in the field of the open cluster Trümpler 18. Vazquez & Feinstein (1990) studied the cluster and found that GH Car is very likely to be a member based on spatial position, derived M_v, intrinsic colours and age. They determined a mass of 5.83$\pm$0.5 M$_\odot$.

We took data on 27 nights and divided them into two seasonal subsets: the first is at 2004/2005 and the second was obtained in 2006. Phasing them, we determined the γ-velocities as –6 km s^{-1} and –3 km s^{-1}, respectively. The phased radial velocity curves are shown in Fig. 9.2.

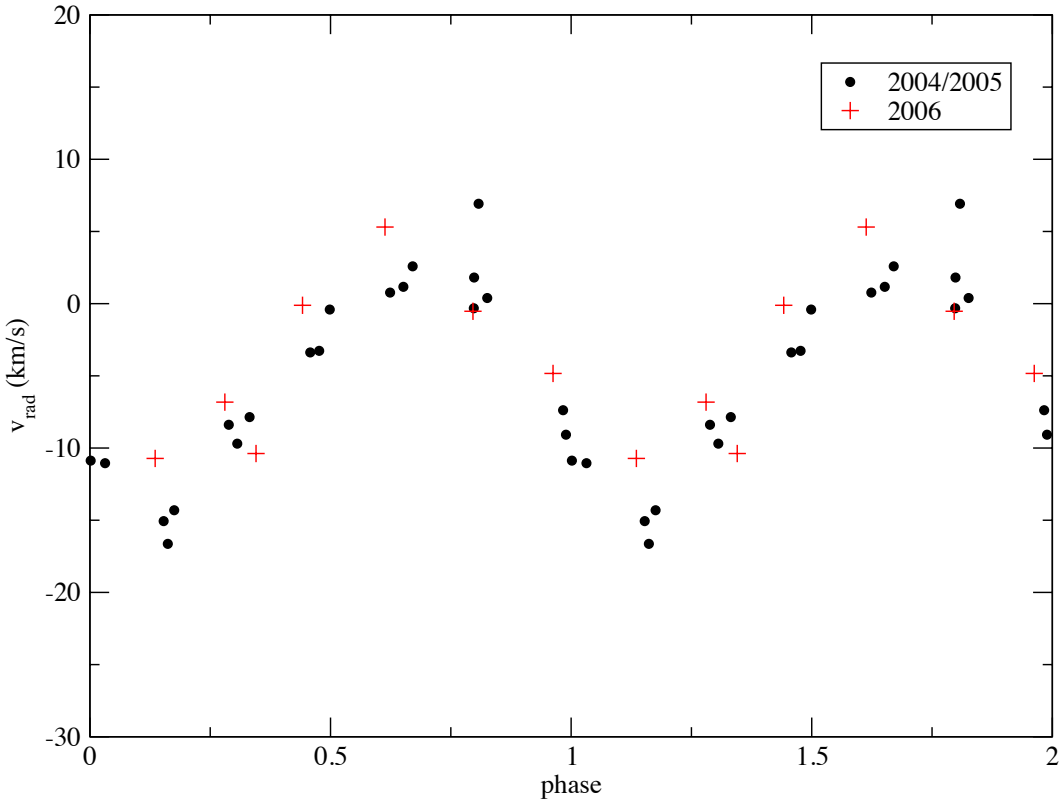

Figure 9.2 Phased radial velocity curve of GH Car. There is a ∼3 km s^{-1} of γ-velocity shift between our two seasons of data.

9.3.4 AY Sagittarii

AY Sgr (HIP 90110) is a Type I Cepheid with a pulsation period of ∼6.57 days and a mean magnitude of V∼10.0 mag. Photometry of AY Sgr was obtained by Walraven, Muller & Oosterhoff (1958); Schaltenbrand & Tammann (1971); Groenewegen (1999). Only one radial velocity measurement can be found in the literature about AY Sgr which determined v_γ=–25 km s^{-1} (Joy, 1937).

We determined the γ-velocity as –15 km s^{-1} from the data we took on 22 nights in total. The phased radial velocities are shown in Fig. 9.8. The comparison with the only available measurement in the literature (Joy, 1937) reveals an ∼10 km s^{-1} velocity shift, so that there is no doubt about the existence of a companion.

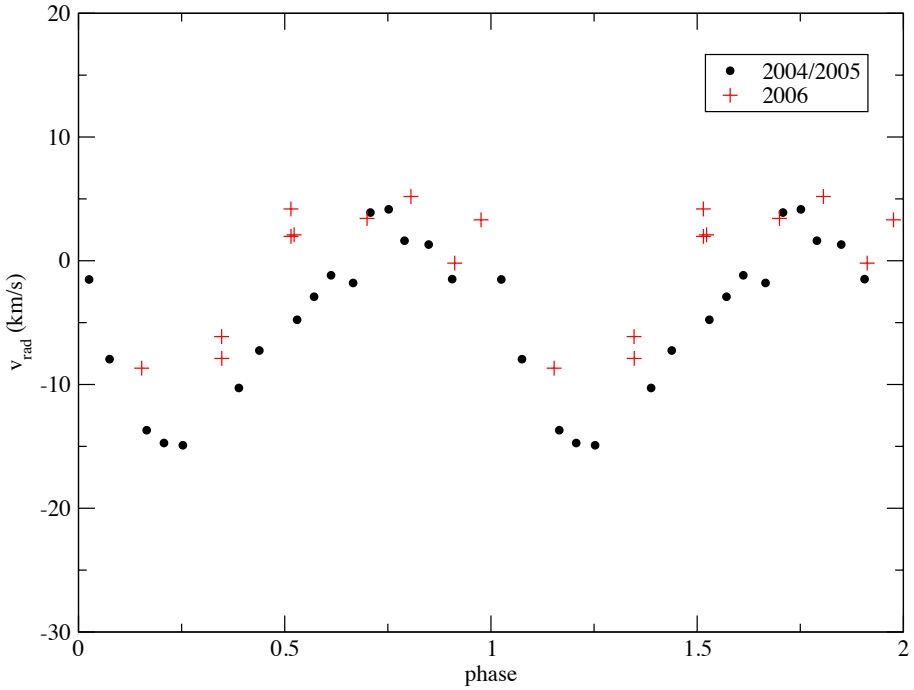

Figure 9.3 Phased radial velocity curve of V419 Cen. There is a $\sim$4 km s^{-1} of γ-velocity shift between our two seasons of data.

9.3.5 V419 Centauri

V419 Cen (HD 100148; HIP 56176) is a Type I Cepheid with pulsation period of $\sim$5.507 days and a mean magnitude of V$\sim$8.2 mag. Stibbs (1955) has obtained the first radial velocity curve and determined –17.2 km s^{-1} for the γ-velocity. It has been included in the following photometric studies: O'Connell (1955); Walraven, Muller & Oosterhoff (1958); Irwin (1961); Stobie (1970); Tsvetkov (1985); Eggen (1996); Groenewegen & Oudmaijer (2000); Berdnikov, Dambis & Vozyakova (2000); Caldwell et al. (2001). Radial velocity measurements were obtained by Lloyd Evans (1968, 1980).

Medium resolution spectra were taken on 26 nights. We divided the data into two subsets and determined the γ-velocities as –5 km s^{-1} and –1 km s^{-1} in 2004/2005 and 2006, respectively (Fig. 9.3). This shows the center of mass shift on its own, so the binary nature of V419 Cen. In addition, comparing our data with ones in the literature, the γ-velocity shift is more unambiguous: $v_\gamma \approx$–16 km s^{-1} was determined in Stibbs (1955) and in Lloyd Evans (1968), so there is a $\sim$10 km s^{-1} γ-velocity shift since the data obtained almost half a century ago.

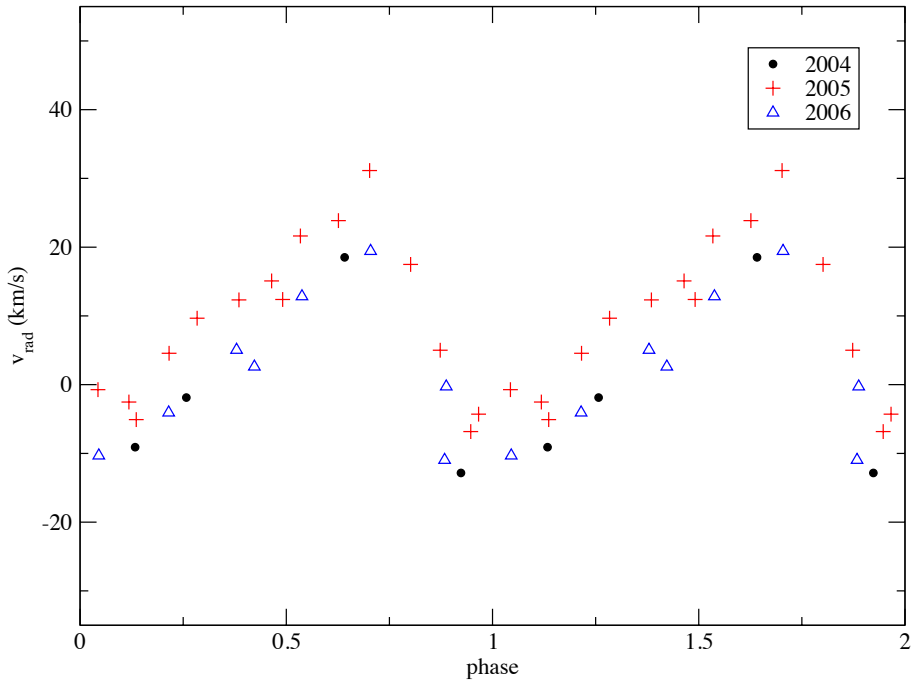

Figure 9.4 Phased radial velocity curve of ST Vel. Yearly subsets show a ∼8 km s^{-1} of γ-velocity shift.

9.3.6 ST Velorum

ST Vel (HIP 42929) is a Type I Cepheid with a pulsation period of ∼5.86 days and a mean magnitude of V∼9.6 mag. Its variability was discovered by Cannon et al. (1909). The first photometric study was done by Walraven, Muller & Oosterhoff (1958) then later by Schaltenbrand & Tammann (1971); Eggen (1996); Groenewegen (1999); Caldwell et al. (2001). The γ-velocity was first determined by Pont, Mayor & Burki (1994) as 7.4 km s^{-1}. Chemical composition was determined by Lemasle et al. (2007).

We obtained spectra on 27 nights. The phased radial velocities are shown in Fig. 9.4, where the γ-velocity change is obvious. The data are divided into yearly subsets, so the center of mass velocity was determined as follows: v$_\gamma$ ≈3 km s^{-1} in 2004, v$_\gamma$ ≈11.3 km s^{-1} in 2005 and v$_\gamma$ ≈3 km s^{-1} in 2006.

9.4 Velocity differences

The atmospheres of Cepheids are strongly affected by velocity gradients and shock waves. There are velocity differences between the photospheric (metal) and upper atmospheric (hydrogen) velocities, which are greatest during the outward acceleration phases (Wallerstein et al., 1992; Vinkó et al., 1998). The difference varies from star to star and it depends on the velocity gradient between the photosphere and the upper atmosphere, as well as on the phase difference between the motion of these two regions (Vinkó et al., 1998).

The phase diagrams of our data also show these differences (see Fig. 9.6-9.10). The maximum velocity differences are plotted against the period (black dots) in Fig. 9.5. For comparison we also show the data of Vinkó et al. (1998) in the same plot with different symbols (red crosses). Our data clearly support the previous results: the longer the period, the larger the maximum velocity difference. At $\mathrm{P} > 10\ \mathrm{d}$ the velocity difference function sharply increases. Vinkó et al. (1998) suggested an uncertain saturation effect at $\mathrm{P} > 20\ \mathrm{d}$ based on only a few stars. Our sample is not large enough to confirm this hypothesis.

It is worth noting that the overall period dependence of the maximum velocity differences is strikingly similar to that of the Fourier parameter R_{21} of the radial velocity curves (Kovács, Kisvarsányi & Buchler, 1990). The interpretation of the latter is the 1:2 resonance of the Cepheid pulsations, which imply that the maximum velocity differences are surprisingly good indicators of the phenomenon. Potentially, this might be used to study Cepheid pulsations in a novel way via combining hydrodynamic models with solving the radiative transfer equation for various atomic transitions and hence identify the atmospheric layers, whose velocities we measure.

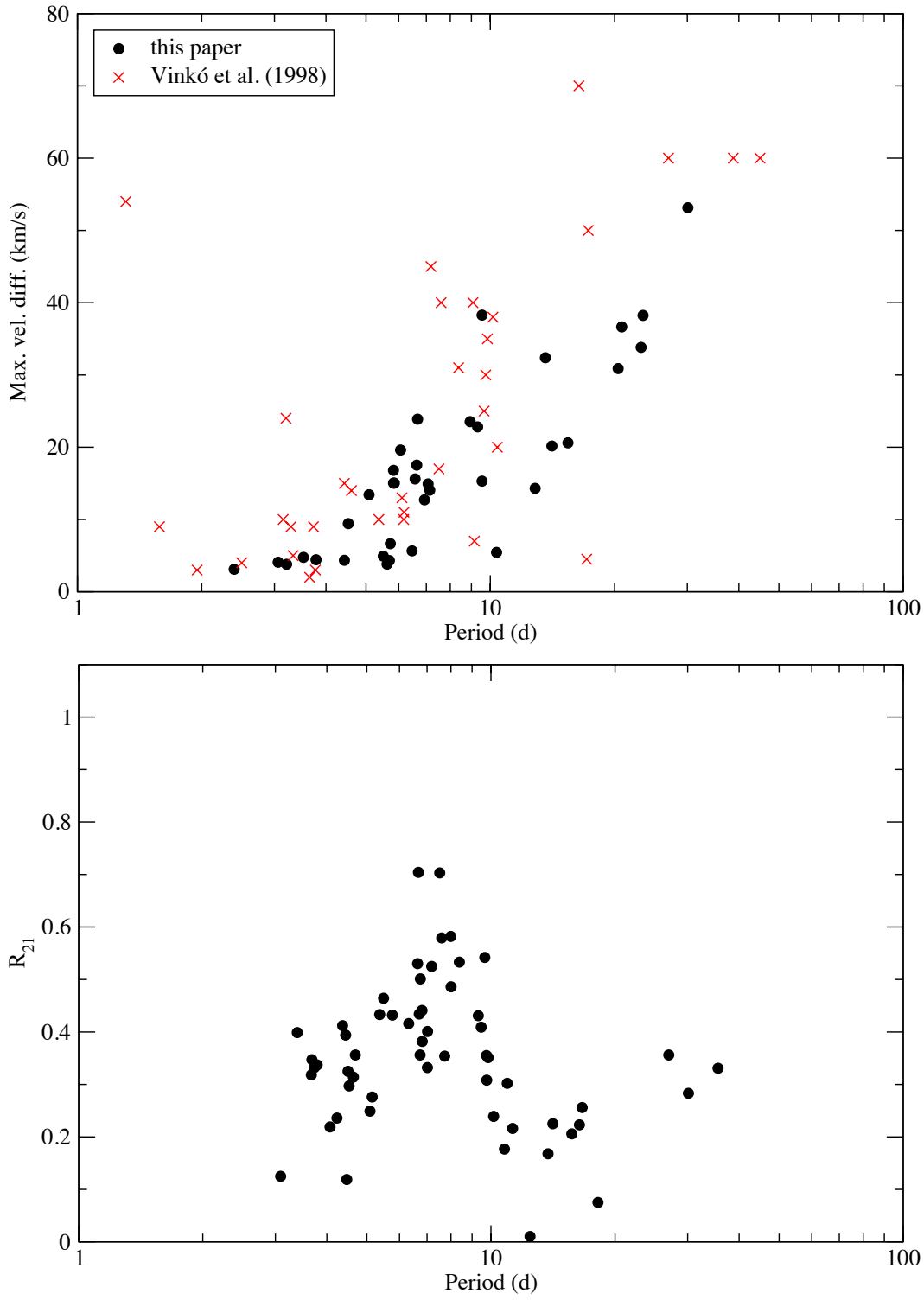

Figure 9.5 Top panel: Maximum velocity difference against pulsation period. Black dots represent data from our observations, red crosses are data from Vinkó et al. (1998). Bottom panel: Amplitude ratio R_{21} vs period (Kovács, Kisvarsányi & Buchler, 1990).

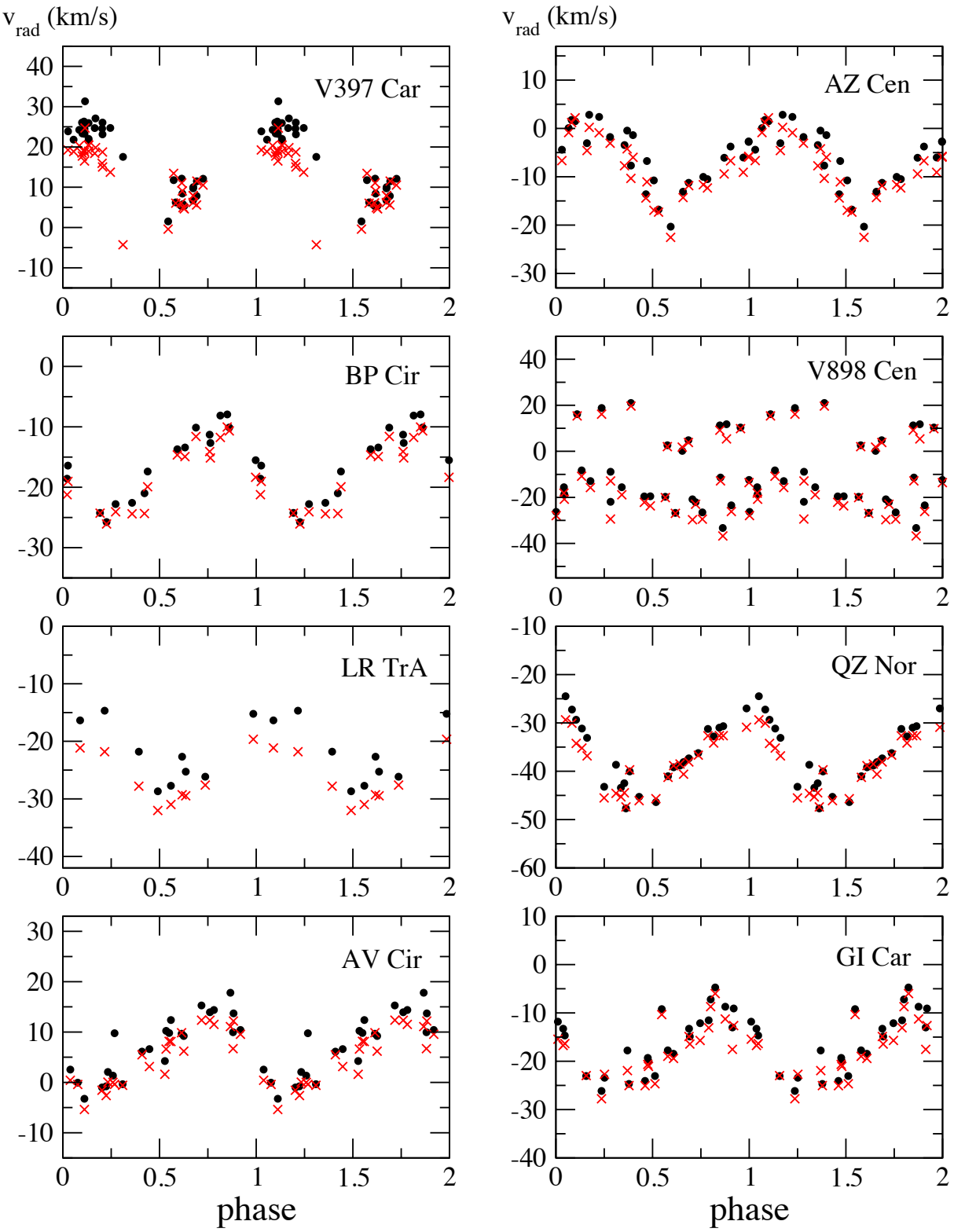

Figure 9.6 Phased radial velocity curves. Black dots are measured from the Hα line, red crosses are measured from the metallic line between 5950 Å and 6530 Å.

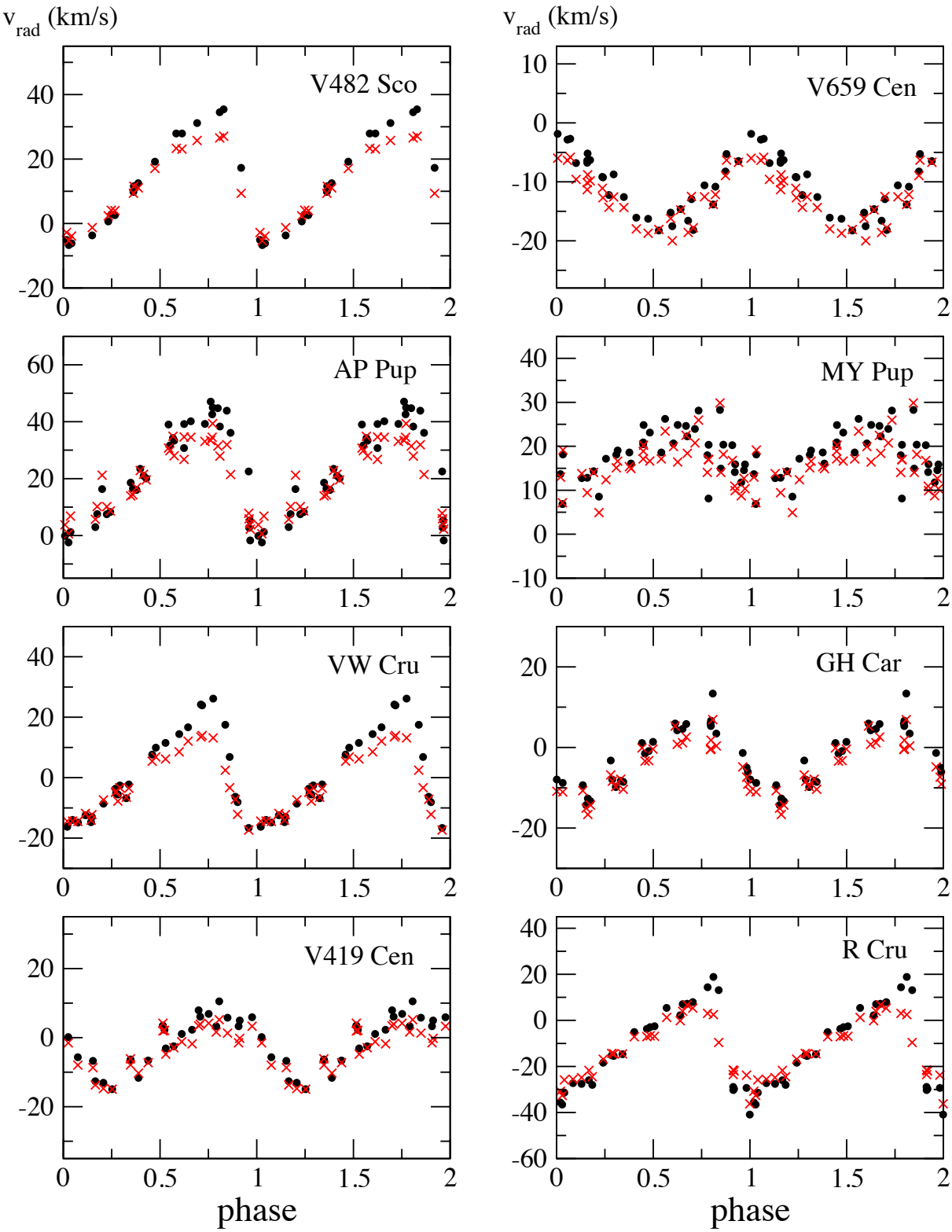

Figure 9.7 Same as Fig. 9.6, but for a different set of stars.

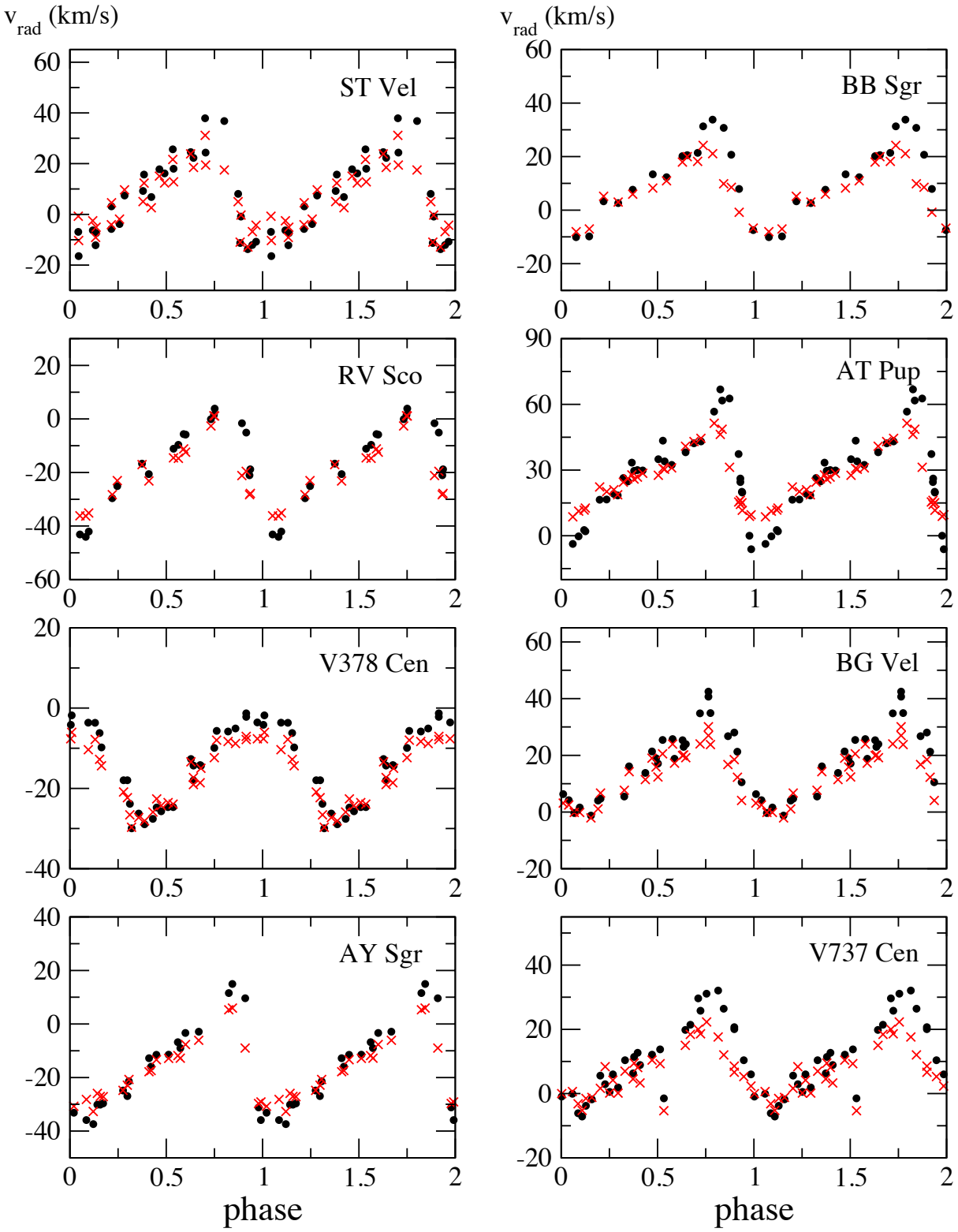

Figure 9.8 Same as Fig. 9.6, but for a different set of stars.

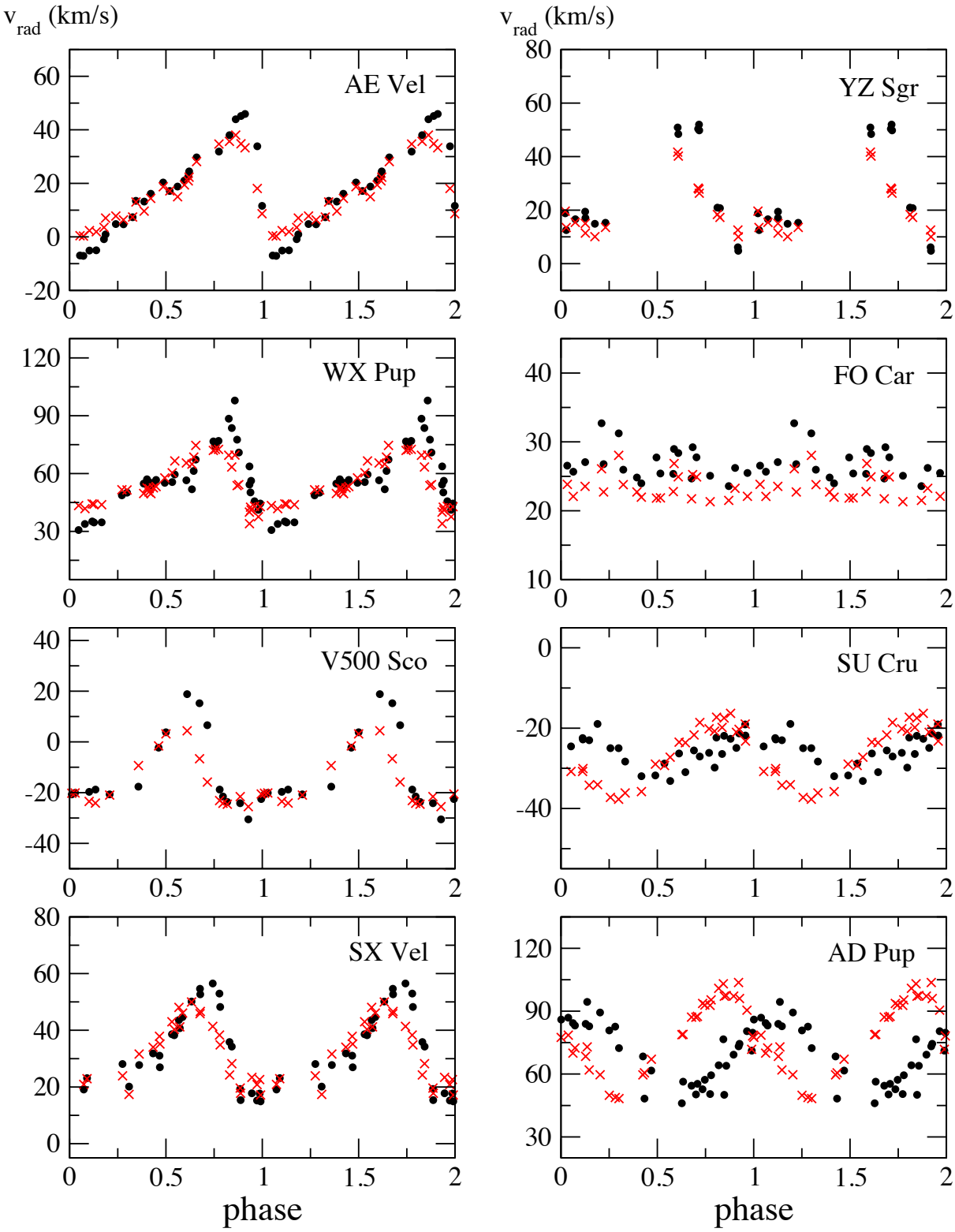

Figure 9.9 Same as Fig. 9.6, but for a different set of stars.

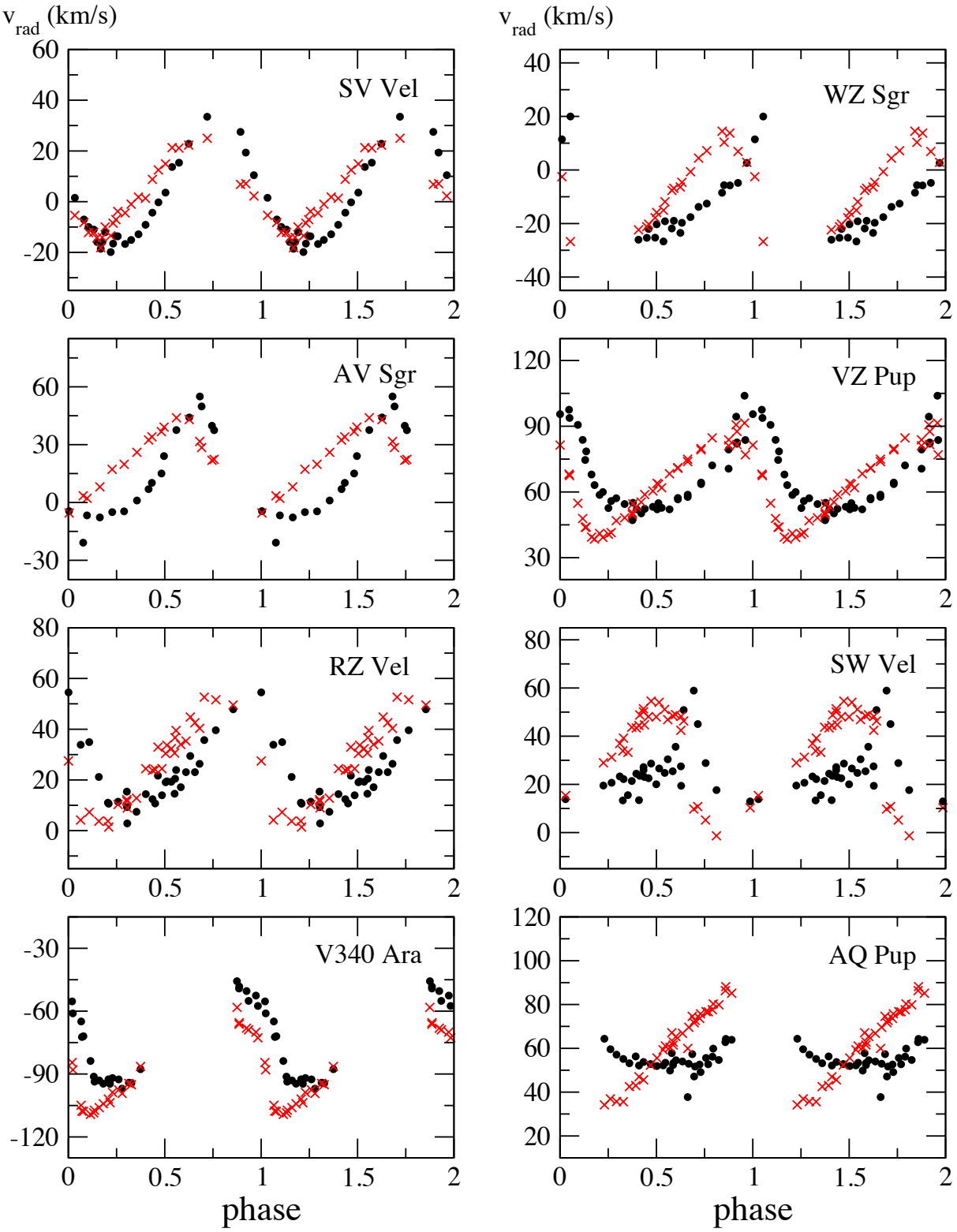

Figure 9.10 Same as Fig. 9.6, but for a different set of stars.

Chapter 10

Summary and future work

10.1 Summary of the thesis

In this thesis, I presented the results of my research done on different types of variable stars using the publicly available dataset obtained by the MACHO Project in the Large Magellanic Cloud and own photometric and spectroscopic observations. The aim of the project was to deepen our knowledge of interplay between pulsations and binarity. The achievements of the thesis are the following:

- I downloaded and reanalysed the photometric data of about 6800 stars in the Large Magellanic Cloud obtained by the MACHO Project and classified as eclipsing binaries. New periods and reclassification of the sample revealed that 3031 stars are genuine eclipsing binary or ellipsoidal variable and the general properties of them was presented. The period distribution is clearly bimodal, reflecting separate groups of more massive blue main-sequence objects and low-mass red giants. Foreground stars were identified using evolutionary models.
- The low-mass red giants in the sample resemble contact binaries and obey a period-luminosity relation, while semidetached systems follow a loose correlation and detached binaries spread uniformly in the P–L plane. The period-luminosity relation of these binaries also revealed that the correct position for sequence E is at periods a factor of 2 greater than previously published, overlapping with the sequence of long secondary periods (LSPs; sequence D).
- The amplitudes of LSPs have properties more similar to pulsations, arguing for pulsation origin of the LSP phenomenon.

- The downloaded MACHO sample contained an RR Lyrae star with enormous rate of period modulation with cycle length of about 8 years that indicated a possible binary nature for this star. Multiple periodicity and amplitude modulation could be unambiguously excluded as a cause of the period modulation. Spectroscopic follow-up observations ultimately rejected the binary hypothesis. The observed behaviour is consistent with that of the RR Lyrae stars with Blazhko effect.
- A photometric and spectroscopic survey of 10 bright high-amplitude δ Scuti stars (HADS) has been carried out. Orbital motion of RS Gru was detected and the data revealed that the companion is a low-mass dwarf star. Multiperiodicity was found in RY Lep and the analysis revealed that the amplitude of the secondary frequency is variable on the time-scale of a few years, whereas the dominant mode is stable. Orbital motion was also detected in the radial velocities. Radial velocities of AD CMi showed cycle-to-cycle variations, and the first radial velocity curves of ZZ Mic and BE Lyn were obtained. We confirmed and updated our present knowledge of BQ Ind, CY Aqr, XX Cyg, DY Her and DY Peg.
- Radial velocity survey of 40 Cepheid variables led to the discovery of 6 new spectroscopic binary Cepheids. The analysis of the atmospheric and photospheric lines revealed that metallic lines are more suitable for extracting radial velocity curves than hydrogen lines.
- HH Nor is an optical double system that carried the potential of being the first RR Lyrae star in an eclipsing binary system. Spectroscopic observations of the system revealed no physical connection between the components.

10.2 Suggestions for future work

Eclipsing binaries in the MACHO database

In order to find pulsating components among eclipsing binaries in the MACHO Large Magellanic Cloud database, we need to subtract the eclipsing binary solutions from the light curves, taking into account the binary period changes. For this, we need to calculate the O–C diagram of each system, fit it with an appropriate polynomial and correct the period for the subtraction.

Since the MACHO data are only sampled at one point per day (or less), the determination of times of minimum is not as simple as in the case of a closely spaced

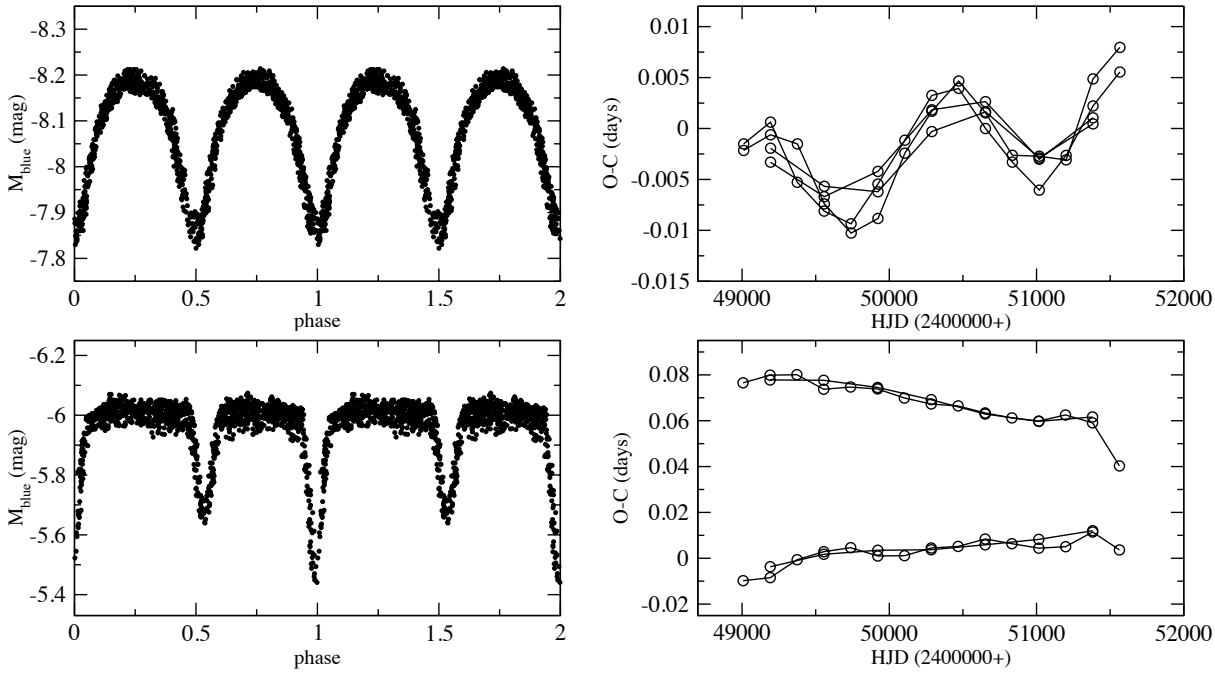

Figure 10.1 Examples for eclipsing binaries from the MACHO database with light-time effect (top panels) and apsidal motion (bottom panels). Left panels show the phase diagrams, while right panels the O–C diagrams.

observations. As it is seen in the top panel of Fig. 5.7, most stars have periods shorter than 10 days, so they are poorly sampled by MACHO. In order to construct the O–C diagrams, we divided the datasets into 50-day and 100-day long subsets and determined the times of minimum of these subsets using the center1d algorithm. Sample O–C diagrams are shown in Fig. 10.1.

The preliminary O–C diagrams led to the discovery of about 40 eclipsing binaries with apsidal motion, 45 systems with cyclic period changes and about 80 stars with parabolic O-C diagrams. The next step is to fit the O–C diagrams with appropriate polynomials (or sine in case of LITE) and draw statistical conclusions from the results.

Taking into account the period changes, we can subtract the eclipsing binary light curves from the data and we can analyse the residuals in order to search for secondary variations, such as pulsation, spot activity, etc.

High-amplitude δ Scuti stars

The next step is to perform an abundance analysis on RS Gru and BE Lyn, using the high-resolution spectra we obtained. In addition, these spectra offer a unique view of pulsating HADS atmosphere. By measuring velocities of lines of different excitation potentials, we will be able to trace motions of layers at different optical depths. A simple one-zone model (developed originally by Stellingwerf (1972)) could then be used to constrain mean dynamical properties of the pulsating atmosphere.

In Derekas et al. (2009), we estimated that the companion of RS Gru is a a low-mass dwarf star. As a further analysis of the system, we would like to examine the high-resolution spectra in order to detect the secondary component, which is likely to be an underluminous dwarf star. The greatest chance of detection is in the blue or the red end of the UCLES spectra. If it is detected, making RS Gru a double-lined spectroscopic binary HADS, then it would allow us measuring dynamic mass after having further observations covering the full orbital phase. Mass measurement would be a crucial input in interpreting evolutionary status of RS Gru.

Spectroscopic survey of Cepheids

We monitored 40 Cepheid variable spectroscopically for 2 years in order to detect binarity. The preliminary results show that we discovered at least 6 new spectroscopic binary Cepheids in our sample. The preliminary results were discussed in Chapter 9. Further analysis of the data is still in progress.

The next steps include period search for the binary Cepheids, absorption line analysis in the spectra and determination of physical parameters using our spectroscopic data and publicly available photometry.

Appendix A

Full log of observations of high-amplitude δ Scuti stars

This appendix contains the log of observations of high-amplitude δ Scuti stars. The abbreviations at the instruments are the following:

Sz40 – Szeged Observatory (Hungary), 0.4 m

APT50 – Siding Spring Observatory (Australia), 0.5 m

SSO60 – Siding Spring Observatory (Australia), 24″/0.6 m

P60 – Piszkéstető Station (Hungary), 0.6 m

MH150 – Fred Lawrence Whipple Observatory (USA), 1.5 m

SSO230 – Siding Spring Observatory (Australia), 2.3 m

AAT – Anglo-Australian Observatory (Australia), 3.9 m

Table A.1 Journal of observations.

Date	Filter	Instrument	Data points	Obs. length
RS Gru				
2003–10–07	B, V, I	SSO60	93	3.6 h
2003–10–09	$B.V, I$	SSO60	145	4.4 h
2003–10–11	B, V, I	SSO60	125	2.9 h
2003–10–12	B, V, I	SSO60	121	2.9 h
2004–10–02	B, V, I	SSO60	141	3.6 h

Table A.1 -continued.

Date	Filter	Instrument	Data points	Obs. length
RS Gru				
2003–10–09	*spec.*	SSO230	151	3.9 h
2004–09–25	*spec.*	SSO230	146	3.3 h
2004–09–26	*spec.*	SSO230	170	3.4 h
2004–09–27	*spec.*	SSO230	99	2.3 h
2004–09–28	*spec.*	SSO230	14	0.3 h
2005–05–28	*spec.*	SSO230	14	0.7 h
2005–05–29	*spec.*	SSO230	179	3.8 h
2005–05–30	*spec.*	SSO230	203	4.1 h
2005–05–31	*spec.*	SSO230	161	4.2 h
2005–06–01	*spec.*	SSO230	86	3.4 h
2005–06–02	*spec.*	SSO230	57	1.4 h
2005–08–17	*spec.*	SSO230	116	2.9 h
2005–08–18	*spec.*	SSO230	125	3.2 h
2005–08–21	*spec.*	SSO230	8	1.1 h
2005–08–22	*spec.*	SSO230	37	3.5 h
2005–08–23	*spec.*	SSO230	98	3.4 h
2006–07–21	*spec.*	AAT	40	4.2 h
RY Lep				
2004–10–25	I	APT50	190	3.3 h
2004–10–28	I	APT50	246	3.7 h
2004–10–29	I	APT50	335	4.9 h
2004–11–24	I	APT50	105	1.9 h
2004–11–25	I	APT50	366	5.8 h
2004–11–26	I	APT50	345	6.1 h
2004–11–27	I	APT50	385	6.0 h
2004–11–28	I	APT50	380	6.2 h
2004–12–24	I	APT50	98	1.4 h
2004–12–25	I	APT50	60	1.2 h
2004–12–27	I	APT50	324	4.7 h
2004–12–28	I	APT50	464	6.7 h
2004–12–29	I	APT50	471	6.8 h
2004–12–30	I	APT50	419	6.6 h
2005–01–06	I	APT50	144	2.1 h
2005–01–07	I	APT50	140	2.0 h
2005–01–08	I	APT50	137	1.9 h
2005–01–09	I	APT50	135	1.9 h
2005–01–10	I	APT50	130	1.9 h
2005–01–11	I	APT50	128	1.9 h
2004–02–05	*spec.*	SSO230	178	4.5 h
2004–02–06	*spec.*	SSO230	134	3.9 h
2004–10–26	*spec.*	SSO230	28	1.3 h
2004–10–27	*spec.*	SSO230	75	3.9 h
2005–12–19	*spec.*	SSO230	233	5.5 h
2005–12–20	*spec.*	SSO230	203	5.5 h

Table A.1 -continued.

Date	Filter	Instrument	Data points	Obs. length
AD CMi				
2004–02–04	$spec.$	SSO230	63	4.9 h
2004–02–07	$spec.$	SSO230	69	4.3 h
2004–02–08	$spec.$	SSO230	47	2.6 h
BQ Ind				
2004–10–25	I	APT60	153	3.5 h
2004–10–26	I	APT60	46	1.1 h
2004–10–27	I	APT60	156	3.6 h
2004–10–28	I	APT60	133	3.0 h
2004–10–29	I	APT60	120	2.8 h
2004–10–30	I	APT60	98	2.2 h
ZZ Mic				
2004–10–27	B, V	SSO60	148	2.7 h
2004–10–29	B, V	SSO60	105	1.7 h
2004–10–30	B, V	SSO60	124	2.1 h
2004–10–27	$spec.$	SSO230	41	2.4 h
CY Aqr				
2003–10–08	V, I	SSO60	193	4.0 h
2003–10–10	V, I	SSO60	85	1.7 h
2003–10–13	B, V	SSO60	175	2.9 h
2004–11–24	I	APT50	43	1.3 h
2004–11–25	I	APT50	47	1.3 h
2004–11–26	I	APT50	33	0.9 h
2004–11–27	I	APT50	45	1.3 h
2004–11–28	I	APT50	49	1.3 h
2007–07–25	V	P60	101	1.2 h
2007–07–26	V	P60	103	1.8 h
2003–10–08	$spec.$	SSO230	87	3.6 h
2004–07–04	$spec.$	SSO230	22	1.6 h
BE Lyn				
2007–10–25	$spec$	MH150	10	1.0 h
2007–10–26	$spec$	MH150	22	2.1 h
2007–10–27	$spec$	MH150	20	2.0 h
XX Cyg				
2007–07–25	V	P60	117	3.2 h
2007–07–27	V	P60	201	3.6 h
2008–07–29	V	Sz40	85	3.3 h
DY Her				
2007–07–22	V	P60	131	2.2 h
DY Peg				
2007–07–23	V	P60	145	2.7 h

Bibliography

Abhyankar, K. D., 1959, ApJ, 130, 834

Abt, H. A., 1983, ARA&A, 21, 343

Agerer, F., & Hübscher, J., 2003, IBVS, No. 5485

Aerts, C., 2007, IAUS, 240, 432

Alcock, C., et al., 1993, ASPC, 43, 291

Alcock, C., et al., 1997a, AJ, 114, 326

Alcock, C., et al., 1997b, ApJ, 490, L59

Alcock, C., et al., 1999, PASP, 111, 1539

Alcock, C., et al., 2000a, AJ, 119, 2194

Alcock, C., et al., 2000c, ApJ, 542, 257

Alcock, C., et al., 2002, ApJ, 573, 338

Alcock, C., et al., 2004, AJ, 127, 334

Alden, H. L., 1935, AJ, 44, 191

Anderson, L. R., & McNamara, D. H., 1960, PASP, 72, 506

Andreasen, G. K., 1983, A&A, 121, 250

Antipin, S. V., Sokolovsky, K. V., & Ignatieva, T. I., 2007, MNRAS, 379, L60

Antonello, E., & Poretti, E., 1986, A&A, 169, 149

Antonello, E., & Morelli, P. L., A&A, 314, 541

Antonello, E., Broglia, P., Conconi, P., & Mantegazza, L., 1986, A&A, 169, 122

Ashbrook, J., 1954, AJ, 59, 6

Aubourg, E., et al., 1995, A&A, 301, 1

Bailey, S. I., 1913, Annals of Harv. Coll. Observ., 78, 1

Balona, L. A., Martin, W. L., 1978a, MNRAS, 184, 1

Balona, L. A., Martin, W. L., 1978b, MNRAS, 184, 11

Balona, L. A., & Stobie, R. S., 1979, MNRAS, 189, 649

Balona, L. A., & Stobie, R. S., 1983, SAAOC, 7, 19

Balona, L. A., & Evers, E. A., 1999, MNRAS, 302, 349

Bedding, T. R., Zijlstra, A. A., 1998, ApJ, 506, 47

di Benedetto, G. P., 2008, MNRAS, 390, 1762

Berdnikov, L. N., Dambis, A. K., & Vozyakova, O. V., 2000, A&AS, 143, 211

Berdnikov, L. N., & Turner, D. G., 2004, Astron. and Astrop. Transactions, 23, 253

Berdnikov, L. N., Ignatova, V. V., & Turner, D. G., 1999, IBVS, No. 4724

Berdnikov, L. N., Leonid N., & Turner, D. G., 2001, ApJS, 137, 209

Bessell, M. S., 1969, ApJS, 18, 195

Bíró et al., 2006, IBVS, No. 5684

Bischof, K. M., & Breger, M., 2002, ASPC, 259, 326

Blake, R. M., Delaney, P., Khosravani, H., Tome, J., & Lightman, M., 2003, PASP, 115, 212

Blazhko, S. N., 1907, Astr. Nachr., 175, 325

Bohusz, E., & Udalski, A, 1980, AcA, 30, 359

Breger, M., 1972, AJ, 171, 539

Breger, M., 1975, ApJ, 201, 653

Breger, M., 1980, ApJ, 235, 153

Breger, M., et al., 1993, A&A, 271, 482

Breger et al., 1995, A&A, 297, 473

Breger, M., 2000, ASPC, 210, 3

Bruntt, H., & Southworth, J., 2008, Journal of Physics: Conference Series, 118, 2012

Caldwell, J. A. R., Coulson, I. M., Dean, J. F., & Berdnikov, L. N., 2001, JAD, 7, 4

Cannon, A. J., Wells, L. D., Leland, E. F., & Pickering, E. C., 1909, Harvard College Observatory Circular, 151, 1

Carter, B. D., Ashley, M. C. B., Sun, Y.-S., & Storey, J. W. V., 1992, Proc. Astron. Soc. Australia, 10, 74

Carroll, B. W., & Ostlie, D. A., 2006, An introduction to modern astrophysics and cosmology, 2nd edition. San Francisco: Pearson, Addison-Wesley

Castellani, V., Degl'Innocenti, S., Marconi, M., Prada Moroni, P. G., & Sestito, P., 2003, A&A, 404, 645

Chadid, M., 2000, A&A, 359, 991

Chadid, M., & Chapellier, E., 2006, A&A, 456, 305

Chadid, M., Kolenberg, K., Aerts, C., & Gillet, D., 1999, A&A, 352, 201

Chadid, M., Wade, G. A., Shorlin, S. L. S., & Landstreet, J. D., 2004, A&A, 413, 1087

Chambliss, C. R., 1971, ApJ, 165, 365

Christensen-Dalsgaard, J., 2004, Solar Physics, 220, 137

Christensen-Dalsgaard, J., & Frandsen, S., 1983, Solar Physics, 82, 469

Christiansen, J.L., Derekas, A., Ashley, M. C. B., Webb, J. K., Hidas, M. G., Hamacher, D. W., & Kiss, L. L., 2007, MNRAS, 382, 239

Christiansen, J.L., et al., 2008, MNRAS, 385, 1749

Churms, J., & Evans, D. S., 1961, Observatory, 81, 25

van Citters, G. W. Jr., 1976, AJ, 81, 766

Claret, A., Rodríguez, E., & Garcia, J. M., 1990, RMxAA, 21, 389

Clarke, D., 2002, A&A, 386, 763

Coates, D. W., Fernley, J. A., Sekiguchi, K., Barnes, T. G., & Frueh, M. L., 1994, MNRAS, 266, 1

Cook, K. H., Alcock, C., Allsman, H. A., et al. 1995, ASP Conf. Ser., 83, 221

Cox, A. N., 1998, ApJ, 496, 246

Cunha, M. S., et al., 2007, A&A Review, 14, 217

Dean, J. F., Cousins, A. W. J., Bywater, R. A., & Warren, P. R., 1977, MmRAS, 83, 69

The DENIS consortium, 2005, Third release of DENIS data (September 2005), Vizier Catalogues, B/denis

Derekas, A., et al., 2003, A&A, 402, 733

Derekas, A., Kiss, L. L., Bedding, T. R., Kjeldsen, H., Lah, P., & Szabó, Gy. M., 2006, ApJ, 650, L55

Derekas, A., et al., 2009, MNRAS, in press

Devor, J., 2005, ApJ, 628, 411

Diethelm, R., 1985, A&A, 149, 465

Dommanget, J., & Nys, O., 2002, Catalogue of the Components of Double and Multiple Stars (CCDM), Observations et Travaux, 54, 5

Dvorak, S. W., 2004, IBVS, No. 5549

Dziembowski, W. A., & Mizerski, T., 2004, Acta Astron., 54, 363

Dziembowski, W. A., Gough, D. O., Houdek, G., & Sienkiewicz, R., 2001, MNRAS, 328, 601

Eddington, A. S., 1941, MNRAS, 101, 182

Eggen, O. J., 1956, PASP, 68, 142

Eggen, O. J., 1983, AJ, 88, 361

Eggen, O. J., 1996, AJ, 111, 1313

Elst, E. W., 1972, A&A, 17, 148

Epstein, I, & Abraham de Epstein, A. E., 1973, AJ, 78, 83

Evans, N. R., 1992, ApJ, 384, 220

Evans, N. R., 1994, ApJ, 436, 273

Evans, N. R., Szabados, L., Udalska, J., 1990, PASP, 102, 981

Eyer, L., & Mowlavi, N., 2008, Journal of Physics: Conf. Ser., 118, 012010

Faccioli, L., Alcock, C., Cook, K., Prochter, G., & Syphers, D., 2005, in Tidal evolution and oscillations in binary stars, ASP Ser., ed. A. Claret, A. Gimnez, & J.-P. Zahn, 333, 75

Farinella, P., & Paolicchi, P., 1978, Ap&SS, 54, 389

Fernley, J. A., et al., 1987, MNRAS, 225, 451

Figer, A., 1980, IBVS, No. 1388

Firmanyuk, B. N., 1976, IBVS, No. 1152

Firmanyuk, B. N., 1982, IBVS, No. 2247

Fitch, W. S., 1973, A&A, 27, 161

Fitzpatrick, E. L., Ribas, I., Guinan, E. F., DeWarf, L. E., Maloney, F. P., & Massa, D., 2002, ApJ, 564, 260

Fox, M. W., & Wood, P. R., 1982, ApJ, 259, 198

Fraser, O. J., Hawley, S. L., Cook, K. H., & Keller, S. C., 2005, AJ, 129, 768

Fu, J. N., Jiang, S. Y., 1996, IBVS, No. 4325

Fu, J. N., & Jiang, S. Y., 1999, Delta Scuti Star Newsletter, 13, 9

Fu, J. N., Sterken, C., 2003, A&A, 405, 685

Fu, J. N., Jiang, S. Y., & Liu, Y. Y., 1994, IBVS, No. 3970

Fu, J. N., Sterken, C., & Barrera, L., 2004, ASPC, 318, 346

Fu, J. N., et al., 2008, AJ, 135, 1958

Garrido, R., Garcia-Lobo, E., & Rodríguez, E., 1990, A&A, 234, 262

Gáspár, A., et al., 2003, A&A, 410, 879

Gautschy, A., Saio, H., 1995, Annual Review of Astron. and Astrop., 33, 75

Gautschy, A., Saio, H., 1996, Annual Review of Astron. and Astrop., 34, 551

Geyer, E. H., & Hoffmann, M., 1975, A&AS, 21, 177

Gieren, W., et al., 2008, ApJ, 683, 611

Giuricin, G., Mardirossian, F., & Mezzetti, M., 1983, A&A, 119, 218

Gontcharov, G. A., 2006, Astron. Lett., 32, 759

Groenewegen, M. A. T., 1999, A&AS, 139, 245

Groenewegen, M. A. T., 2007, A&A, 474, 975

Groenewegen, M. A. T., & Oudmaijer, R. D., 2000, A&A, 356, 849

Guinan, E. F., et al., 1998, ApJ, 509, 21

Handler et al., 2000, JAD, 6, 4

Hardie, R. H., & Tolbert, C. R., 1961, ApJ, 134, 581

Hart, J., et al., 1996, PASP, 108, 220

Hilditch, R. W., 2001, An Introduction to Close Binary Stars, Cambridge University Press

Hinkle, K. H., Lebzelter, T., Joyce, R. R., & Fekel, F. C., 2002, AJ, 123, 1002

Hintz, E. G., & Joner, M. D., 1997, PASP, 109, 639

Hintz, E. G., Joner, M. D., Ivanushkina, M., & Pilachowski, C. A., 2004, PASP, 116, 543

Hoffmeister, C., 1933, Astr. Nachr., 247, 281

Hoffmeister, C., 1934, Astr. Nachr., 253, 195

Hoffmeister, C., 1935, Beobachtungszirkular, 16, 45

Hoffmeister, C., 1956, Veröff. Sonneberg Sternw., 3, 1

Houdashelt, M. L., Bell, R. A., Sweigart, A. V., & Wing, R. F., 2000, AJ, 119, 1424

Howe, R., Komm, R. W., & Hill, F., 2002, ApJ, 580, 1172

Huber, J. P., Bedding, T. R., O'Toole, S. J., 2003, aahd.conf., 421

Hurta, Zs., Pócs, M. D., & Szeidl, B., 2007, IBVS, No. 5774

Hübscher, J., 2005, IBVS, No. 5643

Hübscher, J., 2007, IBVS, No. 5802

Hübscher, J., & Walter, F., 2007, IBVS, No. 5761

Hübscher, J., Paschke, A., & Walter, F., 2005, IBVS, No. 5657

Hübscher, J., Paschke, A., & Walter, F., 2006, IBVS, No. 5731

Irwin, J. B., 1961, ApJS, 6, 253

Ita, Y., et al., 2002, MNRAS, 337, L31

Ita, Y., et al., 2004a, MNRAS, 347, 720

Ita, Y., et al., 2004b, MNRAS, 353, 705

Jiang, S. Y., 1987, ChA&A, 11, 343

Johnson, A., Whelan, D., Edinger, B., Bailey, B., Smith, K., Malmrose, M., & Palen, S. E., 2004, BAAS, 36, 740

Joner, M. D., Laney, C. D., 2004, AAS, 205, 5414

Jørgensen, H. E., & Grønbech, B., 1978, A&A, 66, 377

Jorissen, A., Mowlavi, N., Sterken, C., & Manfroid, J., 1997, A&A, 324, 578

Joy, A. H., 1937, ApJ, 86, 363

Jurcsik, J., Clement, C., Geyer, E. H., & Domsa, I., 2001, AJ, 121, 951

Jurcsik, J., Benkő, J. M., & Szeidl, B., 2002, A&A, 396, 539

Jurcsik, J., et al., 2006, AJ, 132, 61

Jurcsik, J., et al., 2008, MNRAS, 391, 164

Jurcsik, J., et al., 2009, MNRAS, in press

Kalimeris, A., Rovithis-Livaniou, H., & Rovithis, P., 1994, A&A, 282, 775

Kämper, B.-C., 1985, IBVS, No. 2802

Keeley, D. A., 1970, ApJ, 161, 657

Kervella, P., Bersier, D., Mourard, D., Nardetto, N., & Coud du Foresto, V., 2004, A&A, 423, 327

Khokhuntod, P., Fu, J. N., Boonyarak, C., Marak, K., Chen, L., & Jiang, S. Y., 2007, ChJAA, 7, 421

Kholopov et al. 1985-1988, General Catalogue of Variable Stars, Vol. III, Nauka, Moscow

Kholopov, P.N. et al., 2003, General Catalogue of Variable Stars Version 1.4, `http://www.sai.msu.su/groups/cluster/gcvs/gcvs`

Kilambi, G. C., & Rahman, A., 1993, BASI, 21, 47

Kim, C., 1990, Ap&SS, 168, 153

Kim, C., & Joner, M. D., 1994, Ap&SS, 218, 137

Kim, S.-L., Lee, J. W., Youn, J.-H., Kwon, S.-G., & Kim, C., 2002, A&A, 391, 213

Kim, S.-L., Lee, J W., Kwon, S.-G., Youn, J.-H., Mkrtichian, D. E., & Kim, C., 2003, A&A, 405, 231

Kinman, T. D., 1961, Royal Obs. Bull., 37, 151

Kiss, L. L., & Szatmáry, K., 1995, IBVS, No. 4166

Kiss, L. L., & Vinkó, J., 2000, MNRAS, 314, 420

Kiss, L. L., et al., 2002, A&A, 394, 943

Kiss, L. L., & Bedding, T. R., 2003, MNRAS, 343, L79

Kiss, L. L., & Bedding, T. R., 2004, MNRAS, 347, L83

Kiss, L. L., & Lah, P., 2006, Mem. S. A. It., 77, 303

Klingenberg, G., Dvorak, S. W., & Robertson, C. W., 2006, IBVS, No. 5701

Koen, C., 1996, MNRAS, 283, 471

Koen, C., & Lombard, F., 1995, MNRAS, 274, 821

Kolenberg, K., 2008, Journal of Physics: Conf. Ser., 118, 012060

Kolenberg, K., et al., 2006, A&A, 459, 577

Kolenberg, K., et al., 2009, MNRAS, in press

Kopal, Z., 1955, Ann. d'Ap., 18, 379

Kovács, G., Kisvarsányi, E. G.. Buchler, J. R., 1990, ApJ, 351, 606

Kurtz, D. W., & Marang, F., 1995, MNRAS, 276, 191

Kučinskas, A., et al., 2006, A&A, 452, 1021

Lacy, C. H. S., Torres, G., Claret, A., & Vaz, L. P. R., 2005, AJ, 130, 2838

Lah, P., Kiss, L. L., & Bedding, T. R., 2005, MNRAS, 359, 42L

Lafler, J., & Kinman, T. D., 1965, ApJS, 11, 216

Laney, C. D., Joner, M., & Schwendiman, L., 2002, ASPC, 256, 173

Laney, C. D., Joner, M., & Rodríguez, E., 2003, ASPC, 292, 203

Leavitt, H. S., & Pickering, E. C., 1912, Harvard College Observatory Circular, 173, 1

Lee, Y. W., 1991, ApJ, 367, 524

van Leeuwen, F., 2007, Astrophys. Space Sci. Lib., 350

Lemasle, B., Franois, P., Bono, G., Mottini, M., Primas, F., & Romaniello, M., 2007, A&A, 467, 283

Lenz, P., Breger, M., 2005, Comm. Asteroseis., 146, 53

Leung, K.-C., 1968, AJ, 73, 6

Liu, Y. Y., et al., 1996, A&AS, 120, 179

Lloyd Evans, T., 1968, MNRAS, 141, 109

Lloyd Evans, T., 1980, SAAO Circ., 1, 257

Lombard, F., 1998, MNRAS, 294, 657

Lombard, F., & Koen, C., 1993, MNRAS, 263, 309

Maceroni, C., & Rucinksi, S. M., 1999, AJ, 118, 1819

Madore, B. F., 1975, ApJS, 29, 219

Mahdy, M. A., 1987, IBVS, No. 3055

Mahdy, H. A., Soliman, M. A., & Hamdy, M. A., 1988, IBVS, No. 3276

Makarenko, E. N., 1971, Soviet Astronomy, 14, 970

Mazeh, T., Tamuz, O., North, P., 2006, MNRAS, 367, 1531

McAlary, C. W., & Wehlau, W. H., 1979, AJ, 84, 1211

McNamara, D. H., 1985, PASP, 97, 715

McNamara, D. H., 2000, ASPC, 210, 373

McNamara, D. H., & Feltz, K. A. Jr., 1976, PASP, 88, 510

McNamara, D. H., Powell, J. M., & Joner, M. D., 1996, PASP, 108, 1098

Michalska, G., & Pigulski, A., 2005, A&A, 434, 89

Mkrtichian, D. E., Kusakin, A. V., Gamarova, A. Yu., & Nazarenko, V., 2002, ASP Conf. Ser., 259, 96

Mkrtichian, D. E., et al., 2004, A&A, 419, 1015

Mkrtichian, D. E., Rodríguez, E., Olson, E. C., Kusakin, A. V., Kim, S.-L., Lehmann, H., Gamarova, A. Yu., & Kang, Y. W., 2005, ASP Conf. Ser., 333, 197

Mkrtichian, D. E., et al., 2006, Ap&SS, 304, 169

Moffett, T. J., Barnes, T. G. III, Fekel, F. C., Jefferys, W. H., & Achtermann, J. M., 1988, AJ, 95, 153

Monet, D. G. et al., 2003, AJ, 125, 984

Moskalik, P., & Gorynya, N. A., 2005, Acta Astron., 55, 247

Munari, U., Sordo, R., Castelli, F., & Zwitter, T. 2005, A&A, 442, 1127

Nardetto, N., Mourard, D., Mathias, Ph., Fokin, A., & Gillet, D., 2007, A&A, 471, 661

Nather, B., & Warner, R. E., 1972, MNRAS, 156, 315

Nikolaev, S., Drake, A. J., Keller, S. C., Cook, K. H., Dalal, N., Griest, K., Welch, D. L., & Kanbur, S. M., 2004, ApJ, 601, 260

Noda, S., et al., 2004, MNRAS, 348, 1120

Noël, F., 2004, A&A, 413, 725

North, J. R., et al., 2007, MNRAS, 380, 80L

O'Connell, D. J. K., 1955, Ricerche astronomiche, 3, 257

Ohshima, O., et al., 2001, AJ, 122, 418

Olivier, E. A., & Wood, P. R., 2003, ApJ, 584, 1035

Oosterhoff, P. Th., & Walraven, Th., 1966, BAN, 18, 387

Opolski, A., 1984, Acta Astron., 34, 225

Paczyński, B., Szczygiel, D., Pilecki, B., & Pojmański, G., 2006, MNRAS, 368, 1311

Palen, S., & Armstrong, J. C., 2003, BAAS, 35, 1222

Paparó, M., Saad, S. M., Szeidl, B., Kolláth, Z., Abu Elazm, M. S., & Sharaf, M. A., 1998, A&A, 332, 102

Peña, J. H., González, S. F., & Hobart, M. A., 1987, A&AS, 138, 11

Percy, J. R., 1975, A&A, 69, 251

Percy, J. R., 1976, Proc. Solar and Stellar Puls. Conf., 60

Perryman, M. A. C., et al., 1997a, A&A, 323, 49

Perryman, M. A. C., et al., 1997b, The *Hipparcos and Tycho* Catalogues (ESA SP-1200; Noordwjik: ESA)

Petersen, J. O., & Christensen-Dalsgaard, J., 1996, A&A, 312, 463

Petersen, J. O., & Hog, E., 1998, A&A, 331, 989

Petterson, O. K. L., Cottrell, P. L., Albrow, M. D., & Fokin, A., 2005, MNRAS, 362, 1167

Pigulski, A., & Michalska, G., 2007, AcA, 57, 61

Podsiadlowski, P., Rappaport, S., & Han, Z., 2003, MNRAS, 341, 385

Pojmański, G., 2002, Acta Astron., 52, 397

Pont, F., Mayor, M., & Burki, G., 1994, A&A, 285, 415

Popper, D. M., 1966, AJ, 71, 175

Poretti, E., 2001, A&A, 371, 986

Poretti, E., 2003, A&A, 409, 1031

Poretti, E., et al., 2005, A&A, 440, 1097

Poretti, E., et al., 2006, Mem. S. A. It., 77, 219

Powell, J. M., Joner, M. D., & McNamara, D. H., 1995, PASP, 107, 225

Prager, R., 1939, Harv. Coll. Observ. Bull., No. 911, 1

Purgathofer, A., & Schnell, A., 1984, IBVS, No. 2500

Rathbun, P., & Smith, H., 1997, PASP, 109, 1128

Ribas, I., et al., 2000, ApJ, 528, 692

Ribas, I., Fitzpatrick, E. L., Maloney, F. P., Guinan, E. F., Udalski, A., 2002, ApJ, 574, 771

Rodríguez, E., 1999, PASP, 111, 709

Rodríguez, E., 2008, personal communication

Rodríguez, E., & Breger, M., 2001, A&A, 366, 178

Rodríguez, E., Rolland, A., & Lopez de Coca, P., 1988, RMxAA, 16, 7

Rodríguez, E., Rolland, A., & Lopez de Coca, P., 1990, IBVS, No. 3427

Rodríguez, E., Lopez-González, M. J., & Lopez de Coca, P., 2000, A&AS, 144, 469

Rodríguez, E., Rolland, A., Lopez de Coca, P., Garrido, R., & Garcia-Lobo, E., 1990, RMxAA, 21, 386

Rodríguez, E., López de Coca, P., Costa, V., & Martín, S., 1995a, A&A, 299, 108

Rodríguez, E., Rolland, A., Costa, V., & Martín, S., 1995b, MNRAS, 277, 965

Rodríguez, E., Rolland, A., Lopez de Coca, P., & Martín, S., 1996, A&A, 307, 539

Rodríguez, E., et al., 2004, Comm. in Asteroseis., 145, 48

Rodríguez, E., et al., 2004a, MNRAS, 347, 1317

Rodríguez, E., et al., 2004b, MNRAS, 353, 310

Rodríguez, E., et al., 2007, A&A, 471, 255

Rolland, A., Peña, J. H., Lopez de Coca, P., Peniche, R., & Gonzalez, S. F., 1986, A&A, 168, 125

Rucinski, S. M., 1993, PASP, 105, 1433

Rucinski, S. M., 1997a, AJ, 113, 407

Rucinski, S. M., 1997b, AJ, 113, 1112

Rucinski, S. M., 1998, AJ, 115, 1135

Rucinski, S. M., 2002, PASP, 114, 1124

Rucinski, S. M., & Maceroni, C., 2001, AJ, 121, 254

Salaris, M., & Groenewegen, M. A. T., 2002, A&A, 381, 440

Sandquist, E. L., & Shetrone, M. D., 2003, AJ, 125, 2173

Santolamazza, P., Marconi, M., Bono, G., Caputo, F., Cassisi, S., & Gilliland, R. L., 2001, ApJ, 554, 1124

Schaltenbrand, R., & Tammann, G. A., 1971, A&AS, 4, 265

Schechter, P. L., Avruch, I. M., Caldwell, J. A. R., Keane, M. J., 1992, AJ, 104, 1930

Shapley, H., 1948, in Harvard Centennial Symp., Monogr Harv. Obs., No. 7, 249

Shibahashi, H., 2000, ASPC, 203, 299

Simon, N. R., & Teays, T. J., 1982, ApJ, 261, 586

Smith, H. A., 1995, RR Lyrae Stars, Cambridge University Press

Smith, H. A., 1997, Balt. Astr., 6, 89

Sollazzo, C., Russo, G., Onnembo, A., & Caccin, B., 1981, A&A, 99, 66

Soszyński, I., et al., 2003, Acta Astron., 53, 93

Soszyński, I., et al., 2004a, Acta Astron., 54, 129

Soszyński, I., et al., 2004b, Acta Astron., 54, 347

Soszyński, I., 2008a, personal communication

Soszyński, I., et al., 2008b, Acta Astron., 58, 163

Southworth, J., Bruntt, H., 2007, IAUS, 239, 157

Soydugan, E., Soydugan, F., Demircan, O., & İbanoğlu, C., 2006, MNRAS, 370, 2013

Sperl, M., 1998, Comm. Astr. Seis., 111

Stellingwerf, R. F., 1972, A&A, 21, 91

Stellingwerf, R. F., 1978, ApJ, 224, 953

Sterken, C., Fu, J.-N., & Brogt, E., 2003, ASPC, 292, 121

Stibbs, D. W. N., 1955, MNRAS, 115, 363

Stobie, R. S., 1970, MNRAS, 148, 1

Stothers, R., 1980, PASP, 92, 475

Stothers, R. B., 2006, ApJ, 652, 643

Strohmeier, W., 1964a, IBVS, No. 51

Strohmeier, W., Knigge, R., & Ott, H., 1964, IBVS, No. 66

Struve, O., 1949, AJ, 54, 137

Szabados, L. 2003, IBVS, No. 5394

Szabados L., 2006, Communications from the Konkoly Observatory, Proc. of the Detre Centennial Conference; editors: L.G. Balazs, L. Szabados, A. Holl, 104, 105

Szeidl, B., 1975, IAUS, 67, 545

Szakáts, R., Szabó, Gy. M., & Szatmáry, K., 2008, IBVS, No. 5816

Székely G.J., & Rizzo M.L., 2004, InterStat, 2004 November, 5

Sweigart, A. V., & Renzini, A., 1979, A&A, 71, 66

Tamuz, O., Mazeh, T., North, P., 2006, MNRAS, 367, 1521

Tsvetkov, Ts. G., 1985, Ap&SS, 117, 227

Udalski, A., Kubiak, M., & Szymański, M., 1997, Acta Astron., 47, 319

Udalski, A., 2003, Acta Astron., 53, 291

Ulas, B., & Demircan, O., 2007, IAUS, 240, 459

Vinkó, J., 1993, MNRAS, 260, 273

Vinkó, J., Remage Evans, N., Kiss, L. L., & Szabados, L., 1998, MNRAS, 296, 824

Wade, R. A., Donley, J., Fried, R., White, R. E., & Saha, A. 1999, AJ, 118, 2442

Wallerstein, G., Jacobsen, T. S., Cottrell, P. L., Clark, M., Albrow, M., 1992, MNRAS, 259, 474

Walraven, Th., Muller, A. B., & Oosterhoff, P. Th., 1958, Bulletin of the Astronomical Institutes of the Netherlands, 14, 81

Walraven, Th., Walraven, J., & Balona, L. A., 1992, MNRAS, 254, 59

Vazquez, R. A., & Feinstein, A., 1990, A&AS, 86, 209

Wehlau, A., Nemec, J. M., Hanlan, P., & Rich, R. M., 1992, AJ, 103,1583

Willems, B., 2003, MNRAS, 346, 968

Willems, B., & Aerts, C., 2002, A&A, 384, 441

Wilson, R. E., 1971, IBVS, No. 5076

Wilson, R. E., 2007, IAUS, 240, 188

Wilson, R. E., & Devinney, E. J., 1971, ApJ, 166, 605

Wolk, S. J., 1996, Watching the Stars go 'Round and 'Round, PhD thesis, State Univ. New York at Stony Brook

Wood, P. R., et al., 1999, IAUS, 191, 151

Wood, P. R., 2000, PASA, 17, 18

Wood, P. R., Olivier, E. A., & Kawaler, S. D., 2004, ApJ, 604, 800

Wyithe, J. S. B., & Wilson, R. E., 2001, ApJ, 559, 260

Wyrzykowski, L., et al., 2003, Acta Astron., 53, 1

Wyrzykowski, L., et al., 2004, Acta Astron., 54, 1

Zakrzewski, B., Ogloza, W., & Moskalik, P., 2000, Acta Astron., 50, 387

Zebrun, K., et al., 2001, Acta Astron., 51, 317

Zessewitch, B. P., 1950, Astron. Circ. USSR, 100, 18

Zhou, A. Y., Fu, J. N., & Jiang, S. Y., 1999, Ap&SS, 268, 397

Zissel, R., 1968, AJ, 73, 696

Zwintz, K., 2008, ApJ, 673, 1088

Zwintz, K., & Weiss, W. W., 2006, A&A, 457, 237